ENGINEERING ANTIBODY FRAGMENTS WITHOUT DISULFIDE BONDS: A POTENTIAL CHEMOTHERAPEUTIC AGENT FOR BREAST CANCER

By

JENNIFER ALICE TONZELLO

A DISSERTATION PRESENTED TO THE GRADUATE SCHOOL
OF THE UNIVERSITY OF FLORIDA IN PARTIAL FULFILLMENT
OF THE REQUIREMENTS FOR THE DEGREE OF
DOCTOR OF PHILOSOPHY

UNIVERSITY OF FLORIDA

2000

This work is dedicated in loving memory to my grandmothers
Domenica Tonzello and Catherine O'Sullivan
for their images of strength, perseverance and love.

ACKNOWLEDGMENTS

I would like to give my gratitude to everyone who helped and encouraged me through these years and made the completion of this work possible.

During my career as a graduate student in the chemistry department I was blessed with many mentors, colleagues and wonderful friends. I would like to thank Dr. Jon Stewart for the opportunity to work in his group and for his advice and guidance with my doctoral research. The constant support for methods and substrates from the Benkovic Laboratory was appreciated. I would also like to thank the Benner group, Horenstein group and Hudlicky group for donating supplies and ideas for my research project. Dr. Horenstein and Dr. Battiste has especially contributed to my graduate career with their interest and support. Dr. Michael DiGiovanna made the biological application of this project possible with the generous donation of the cDNA of the PN2A antibody. The DiGiovanna laboratory at Yale University, especially Katerine Kasowitz, provided the ELISA data for the binding of the scFv PN2A fragments.

As a member of the Stewart Group I have made many wonderful friendships and have had the benefit of working with talented scientists. Sonia Rodríguez has become a cherished friend and her insightful chats about science were invaluable to my career. Carlos Martinez had a special way in bringing a smile to my face and was always a complete source for any chemistry question I ever had. Every time I entered the lab I awaited the cheerful greeting of Kavitha Vedhanayakam. Kavitha's cheerful attitude and supportive ear will be missed. I would also like to thank Brian Kyte for not only making me realize the value of a knee and a good friend, but also for continuing the work on the light chain of scFv 43C9. Aris Polyzos provided a lighthearted environment with the ability to supply me with any detail I needed to know. I was also fortunate to spend time with Leslie Tuchman, Iwona Kaluzna and Debbie Boroughs, and I am confident that they will enhance the Stewart Group. Lisa Manning, Kersten Schroder, Catherine Charron, Tricia Pokey and Mike Sismour always brought a refreshing attitude towards research. I was also fortunate to develop friendships with Bart Neff and Jun Zhu in the Stewart Group and Darwin Ang, Scott Kassel, Stefan Lutz, Kim Millar, Ben Novak, Melissa Petruska, Lee Raley and Mike Roper in the Chemistry Department.

During my stay at the University of Florida I was also fortunate to make many lasting and close friendships. I would like to especially acknowledge Joy Méndez, Eve Hunovice and Julia Cordek. Joy Méndez was the first close friendship I made in graduate school. During our many long and intensive study sessions we fantasized of working together after graduate school. I am pleased that we will have this opportunity and that I have such a dear friend to work with. Eve Hunovice had a special way of making me smile and I was so lucky to have her close friendship during our final years of graduate school. Even before entering graduate school Julia Cordek was a close friend who shared so many of my opinions and tastes. During our time at the University of Florida we were able to nurture our friendship where we became inseparable. She has been my personal cheerleader during my graduate career.

Ever since I was five I've shared my dreams and closest thoughts with my best friend Rebecca Devereaux. Her friendship has brightened my life with laughter, understanding and love. Even during my graduate studies Becky lent an interested ear to my experiences and has encouraged me throughout my life.

I have been truly blessed with the unconditional love, guidance and support of my cherished parents, Alice and Anthony Tonzello. Their encouraging words have helped me to build confidence throughout my life and to succeed at anything I put my mind to. This accomplishment is a direct reflection of the strength and hope their love has given me. The strength and guidance throughout my life is indebted to God the almighty father.

TABLE OF CONTENTS

page

ACKNOWLEDGMENTS iii

LIST OF TABLES x

LIST OF FIGURES xii

ABSTRACT xiv

CHAPTERS

1 BACKGROUND AND INTRODUCTION

- Advancements in Antibody Design 2
  - Antibody Structure and Development of Useful Constructions 2
    - Antibody structure 2
    - Common antibody fragments 2
- Antibodies Used in Chemistry 5
  - Catalytic Antibodies 5
- Antibodies Used for Therapeutic Applications 7
  - Immunotoxins 7
  - Intrabodies 10
- Engineering Antibodies into Stable Folded Proteins 15
  - Unique Antibodies 16
  - Model Predictions for Effective Mutations 16
  - Engineered Disulfide-Less Antibodies 17
  - Stability Studies of Engineered Antibody Fragments 17
  - Discussion of Engineered Antibodies 21
    - Antibody McPC603 21
    - Antibody REI$_v$ 22
    - Antibody ABPC48 23
    - Antibody hu4D5-8 26
    - Antibody scFv13 27
    - Antibody 03/01/01 28
- Guidelines to Increase Stability in Engineered Antibodies 30
  - Insight into Folding Pathway from Denaturation Curves 30
    - Models derived from stability data 30
  - General Considerations to Increase Proper Folding 32

Interface interactions between domains....32
Proline cis/trans-isomerization....32
The Need for a General Method....33
Introduction to Research Goal....34
The Model System scFv 43C9....34
Plan for Reengineering....36
Discussion of Methods for Antibody Production....39
In Vivo Protein Folding....39
In Vitro Refolding Methods for Antibody Fragments....41
Identification of Functional and Stable V_H Disulfide-less Mutants....42
Biological Application....42
Role of ErbB-2 in Cancer....42

2 EXPRESSION AND ISOLATION OF ANTIBODY FRAGMENTS

Strategies to Isolate Correctly Folded and Active scFv 43C9....44
In Vivo Expression in Bacteria Strains....44
Expression of wt scFv 43C9....45
Tools needed to design an alternate synthesis of scFv 43C9....46
Searching for an *In Vivo* Protocol for scFv 43C9 Mutants....47
Attempts to directly produce soluble wt 43C9 scFv/c-myc/his_6....47
Construction of alternative expression systems carrying a strong T7 promoter....51
In Vitro Refolding from Inclusion Bodies....54
Immobilized refolding of over-expressed scFv 43C9....54
Design of a batch refolding procedure for wt scFv 43C9....58
Characterization of chromatography elution pattern....64
Expression of scFv 43C9 V_H disulfide mutants....68

3 BINDING AND STABILITY STUDIES OF WILD-TYPE AND V_H DISULFIDE MUTANT SCFV 43C9 PROTEINS

Methods Investigated for the Binding Activity of scFv 43C9....72
Ester Hydrolysis Kinetics....72
Hydrolysis of *p*-nitrophenyl acetate....73
Synthesis of *p*-chlorophenyl ester....73
Hydrolysis of *p*-chlorophenyl ester....74
Electrospray Mass Spectroscopy....76
Binding Studies Using Fluorescence Spectroscopy....77
Fluorescence Spectroscopy of scFv 43C9....78
Quantitative Binding Measurements....79
Active antibody concentrations....79
Measurement of thermodynamic dissociation constants....80
Fluorescence Assays of scFv 43C9....82
Titration of scFv 43C9 with the Phosphonate Antigen....82
Quantitating Dissociation Constants for scFv 43C9....83
Stability of scFv Fragments....85

Guanidine Denaturation Studies 86
Denaturation of scFv 43C9 87
Data Interpretation 87
Wt scFv 43C9 Denaturation Curves 88
Denaturation Studies of the V_H Mutant Library 89
Predicted Folding Pathway of the wt scFv and V_H Mutants 93

4 CONSTRUCTION OF SCFV PN2A

Biological Application of Reengineered Antibody Fragments 94
Creating a scFv Fragment from a Monoclonal Antibody..........95
Construction of ScFv PN2A 95
Isolation of Fab chains of mAb PN2A..........95
Isolation of the light and heavy chains of the variable domain 98
Construction of scFv PN2A 99
Expression of scFv PN2A 102
scFv PN2A Expressed with a c-Myc Tag from pJAT21 102
Test inductions..........102
Batch refolding..........103
Expression of scFv PN2A with a c-Myc and His_6 Tag..........104
Test inductions and isolation from *in vivo* isolation methods..........104
In vitro batch refolding 104
Binding Studies of scFv PN2A..........105
ELISA screening..........105
Fluorescence studies 106
Future Work to Increase the Binding Selectivity of scFv PN2A 107
Correcting the *pelB* Leader Sequence..........107

5 CONCLUSIONS

Project Goal 108
Engineering the Model System scFv 43C9 108
Production of Disulfide-less Heavy Chain Mutants..........109
Characterization of the V_H Disulfide-less Mutants of scFv 43C9..........109
Proportion of Functional Protein 109
Binding Assays 110
Guanidine Denaturation Experiments..........111
Stability studies..........111
Classification of scFv 43C9 V_H mutants..........111
Engineering Monoclonal Antibody PN2A..........112
Construction of scFv PN2A and Binding Studies..........112
Tailoring the Binding of scFv PN2A..........112
Long-Term Goal of the Project 112

6 EXPERIMENTAL

Molecular Biology 114
  Biochemicals and Media 114
  Vectors 114
  Primers 115
  Conditions for PCR 115
  E. coli Strain Genotypes 115
  Maintenance of *E. coli* Strains 116
  Recombinant DNA Techniques 116
Test inductions of expression plasmids 117
  Materials and Equipment 117
  General 117
  Experimental Procedures 117
    Induction 117
    Sample preparation 118
    Separation by gel electrophoresis 118
    Western blots 119
  Materials and Equipment 119
  General 120
  Experimental Procedures 120
  Protein Concentration 121
  Molecular Weight Determination by Size Exclusion 122
    Materials and equipment 122
    Experimental procedure 122
Assays for scFv 43C9 Activity and Binding 123
  Kinetic Assays 123
    Materials and equipment 123
    Experimental procedure 123
  Fluorescence Assays 123
    Materials and equipment 123
    Experimental procedure 124
Organic Synthesis 125
  Chemicals and General Procedures 125
  Synthesis of Substrates 126

APPENDIX A EXPLANATION OF ABBREVIATIONS 127

APPENDIX B FLUORESCENCE QUENCHING PLOTS 128

APPENDIX C SEQUENCES 144

REFERENCES 149

BIOGRAPHICAL SKETCH 156

LIST OF TABLES

Table page

Table 1-1. Summary of known intrabodies in literature. This table includes comments on the stability and expression levels of each antibody. Assays to determine the presence, the stability and the effects of the antibody were determined by one of the following: (a) intracellular expression and binding in cytoplasm by immunofluorescence, (b) immunofluorescence to a tag showing antibody intracellular expression, (c) inhibition of meiotic maturation of *Xenopus* oocytes, (d) inhibition of infected cell growth, (e) degradation of an unstable antibody expressed inside a cell, (f) selective growth of *E. coli* expressing the cloned antibody, (g) decrease in antigen due to antibody expression, (h) immunoprecipation of antigen by the expressed antibody, (i) kinetic activity of intracellular expressed antibodies, (j) stability of antibody determined by guanidine denaturation, (k) location and expression level of antibody using western blot and (l) ELISA experiments showing antigen binding....14

Table 1-2. Summary of engineered antibodies. Sequence numbering as described by Kabat *et. al.,* 1987....19

Table 1-3. Denaturation studies of stabilizing mutations. [Urea] and [Gdn] concentration reflect the midpoint of unfolding from published plots. (ss) indicates a fragment with one intrachain disulfide bond, (ss^2) indicates two intrachain disulfide bonds, (-) appears if an intrachain disulfide bond is missing, and (--) shows a disulfide-free fragment. Data entries in a single row are match to the respective scFv by superscript letters (^{a,b})....20

Table 1-4. Primers used to mutate scFv 43C9....38

Table 2-1. Primers used to construct pJAT2....51

Table 2-2. Conditions explored to optimize the refolding of immobilized scFv 43C9. Two scFv's (43C9 and PN2A) were tested. The percent of eluted scFv that was active was determine by fluorescence assays when a significant amount of scFv was isolated....58

Table 2-3. This table organizes information from three *in vitro* refolding experiments for wt scFv 43C9. Concentrations of protein samples refolded and separated by polyCAT-A chromatography are listed. The eluted peaks from chromatography were assayed for scFv concentration by absorbance at 280 nm and by fluorescence titration....63

Table 2-4. Molecular weight determination of the three peaks isolated by the PolyCAT-A column for wt scFv 43C9....65

Table 2-5. Active protein present for wt scFv 43C9 eluted in peak A and B and quantification of binding ability from fluorescence hapten quenching. (N/D represents data that was not determined....67

Table 2-6. Summary of protein isolation for the V_H disulfide mutants....................71
Table 3-1. Summary of percent of active refolded scFv comparing the isolated scFv concentration determined from fluorescence titration experiments *versus* protein absorbance at 280 nm...83
Table 3-2. K_D Values for the Fluorescence Quenching for scFv 43C9. [a]Benkovic *et al.*, 1990, *Science*, **250**, 1135-1139. [b] Gibbs *et al.*, 1991, *Proc. Natl. Acad. Sci. USA*, **88**, 4001-4004 and Stewart *et al.*, 1994, *Biochemistry*, **33**, 1994-2003. Plots are included in Appendix B and plots showing poor fits to the quadratic relationship is indicated with (poor). If a quadratic relationship did not fit data at all (no quenching) was entered in the table...85
Table 3-3. Results from Denaturation of scFv with Guanidine...90
Table 4-1. Collection of primers used for PCR amplification of Fab Fragment. 98
Table 4-2. Summary of primers used to amplify the variable fragment of each chain......99
Table 4-3. Binding study of scFv PN2A with c-myc-his$_6$ tag. 106
Table 5-1. Grouping of V_H mutants on the basis of percentage of active scFv produced from refolding. 110
Table 6-1. *E. coli* strains used in this work and their genotype......................................115

LIST OF FIGURES

Figure page

Figure 1-1. Schematic depiction of an antibody showing the disulfide bonds (black bands), different domains and fragments of antibodies (F_v, Fab and Fc). 3
Figure 1-2. Antibody fragment constructions. 5
Figure 1-3. Catalysis of ester hydrolysis using a catalytic antibody that recognizes a transtion state analog 7
Figure 1-4. Cellular effects from immunotoxins. 8
Figure 1-5. Cross section of the expression of intrabodies inside the reductive lumen of the ER 12
Figure 1-6. Removal of the light chain disulfide bond from scFv ABPC48 using site-directed mutagenesis and DNA shuffling. 24
Figure 1-7. Mutagenesis of scFv13, and selection of functional disulfide-less mutants expressed inside bacteria 28
Figure 1-8. Depictions of the denaturing curves expected from scFv fragments of each class. The Y-axis is the fraction of denatured protein and the X-axis is the concentration of denaturant 30
Figure 1-9. The transition state analog (TSA) against which mAb 34C9 was raised. Ab 43C9 catalytic antibody catalyzes the ester and amide hydrolysis by lowering the energy barriers of transition states. 34
Figure 1-10. The Ab 43C9 catalyzed ester hydrolysis mechanism from mutagenesis studies on active site residues. 35
Figure 1-11. Strategy for removing the disulfide bonds. 36
Figure 1-12. Procedure for site-directed mutagenesis of each domain 37
Figure 2-1. Plasmid constructs of pJS118 and pTG119. 46
Figure 2-2. Construction of pJAT3 48
Figure 2-3. Construction of pJAT5 49
Figure 2-4. Western Blots and SDS-PAGE of IPTG induction of BL21(DE3)pJAT3 50
Figure 2-5. Construction of pJAT2 52
Figure 2-6. Construction of pJAT11 53
Figure 2-7. Construction of the expression plasmid pJAT30. 60
Figure 2-8. Elution patterns of wt scFv 43C9 secreted from BL21(DE3) and of the *in vitro* batch refolding wt scFv 43C9. The dotted line represents the linear increase to 25 mM calcium acetate buffer. Y-axis for both plots is 0.2 absorbance units (280 nm) 63
Figure 2-9. Protein standards for molecular weight determination 65
Figure 2-10. Construction of mutant expression vectors pJAT31-pJAT40 68
Figure 2-11. Chromatograms from the separation of scFv fragments by polyCAT-A chromatography. Dotted line represnets increasing buffer gradient. 70

Figure 3-1. Hydrolysis reactions followed by kinetic assays. 73
Figure 3-2. Synthesis of *p*-chlorophenyl ester 74
Figure 3-3. Observed catalyzed hydrolysis of p-chlorophenyl ester with scFv 43C9 corrected for background hydrolysis is in the absence of scFv 43C9........................75
Figure 3-4. Ligands used in binding assays of scFv 43C9. 78
Figure 3-5. Quenching of scFv 43C9 fluorescence by the phosphonate antigen.............79
Figure 3-6. Fit used to determine K_D of the quenching ligand...80
Figure 3-7. Model used to fit guanidine denaturation data...88
Figure 3-8. Guanidine denaturation of three stocks of refolded wild type scFv 43C9 isolated from polyCAT-A column chromatography....................................89
Figure 3-9. Guanidine denaturation of wt scFv 43C9 isolated from secretion into the media and from *in vitro* batch refolding compared to the V_H mutants of scFv 43C9 isolated from *in vitro* batch refolding. 91
Figure 3-10. Guanidine denaturation curves with the calculated experimental error of in vitro batch refolded wt and VH mutant scFv 43C9 presented in Figure 3-9.............92
Figure 4-1. Scheme for isolation of V_L and V_H domains of scFv PN2A..........................97
Figure 4-2. Construction of pJAT21 101
Figure 4-3. Construction of pJAT22..102
Figure 4-4. Test inductions and isolation of the myc tagged scFv PN2A. 103
Figure 4-5. Accumulation of scFv PN2A with c-myc and his6 as inclusion bodies in BL21(DE3) cells and the eluted fractions of the immobilized *in vitro* refolding....104

Abstract of Dissertation Presented to the Graduate School
of the University of Florida in Partial Fulfillment of the
Requirements for the Degree of Doctor of Philosophy

ENGINEERING ANTIBODY FRAGMENTS WITHOUT DISULFIDE BONDS: A POTENTIAL CHEMOTHERAPEUTIC AGENT FOR BREAST CANCER

By

Jennifer Alice Tonzello

May 2000

Chairman: Dr. Jon D. Stewart
Major Department: Chemistry

The introduction of antibodies inside the cytoplasm of cells provides a powerful tool for manipulating intracellular metabolism. The long-term goal of this project is to convert an antibody representative of those found in Nature into one that can fold in the reducing environment of the cytoplasm. A well-characterized antibody was first reconstructed to provide a general method for creating functional antibody fragments in reducing environments.

The model single-chain variable fragment (scFv) 43C9 was engineered by removing one of the two disulfide bonds. Site-directed random mutagenesis was completed for the two cysteine residues of each disulfide bond, located at H92 and H22 of the heavy chain and L23 and L88 of the light domain of scFv43C9. A disulfide-less chain was then paired with the wild-type partner to create the mutant scFv's. A preliminary screening provided ten scFv's that lacked a disulfide bond in the heavy chain while retaining the disulfide bond in the light chain. These disulfide-less heavy chain mutant scFv's were assayed for antigen and product binding to quantitatively determine the best mutant. The stabilities of the mutants was also determined using denaturation experiments. This revealed that two single mutants (C-H92-P and C-H92-A) and two double mutants (C-H22-A, C-H92-A and C-H22-A, C-H92-T) possessed binding affinities close to that of the wild-type scFv. Even though the stability of these mutants was less than that of the wild type scFv, we hope to pair these heavy chain mutants with a similarly-engineered light chain mutant to provide a disulfide-less scFv 43C9.

The results from engineering a disulfide-less derivative of scFv 43C9 will be used as a guide for engineering the monoclonal antibody (mAb) PN2A into a form capable of folding in the reducing environment of a cell. Monoclonal antibody PN2A recognizes the intracellular portion of p185, and this study plans to engineer mAb PN2A into a derivative capable of blocking the mitogenic cascade inside a living cell. As a first step mAb PN2A has been converted to a scFv derivative that was tested for binding affinity through enzyme-linked immunosorbant assays (ELISA). These assays indicated that the binding specificity of scFv PN2A was decreased compared the monoclonal antibody. Once the specificity of the scFv has been increased, scFv PN2A will be transformed into a disulfide-less scFv using the data from the model scFv 43C9 as a guide.

CHAPTER 1
BACKGROUND AND INTRODUCTION

Conventional approaches to cancer treatment are limited to toxic removal methods, such as radiation or chemotherapy, or surgical excision of tumor masses. New strategies are being investigated to target cancer cells directly, and many of these approaches incorporate elements of the immune system.

The advent of monoclonal antibodies in 1975 provided a source for both specific and selective reagents for research. Since that time, efforts to incorporate antibodies into a number of intracellular compartments have provided powerful tools for disease therapy. A key challenge in this field is to maintain a stable and functional antibody in a non-natural environment. The free thiols that are found in a high concentration in the cytoplasm of cells reduce the disulfide bonds that maintain antibody stability.

The goal of this project is to provide a general strategy and a successful example of an antibody engineered for stability in the cytoplasm. For maximal utility, it is important that the model does not contain unusual features or robust folding. Removal of the disulfide bonds by site-directed random mutagenesis of the cysteine residues poses the greatest challenge. The resulting collection of mutants is then examined for antigen binding and folding stability. Because the cysteine residues involved in antibody disulfide bonds are located in the conserved regions of the protein, it is predicted that appropriate mutations identified for the model antibody can be applied to antibodies in general. The clinical utility of disulfide-less antibodies will be tested by producing an intracellular derivative of an antibody that is specific for the intracellular domain of the oncoprotein p185.

Advancements in Antibody Design

Antibody Structure and Development of Useful Constructions

Antibody structure

Common antibodies, such as immunoglobulin G, consist of four polypeptides or "chains" as illustrated in Figure 1-1.[1,2] Two identical heavy chains and two identical light chains associate to form the functional IgG molecule. Intra- and inter-domain disulfide bridges stabilize the tertiary and quaternary structures of the protein. These disulfides are inaccessible to solvent and contribute significantly to the folding and stability of the protein.[3]

Common antibody fragments

F_c and Fab fragments. The full IgG can be enzymatically digested into two major portions: the F_c, which contains a sequence and structure that are conserved between antibodies of a given host, and the Fab, which contains the antigen binding pocket.[2] The Fab fragment is commonly used in combinatorial libraries of antibodies and can be expressed in functional form in *Escherichia coli* (*E. coli*).[7] The variable fragment (F_v), indicated in Figure 1-1 by a darker gray color, consists of the heavy (V_H) and light (V_L) variable chains that form the antigen binding pocket.

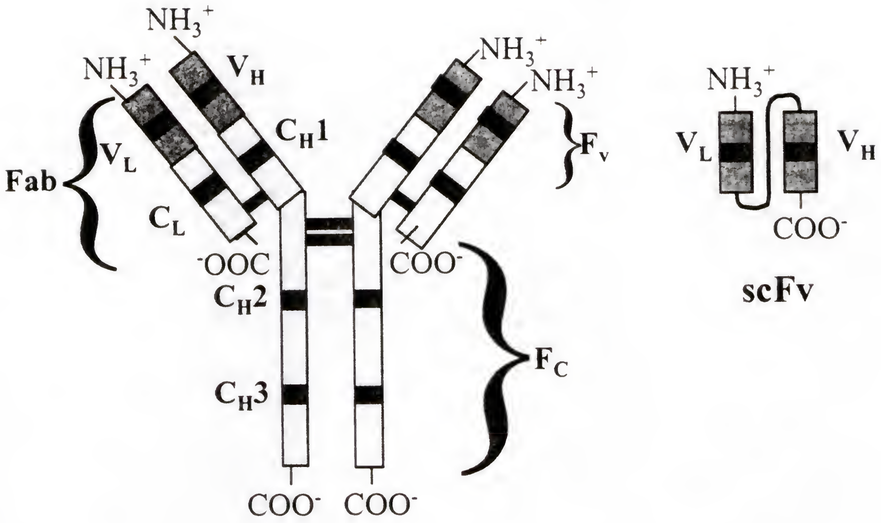

Figure 1-1. Schematic depiction of an antibody showing the intra- and interchain disulfide bonds (black bands), different domains and functional fragments of antibodies (F_v, Fab and Fc).

Variable fragment (F_v). The variable domain of this heterodimer fragment consists of β-sheets that are organized into a β-barrel. The antigen binding pocket is formed by the six variable loops that connect the strands of the β-sheets of each domain. These regions are also referred to as the complementary determining regions (CDRs). The β-sheets form a conserved structure known as the framework region (FR) that is stabilized by two intra-chain disulfide bonds located between H22 and H92 in the heavy chain and between L23 and L88 of the light chain (amino acid positions are numbered according to Kabat[4]). The F_v heterodimer can exist as a functional protein if the large hydrophobic interface between the two chains is sufficient to stabilize the antigen binding pocket. One attractive feature of F_v fragments is their small size that allows them to penetrate tumor cells faster than the larger parent antibody.[5] Furthermore, the lack of a constant domain in an F_v fragment also makes it less immunogenic in humans.[6]

Single-chain variable fragment (scFv). Unfortunately, only a few F_v heterodimers are resistant to dissociation of the heavy and light chains. This problem can be overcome by using a covalent linker to keep the two domains together in a functional form. Figure 1-2 illustrates some common F_v fragments produced by protein engineering. The single-chain variable fragment (scFv) is produced by connecting the N- and C-terminal ends of the two chains with a flexible polypeptide sequence to resist dissociation.[7] Introducing a disulfide bond at the interface between the two domains (dsFv) has also stabilized Fv fragments. The dsFv is typically more stable than the other fragments and tends to maintain a binding affinity better than the corresponding scFv.[5] A scFv with a disulfide bond in the interface (ds-scFv) has also been synthesized and is useful when extra stability is required to maintain an active F_v.[8] The inherent stability of the antibody and the intended use of the protein generally dictates which construct in Figure 1-2 is adopted.

Other antibody fragments. Other recombinant antibody derivatives such as bispecific bivalent F_v's [$(scFv)_2$] also have specific uses. A construct of this type of F_v involves connecting two independent scFv fragments with a third flexible polypeptide linker.[5] A $(dsFv)_2$ has a similar construct except an additional disulfide bond replaces the linker.[5] The advantage of these fragments is their ability to bind two epitopes on the same antibody molecule. A diabody is another bivalent F_v that has a shortened polypeptide linker between the light and heavy chains of an F_v.[5] The short linker inhibits pairing of the heavy and light chains of one F_v and results in the mispairing between complementary domains of two F_v's.

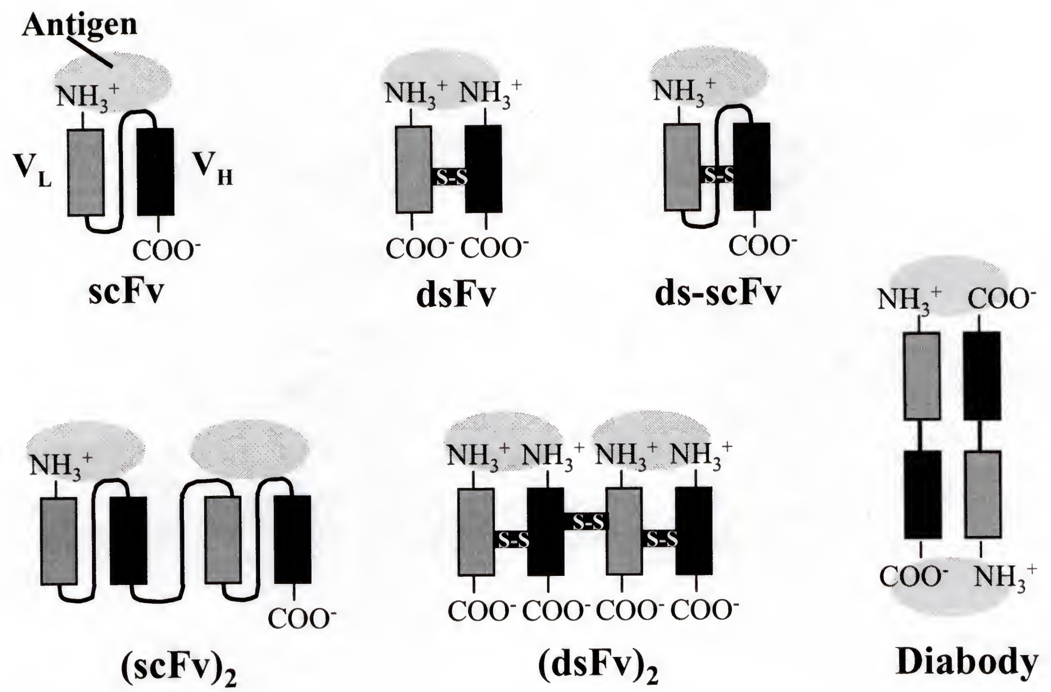

Figure 1-2. Antibody fragment constructions.

Antibodies Used in Chemistry

Catalytic Antibodies

The immune system can provide a repertoire of proteins possessing high affinity to nearly any antigen. Pauling was the first to suggest that this reservoir might also be useful for catalysts.[9] Antibodies with higher binding affinity for the transition state of a reaction than the reactants or products could behave as a catalyst.[10] This application at first seems impossible given the functional differences between enzymes and antibodies. An enzyme assists in the acceleration of intra-molecular bond cleavage and the formation of new bonds, whereas antibodies are produced to bind molecules in their ground states. This significant difference can be overcome by tailoring the binding selectivity of the antibody to match that of an enzyme.[11] Catalytic antibodies are produced by immunization with a transition state analog (TSA) that mimics the transition state for the reaction.[10] The catalytic antibody can act as a catalyst to accelerate reaction rates by mechanisms similar to those of natural enzymes or by novel mechanisms.

The first deliberately produced catalytic antibody was reported in 1986 and accelerated ester hydrolysis.[10] This new tool for catalysis was developed from Pauling's theory that the binding energy of the antibody to the TSA could decrease the energy barrier of a reaction (Figure 1-3).[7] This can be approached by either increasing the ground state energy of a substrate or decreasing the transition state energy of the reaction. Catalytic antibodies are still being developed and have provided scientists with unique catalysts and therapeutic agents.[10-13]

A catalytic antibody of special interest to this project is the monoclonal antibody (mAb) 43C9. ScFv 43C9 was developed to catalyze ester and amide hydrolysis as a model for antibodies capable of hydrolyzing peptide bonds. This catalytic antibody was chosen as the model system for creating the disulfide-less scFv. The scFv 43C9 was chosen because it represents a common antibody that does not contain unusual, robust folding stability that would skew the mutations required to remove the disulfide bonds. In addition, the catalytic mechanism and three-dimensional structure[14] of this antibody are known. Finally, the binding affinities for a number of ligands are also known.[15-17] This wealth of knowledge made scFv 43C9 an excellent model to determine the mutations that produced a stable and functional disulfide-less scFv.

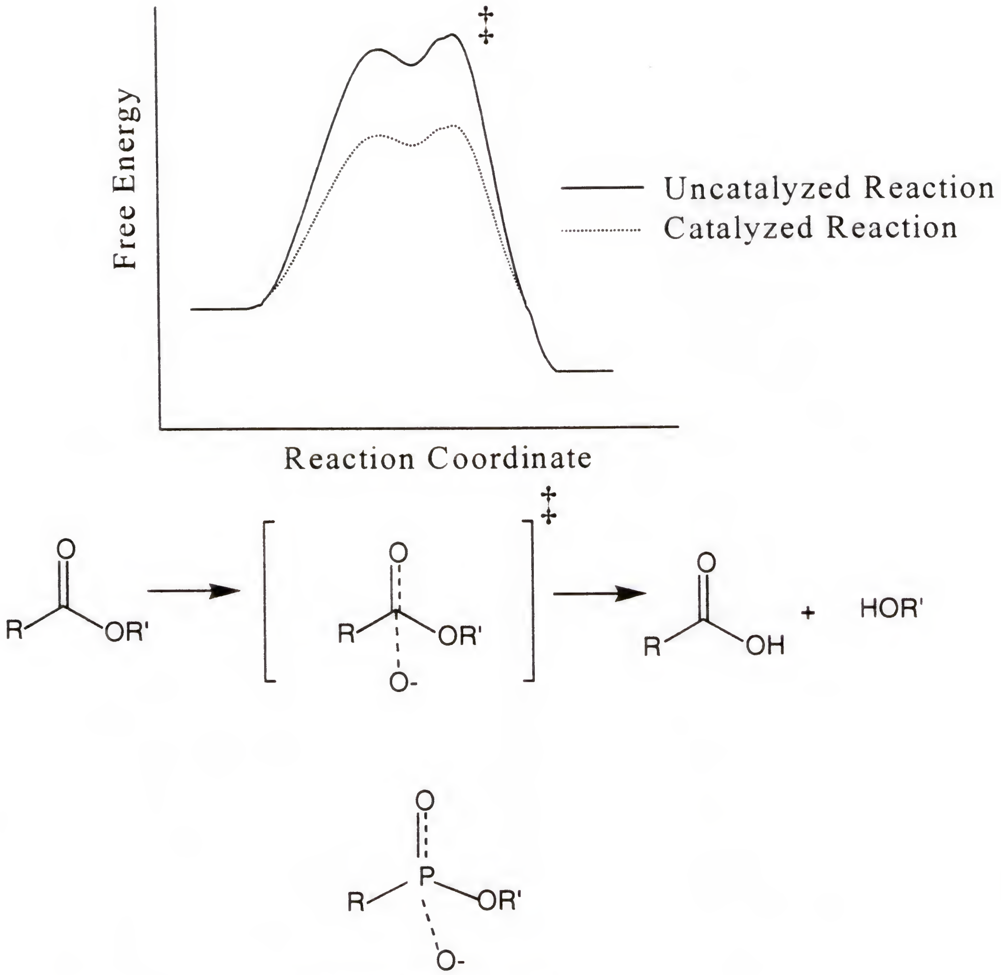

Transition State Analog

Figure 1-3. Catalysis of ester hydrolysis using a catalytic antibody that recognizes the transition state analog.

Antibodies Used for Therapeutic Applications

Immunotoxins

One approach for cancer treatment is to target the cancer cells directly by delivering a cytotoxic agent to the cell. The combination of antibody fragments with cytotoxic agents yields a fusion protein known as an immunotoxin. A schematic of the function of an immunotoxin is illustrated in Figure 1-4. The antibody portion recognizes a receptor that is displayed on the cell surface of tumors or infected cells. Two classes of molecules have been identified as being an excellent antigen for the immunotoxin. One class is composed of target molecules such as growth factors, cytokines, lymphokines, polypeptide hormones, and other cell recognition proteins, while the second class is composed of monoclonal antibodies.[18] Once an immunotoxin is docked at the antigen, the cytotoxin is delivered into the cell by endocytosis.

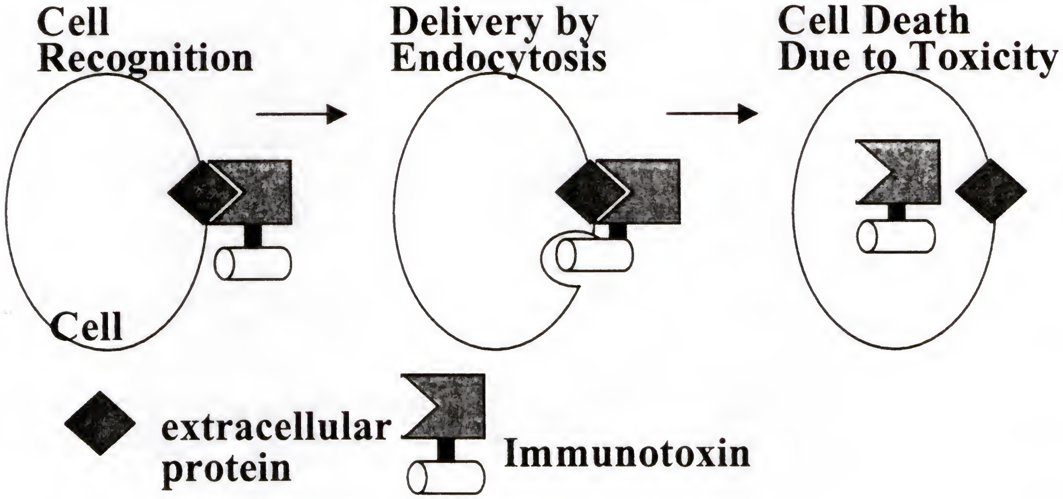

Figure 1-4. Cellular effects from immunotoxins.

Immunotoxins have been used to combat lung, ovarian, breast, stomach and prostate cancers and leukemia.[18,19] In order to appreciate the impact immunotoxins have made in the biological goals of this project, studies involving cancer cells carrying the oncoprotein p185 are emphasized. Research in this area has developed a specific immunotoxin targeted to cancer cells overexpressing the epidermal growth factor receptor (EGFR) and the oncoprotein p185 expressed from oncogene erbB-2.[5,8,20,21]

Overexpression and/or amplification of erbB-2 produces oncoprotein p185 and this protein is commonly found on the surfaces of breast and ovarian tumor cells. The p185 transmembrane protein mimics the EGFR mitogenic signaling and produces uncontrolled and amplified cell division. Developments in the prognosis and treatment of cancer have incorporated agents targeting p185.

Researchers have developed immunotoxins that contain antibody fragments that recognize the extracellular domain of the transmembrane protein p185 and have studied the effects of the delivered toxin. Many of these immunotoxins carry a highly toxic bacterial cytotoxin, *Pseudomonas* exotoxin A.[20] *Pseudomonas* exotoxin A is a potent inhibitor of protein synthesis in mammalian cells. Micrometatasis in immunocompetent animals possessing tumors overexpressing p185 has been prevented with immunotoxins.[20] Other immunotoxins that utilized different antibody fragment constructs that recognize the same receptor were shown to produce a 10-20 fold higher level of cytotoxicity; however, potency only doubled when the antibody fragment of the immunotoxin was improved for antigen binding.[21]

Immunotoxins represent one successful example of using antibodies as therapeutic agents; however, the applications are limited by the need for the presentation of the antigen on the cell surface. Unfortunately, immunotoxins also face an inherent problem of an immune response in the patient to the foreign and highly fatal cytotoxic molecules.[22] Even with the use of immunosuppresive agents, a response to the toxin is observed shortly after exposure.[23,24]

Marasco and co-workers have developed a system that can avoid an immunogenic response.[22] These researchers created an immunotoxin that fuses an antibody to protamine, a small, DNA binding protein that can electrostatically interact with the DNA encoding for a cytotoxin. The antibody of the immunotoxin recognizes the HIV-I envelope glycoprotein gp120. Once the antibody binds gp120, the DNA carried by protamine is delivered into the cell and is transcribed and translated to produce the encoded cytotoxin. In one example of this strategy, HIV-1 infected CD4+ lymphocytes containing surface gp120 were incubated with the immunotoxin-DNA complex. Within 48 hours a significant decrease in cell viability (<1.5%) and protein synthesis (<0.2%) was observed as compared to controls. Advances such as these will help immunotoxin applications in disease and cancer therapy.

One limiting factor of immunotoxins and antibodies in general is the loss of the stabilizing forces of antibody disulfide bonds in reducing environments. Antibodies located in reducing environments inside a cell are unable to recognize intracellular molecules. Researchers have worked diligently to develop this system into one that will allow antibodies to bind intracellular targets because of the invaluable applications this would provide for cancer and disease therapy.

Intrabodies

Antibodies that can bind intracellular proteins may have the potential to manipulate cellular metabolism. Interest in antibodies inside cells (intrabodies) erupted in the early 1990s, although a study as early as 1988 demonstrated that expression of antibodies against the cytoplasmic alcohol dehydrogenase I affected yeast cell growth.[25] Many studies in this field have recorded *in vivo* effects from intrabodies but stability, expression levels and quantitative binding affinities are issues that need to be addressed.[26]

In the normal case, the light and heavy chains of antibodies expressed in mammalian cells are initially translocated into the endoplasmic reticulum (ER) where chaperone molecules play a key role in folding proteins in an oxidative environment. The correctly processed and assembled antibodies are then secreted into the oxidative environment that prevails outside the cell. Efforts to develop cellular systems or antibodies that can deviate from this normal process have been pursued for applications in areas such as human immunodeficiency virus (HIV), cancer, plant pathogenicity and leukemia research.

Normal exocytosis of antibodies has been manipulated by capturing them in the ER. Secretory scFv's are anchored to membrane receptors by a C-terminal peptide (KDEL) tag and the antibody domains remain in the oxidative environment of the lumen in eukaryotic cells (Figure 1-5). Antibodies in this compartment have been used to deter the growth of cells infected by HIV-1[27] and cancer cells that overexpress erbB-2[29-31] by capturing these proteins and preventing their normal translocation processes. In one example, an ER-anchored scFv105 competed with CD4 proteins for the binding of the HIV-1 envelope protein gp120 and thereby prevented the transit of the antibody-gp120 complex to the cell surface.[27] Inhibition of gp160 maturation and function by the scFv was shown in cells expressing the antigen.

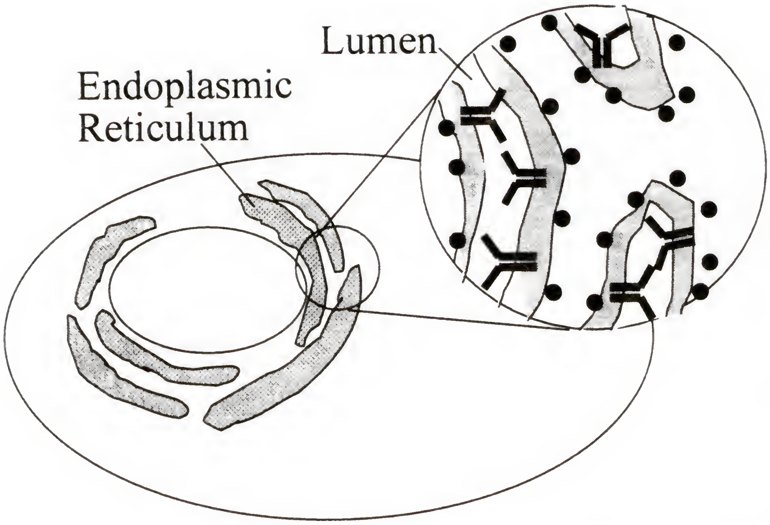

Figure 1-5. Cross section of the expression of intrabodies inside the reductive lumen of the ER.

The inactivation of the cellular oncoprotein erbB-2 was also accomplished using ER-resident intrabodies. Two scFv's were directed to the lumen of the ER (as demonstrated by western blotting), and retention of a stable scFv was independent of the presence or absence of antigen.[29] ScFv expression decreased cell growth by 80% in soft-agar, and the transit of erbB-2 through the ER was limited. The more potent scFv-5R was further tested for impaired cell growth in cells stimulated by NDF (a *neu* differentiation factor).[31] The direct receptors of NDF are erbB-3 and erbB-4, but the ER trapped scFv-erbB-2 complex directly affected NDF signaling. Other research has addressed the problem of delivering the anti-erbB-2 scFv to all neoplastic cells to achieve tumor eradication.[30] Deshane *et al.* developed an adenoviral-mediated delivery to more than 80% of the malignant ascites in ovarian carcinomas and demonstrated survival advantages in treated animals. Further studies in this area have focused on overcoming the limitations of intracellular expression caused by low stability, low expression rates and unpredictable behavior.[32] Researchers have also speculated that rare, stable *in vivo* behavior may be due to the biochemical differences between individual scFv proteins.[31]

Research groups have also tried to target antibody fragments to other intracellular compartments and to the reducing environment of the cytosol itself. Attaching leader sequences to antibodies has allowed them to be trafficked to both the nucleus and mitochondria as shown by immunofluorescence.[33,34] The heavy and light chains of an antibody were also directed independently into the cytoplasm; however, this resulted in low protein expression and rapid degradation of the Fv.[33,34] Addition of antigen seemed to result in higher stability of the F_v; however, others have criticized this work, pointing out that the stability of an antibody should not be dependent on the availability of its ligand.[32]

Cytoplasmic expression of antibody fragments has also been accomplished by microinjections of the scFv mRNA into the cytoplasm. Microinjection of scFv259cyt into *Xenopus* oocytes allowed the expression of anti-$p21^{ras}$ scFv and led to the inhibition of meiotic maturation.[35] These studies only tested the global effects of the antibody fragments on the cells, and the activity of the intrabody was not directly assayed. This study also reported that the cytoplasmic F_v was unstable and subject to degradation. The researchers speculated that the residual activity observed was most likely a cross-reactivity of partially folded molecules with the antigen.[34]

Table 1-1. Summary of known intrabodies in literature. This table includes comments on the stability and expression levels of each antibody. Assays to determine the presence, the stability and the effects of the antibody were determined by one of the following: (a) intracellular expression and binding in cytoplasm by immunofluorescence, (b) immunofluorescence to a tag showing antibody intracellular expression, (c) inhibition of meiotic maturation of *Xenopus* oocytes, (d) inhibition of infected cell growth, (e) degradation of an unstable antibody expressed inside a cell, (f) selective growth of *E. coli* expressing the cloned antibody, (g) decrease in antigen due to antibody expression, (h) immunoprecipation of antigen by the expressed antibody, (i) kinetic activity of intracellular expressed antibodies, (j) stability of antibody determined by guanidine denaturation, (k) location and expression level of antibody using western blot and (l) ELISA experiments showing antigen binding.

Antibody Fragment	**Antigen**	**Expression**	**Assay**	**Ref.**
mAb B1-7	ADH I	Intracellular in yeast	a	25
scFv 105	HIV-1	ER of COS cells	g,d	27,28
scFv Tac	Interleukin2	ER of Jurkat T cells	g	26,36
Fv D11	NGF	ER of COS and NSO cells	g	37
scFv anti-Rev	HIV-1	Intracellular in *E. coli*	b,d,g	33,34, 38,39
scFv 5, scFv 51	ErbB-2	ER	d,k	29
scFv 5	ErbB-2	ER (presence of NDF)	d,g	31
scFv anti-erbB2	ErbB-2	ER	d	30
scFv 259cyt	$P21^{ras}$	Mitochondria, nucleus and cytoplasm in *E.* coli	b,e	32,33, 40
scFv 259cyt	$P21^{ras}$	Colon carcinomas	c,h	41
scFv 259cyt	$P21^{ras}$	*Xenopus* oocytes	c	35
V_L(catalytic antibody Ab17E8)	L-NFMP ester	Soluble intracellular in *E.* coli	i	42,43
V_H and Fv(catalytic antibody Ab17E8)	L-NFMP ester	Soluble & inclusion bodies intracellular in *E. coli*	i	42,43
scFv F8	Anti-viral	Intracellular in transgenic plants	b,j	44,45
Fab(catalytic Ab1F7)	Oxabicyclic hapten	Soluble intracellular in yeast	i	46

In addition to the examples presented here, other intrabodies have been created and their global or specific effects have been determined. Table 1-1 summarizes all of the intrabodies found in literature in chronological order and the antigen that is recognized (antigen descriptions used in the table are presented in Appendix A). This table also includes the host and location of intrabody expression and the assay performed to determine the function. The assays are described in the table caption and are included to specify which intrabodies were shown to have global effects versus the assays completed that determined direct activity. Unfortunately, binding and kinetic constants were only determined for a few intrabodies that were catalytic.

The main obstacle in intrabody research is to produce stable folded antibodies in the reducing environment of the cytoplasm. Disruption of the native disulfide bonds in reducing environments has been shown to result in aggregation of antibodies and loss of activity.[3] Restructuring antibodies for a gain of sufficient folding energy could be used to compensate for the loss of the structural disulfide bonds and lead to viable expression in the cytoplasm.

Engineering Antibodies as Stable Folded Protein

In order to produce intracellular antibodies consistently, a number of researchers have addressed the destabilization of antibodies that occur in a reducing environment.[47-50] Conditions that prevail in the cytoplasm do not allow formation of the disulfide bonds that stabilize the β-sheets of the protein. This loss of folding energy disrupts the active conformation of the protein and results in poor antigen recognition. A few antibodies have been engineered as stable proteins without the stabilization of disulfide bonds. Methods such as site-directed mutagenesis, DNA shuffling and error prone polymerase chain reactions (PCR) have been used to produce disulfide-free antibodies that maintain antigen binding.[47,51,52] Unfortunately, only a few antibodies have been successfully engineered because a general method of producing disulfide-free antibodies has not been developed.

Unique Antibodies

The removal of a disulfide bond from an antibody has been accomplished by genetically engineering antibodies through random mutagenesis and/or rational design. These studies tend to use either naturally robust antibodies that can withstand the destabilization caused by removing a disulfide bond, or unique antibodies that are naturally missing a disulfide bridge in one of the variable domains. Antibodies with the natural deletion of one of the intrachain disulfide bonds are included in the human and mouse V_H and V_L sequences of the Kabat Database (http://immuno.bme.nwu.edu/, March 1996). In this collection there are 17 (0.5%) disulfide-less V_H chains and 18 (0.6%) disulfide-free V_L chains.[53] Caution must be used when studying these particular antibodies because these sequences were determined at the DNA level, and, therefore, do not guarantee the expression of a functional antibody. Nevertheless, many groups employ these proteins and have studied the alternative stabilizing forces of these unconventional proteins. The following section will discuss these engineered antibodies in detail by including the effects of the mutations on antigen recognition and protein stability.

Model Predictions for Effective Mutations

Steipe and coworkers have employed a rational approach to antibody design by determining common residues located in the framework region of aligned antibody sequences.[50] They predicted that introducing invariant amino acids that have been selected through evolution by the immune system will likely add stability to antibodies in which the sequences deviate from these 'ideal' sequences. Two different V_L domains engineered in this way showed an increase in protein stability.[42] Similar results were obtained for mutated V_H domains of a catalytic antibody.[43] The V_H domain of this catalytic antibody, Fv IcaH-501, contained five mutations, and the F_v isolated from the cytoplasm was shown to remain catalytic. The sufficient folding energy produced by the mutations was believed to compensate for the structural loss of the disulfide bridge in the reducing environment of the cytoplasm. Although this type of study has contributed to a general method for stabilizing antibodies, the applicability remains open to question.

Engineered Disulfide-Less Antibodies

Research in this field has supplied a few specific examples of engineered antibodies and has characterized the effects of introduced mutations. Table 1-2 summarizes the antibodies discussed in this section, and also includes the method used to remove the disulfide bonds, the nature of mutations at the cysteine positions (H22, H92, L23 and L88) and other mutations used to increase protein stability. The table also specifies any unusual traits for each antibody in order to highlight those proteins that naturally lack an intrachain disulfide bond or possess unusual intrinsic stability. The binding ability and protein stability of each antibody are presented in the Discussion of Engineered Antibodies in this chapter. The stabilities of the engineered antibodies are commonly compared by observing the effects of a denaturant on the protein folding and stability.

Stability Studies of Engineered Antibody Fragments

Experiments determining the energetic benefits for specific mutations made in an antibody can provide information to explain the intrinsic stabilities of specific antibodies possessing unusually stable folded conformations. Urea and guanidine denaturation experiments give insight into the equilibrium denaturation and stabilities of antibodies. Denaturant-induced unfolding is commonly followed through the spectroscopic properties of a protein such as tryptophan fluorescence. Equilibrium unfolding of antibody fragments can be a simple two-state process between native protein and completely denatured protein. More complex systems, however, can have multiple transitions between intermediate states that accumulate to significant levels from equilibria involving one native and one denatured domain or from interacting domains which are only partially unfolded. Unfortunately, antibodies with these elaborate folding states and stabilizing forces can not be completely characterized with these studies since typical quantitative treatments are based on simple two-state models that interconvert by cooperative transitions. The use of these denaturation studies to understand the effect of mutations on protein stability is included in the following section, and the results from the stability studies are also summarized in Table 1-3.

Table 1-2. Summary of engineered antibodies. Sequence numbering as described by Kabat *et al.*, 1987.

Antibody	**Unusual Traits**	**Mutation Method**	**H22**	**H92**	**L23**	**L88**	**Additional Stabilizing Mutations**	**Refs.**
McPC603	none	site-directed	C	C	C	C	P-H40-A S-H63-A A-H64-D S-H79-N I-H80-T P-L8-A A-L15-L S-L56-P N-L90-Q	50
			A	A	A	A		3
			Y	Y	Y	Y		3
			A	A	C	C		3
			C	Y	C	C		3
REI_v	Bence-Jones protein	site-directed	-	-	C	C		54
			-	-	V	C	Y-L32-H	54
ABPC48	naturally lacks V_H bond	site-directed and random and DNA shuffling	C	Y	C	C	N-H32-S K-H66-R	47,51
			C	C	C	C	N-H32-S K-H66-R T-L8-P	47
			A	V	A	V	N-H32-S K-H66-R T-L8-P	47
hu4D5-8	robust	site-directed	C	C	C	C		
			V	A	V	A		48
13	unique selection method for screening	error prone PCR	C	C	C	C	G-H10-S V-H48-I S-H52-G S-H55-R K-H75-T A-H93-V G-L51-D	52
03/01/01	naturally lacks V_H bond	site-directed	C	S	C	C	Q-H6-E	53
			C	C	C	C	Q-H6-E	53

Table 1-3. Denaturation studies of stabilizing mutations. [Urea] and [Gdn] concentration reflect the midpoint of unfolding from published plots. (ss) indicates a fragment with one intrachain disulfide bond, (ss^2) indicates two intrachain disulfide bonds, (-) appears if an intrachain disulfide bond is missing, and (--) shows a disulfide-free fragment. Data entries in a single row are matched to the respective scFv by superscript letters(^{a,b}).

Antibody	**V_H mutant**	**V_L mutant**	**[Urea]M**	**[Gdn]M**	**Ref**
McPC603					
V_L wt (ss)				0.80	50
V_L (ss)		Q-L79-E		0.65	50
V_L(ss)		N-L90-Q		1.05	50
V_L(ss)		A-L15-L		1.55	50
V_L(REI$_v$)					
V_L wt (ss)			3.9		54
V_L		C-L32-H	4.4		54
V_L (-)		C-L23-V C-L32-H	1.9		54
ABPC48					
ScFv wt (ss),(--)^a			2.8, 2.4^a	1.3	47,57
ScFv (ss^2)	Y-H92-C		5.6	1.7	47,57
ScFv(ss), (--)^a	K-H66-R		2.7^a, 3.8		47,58
ScFv (ss),(--)^a DsFv (--)^b	K-H66-R N-H32-S		3.2^a , 4.7^b	1.4, 3.0^a	47,58
ScFv (--)	K-H66-R N-H32-S Y-H92-V			~3	47
ScFv (ss^2)	K-H66-R N-H32-S	T-L8-P	6	~2.5	47
ScFv (--)	K-H66-R N-H32-S Y-H92-V	T-L8-P	3.9	4.10	47
4D5					
ScFv wt (ss^2)			4.8	1.65	47
ABPC48/4D5	**V_L(D5)**	**V_H(A48)**			
ScFv (ss^2) DsFv (ss^2)^a		K-H66-R N-H32-S		3.1, 3.4^a	47
03/01/01					
ScFv wt-SE (ss)			2.0		53
ScFvTras-SQ (ss)		E-H6-Q	3.2		53
ScFvTras-CE(ss^2)		S-H92-C	3.0		53
ScFvTras-CQ(ss^2)		E-H6-A S-H92-C	3.2		53

Discussion of Engineered Antibodies

Antibody McPC603

Mutagenesis. Monoclonal antibody McPC603 has been engineered using recombinant DNA techniques to study protein stability and to create higher-affinity antigen binding derivatives. The effects of the disulfide bond on expression of active protein were also explored and four mutants of the disulfide bridge were constructed. Plückthun and co-workers studied five derivatives of this antibody: F_v's in which all four cysteines were replaced by alanines, those in which all four cysteines were replaced with tyrosines, a Fab with alanines at H22 and H98 and a scFv with only a C-H92-Y replacement. The mutation C-H92-Y was included because this mutation is found in an antibody naturally lacking a heavy chain disulfide bond. Only this later mutation allowed scFv expression in the periplasm of *E. coli*; however, the scFv precipitated largely due to misfolding. This study therefore demonstrated the importance of disulfide bonds for the complete and correct folding of antibody fragments *in vivo* without additional stabilizing forces.[3]

Stability studies. Mutations at positions surrounding the disulfide bond of the V_L chain shown in Table 1-2 and 1-3 were chosen based on the identities of residues that were most common found at these positions in an assembly of sequences from an immunoglobulin repertoire.[50] The invariant residues of the sequence alignments signify potential stabilizing sites and the conserved regions are predicted to be in constant equilibrium with respect to any induced sequence changes from mutagenesis. The canonical sequence approximation states that Boltzmann's law gives the most probable distribution of amino acids at a specific position, and a statistical "free energy" can be calculated from the frequencies of observation. The amino acid frequency distributions were calculated for all the residues of the V_L domain of McPC603, and ten stabilizing point mutations that introduced the most common amino acid were introduced individually by site-directed mutagenesis. Six of these mutants possessed free energies of folding greater than the wt value and only two destabilized the light chain. Two stabilized mutants (N-L90-Q and A-L15-L) and one destabilizing mutant (Q-L79-E) were investigated further by guanidine denaturation and each behaved as expected. The other mutants listed in Table 1-2 are presented in a later section discussing the folding dependence on cis/trans isomerization of proline residues.

Antibody REI_v

Mutagenesis. The Bence-Jones protein REI_v provides a good example of the use of site-directed mutagenesis to engineer antibodies active in the reducing environment of *E. coli* cytoplasm. Frisch *et al.* constructed a fusion protein between the V_L domain of Ig REI_v and β-lactamase with a truncated leader sequence to confine the fusion protein to the cytoplasm.[54] Site-directed mutagenesis was used to remove the disulfide bond of the V_L domain by converting cysteine-L23 to valine and the loss of the disulfide bridge was compensated by introducing the stabilizing mutation Y-L32-H. Contrary to the wt REI_v fusion protein, the V_L mutant fusion protein was shown to accumulate in the cytoplasm.

Stability studies. Denaturation experiments verified the importance of the stabilizing L32 mutation used in the mutant V_L fusion protein.[54] This mutation compensated for the loss of the disulfide bond and allowed the complex to accumulate in the cytoplasm.

Antibody ABPC48

Mutagenesis to reintroduce disulfide bond. Plückthun and coworkers have restructured the folding of an antibody naturally missing a disulfide bond within the V_H chain. The levan (poly-β-2,6-D-fructose) binding monoclonal antibody (mAb) ABPC48 possessing a tyrosine at position H92 was first assayed for antigen binding by Rudikoff and Pumphrey.[56] Proba *et al.* constructed a scFv fragment of this antibody and reintroduced the disulfide bond in the heavy chain to show the extra stability that this crosslink added to the protein.[57] As expected for this unique antibody, refolding the disulfide-stabilized scFv had much lower refolding yields than the wt scFv, but ELISA results proved that both proteins possessed similar antigen binding abilities. The conformation of the naturally unpaired cysteine of H22 was also determined, and this residue appeared to deviate from the normal buried position within the β-sheet. Mass determination experiments showed that the *in vitro* refolded wt scFv was covalently linked to glutathione, which supported the notion that this side-chain was accessible to solvent and the redox reagents used in refolding. Model predictions suggested that this conformational change allowed for the formation of new hydrogen bonds and thereby compensated for the loss of free energy from the missing disulfide bond.

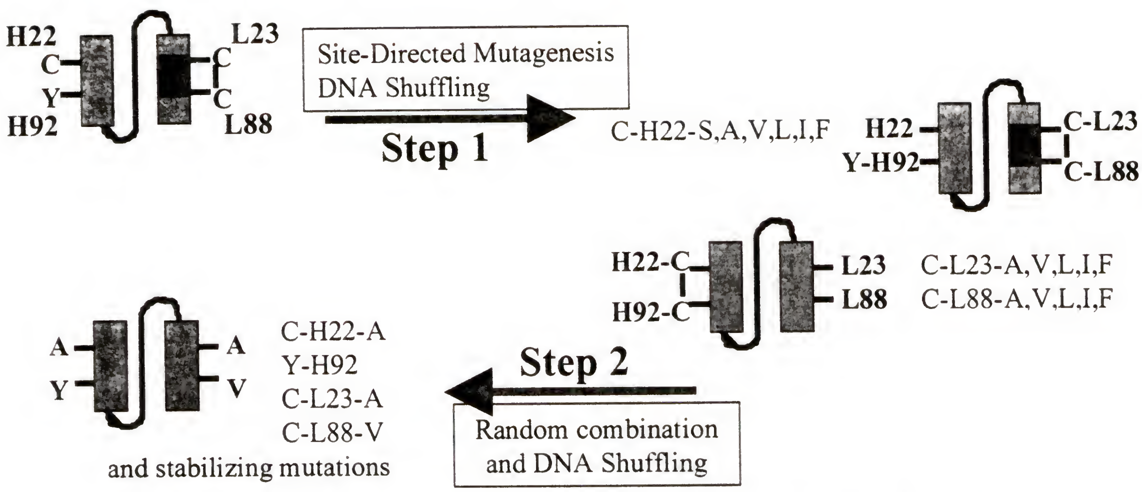

Figure 1-6. Removal of the light chain disulfide bond from scFv ABPC48 using site-directed mutagenesis and DNA shuffling.

Mutagenesis to remove the remaining disulfide bond from ABPC48.

Recombinant DNA techniques have extended the spectrum of mutations of this antibody beyond those somatic mutations produced by the immune system (Figure 1-6). Site-directed mutagenesis and DNA shuffling (step 1) of scFv ABPC48 produced two mutant libraries that were selected on the basis of antigen binding using phage display.[51] In one library, C-H22 (the unpaired cysteine of the V_H domain) was replaced with either Ser, Ala, Val or Leu and the natural mutation of Y-H92 was kept. The second library contained V_L domain mutants with Ala, Val, Leu, Ile or Phe at positions C-L23 and C-L88 paired with a V_H domain having a disulfide bond. The two libraries were randomly combined and submitted to DNA-shuffling and random mutagenesis (step 2) according to Stemmer (1994). Twelve clones produced correctly assembled scFv's, and three disulfide-free sequences were found to contain C-H22-A, C-L23-V, C-L88-A, and Y-H92 along with other random stabilizing mutations. While this mutant fused to phage coat protein demonstrated antigen recognition through ELISA studies, the protein could not be refolded *in vitro*, which directly demonstrated the importance of the additional stabilizing mutations for this antibody. After random mutagenesis, sequence analysis indicated the stabilizing mutation L-H66-R added similar stabilizing forces as the introduction of a disulfide bond. Ninety percent of human V_H chains contain an arginine at this position where it can ideally interact with D-H86. This study exemplifies the benefits of randomization (when the sample set is representative); however, this mutant theoretically could have been constructed by rational design if the researcher was fortunate enough to identify the key L-H66-R mutation.

Stability effects of the reintroduction of a disulfide bond. The gain of folding energy from the reintroduction of the missing disulfide bridge in the V_H chain of ABPC48 was studied. As shown in Table 1-3, this study verified the above average thermodynamic stability of the starting scFv (compare scFv wt (ss) and (--) and scFv Y-H92-C (ss^2)).[57] The flexible polypeptide linker of the wt scFv ABPC48 also appeared to affect the stability of this antibody.[51] Urea denaturation experiments showed the linker influenced the denaturing midpoints of the mutants in a range of 2 to 3 M urea (data not included in Table 1-3).

Stability studies on other mutations. Another study examined the highly stabilizing mutations (K-H66-R and N-H52-S) developed by the lab of Stemmer after analyzing results from DNA-shuffling of scFv ABPC48.[58] The single K-H66-R mutation had the most significant effect on scFv stability, and the stability gained from introducing both mutations was not additive. The influence of an interacting domain on the folding and/or stability of the other domain was also addressed. Stable folding of the

V_H domain was strongly influenced by the stability of the V_L chain, but the V_L domain was unaffected by the V_H chain.

Antibody hu4D5-8

This antibody introduces the concept that global stability is a prerequisite for disulfide removal.[48] ScFv 4D5 recognizes the extracellular domain of p185 (the oncoprotein of erbB-2) and possesses above average thermodynamically stability. Plückthun and co-workers reasoned that this robust antibody would allow the removal of the two disulfide bridges without the need for any additional stabilizing forces.

Mutagenesis. Mutations of scFv 4D5 were introduced to replace the cysteines participating in disulfide bonds with valine and alanine in each chain. These substitutions maintain the steric sizes similar to a disulfide bridge, and the hydrophobicity of these two amino acids is compatible with the hydrophobic interior of the antibody domains. To assess the functionality of these mutants, K_D values were collected for the wild type (194 pM) and mutant (121 pM). The virtually identical K_D values were consistent with the retention of native structure by the mutant. Urea denaturation studies showed that the mutant was more stable than the reduced wt scFv (midpoint denaturation of about 3.1 M and 2.7 M urea) but less stable than the oxidized wt scFv (4.8 M urea).

It was speculated that this stable mutant could provide a framework to act as a surrogate for other antibody functionality. The authors predicted that previous success in CDR loop grafting into this antibody proves the mutant to be a promising framework for grafting different variable loop specificity.

Stability studies of a ABPC48 and hu4D5-8 hybrid. Hybrids of the two scFv's were constructed to allow the stable V_L domain of scFv 4D5 to compensate for the weak

V_L domain of scFv ABPC48.[47] As shown in Table 1-3, this hybrid with both disulfide bonds (scFv ABPC48/4D5 (ss^2)) exhibited dramatically increased stability as shown by a midpoint value of 3.1 M urea compared with values from either of the parent scFv's (scFv ABPC48 (ss^2), 1.7 M and scFv 4D5(ss^2), 1.65 M). This hybrid illustrates a simple method to increase stability with dramatic results; however, the product of hybrids such as these are likely to have unpredictable and perhaps even unusable antigen recognition.

Antibody scFv13

Mutagenesis. Winter and co-workers have used error prone polymerase chain reaction (PCR) to synthesize mutants of scFv 13 in order to mutate a robust immunogloblin that has a natural stability capable of compensating for the loss of intrachain disulfide bridges (Figure 1-7).[52] A key step for using error prone PCR is to establish a suitable screening process. This particular study has the advantage of a convenient screening because scFv13 recognizes nonfunctional dimers of β-galactosidase (AMEF). ScFv13 binding produces active tetramers of AMEF, and the presence of this tetramer allows for growth on selective media. The antibody activation of the tetramer is directly proportional to the concentration of functional scFv, and therefore cell growth directly reflects correctly folded and active mutants. Four rounds of mutation and selection yielded the mutant scFv 13R4 and this scFv recovered the functionality of AMEF to that of normal β-galactosidase. ELISA showed a 2.5 higher signal for scFv13R4 compared to the wt scFv13. *In vitro* activation of AMEF by scFv13R4 was also more than 1000 fold stronger with tenfold less protein. Analysis of the mutant scFv 13R4 revealed that the disulfide bonds were reduced in the cytoplasm but the protein remained folded due to the stabilizing mutations introduced. This is a powerful example of the ability of antibodies to compensate for structural changes. Unfortunately this screening method is extremely limited.

Round	**Mutation**
1	K-H75-T
2	G-H10-S
3	V-H48-I
	S-H52-G
	S-H55-R
	A-H93-V
4	G-L51-D

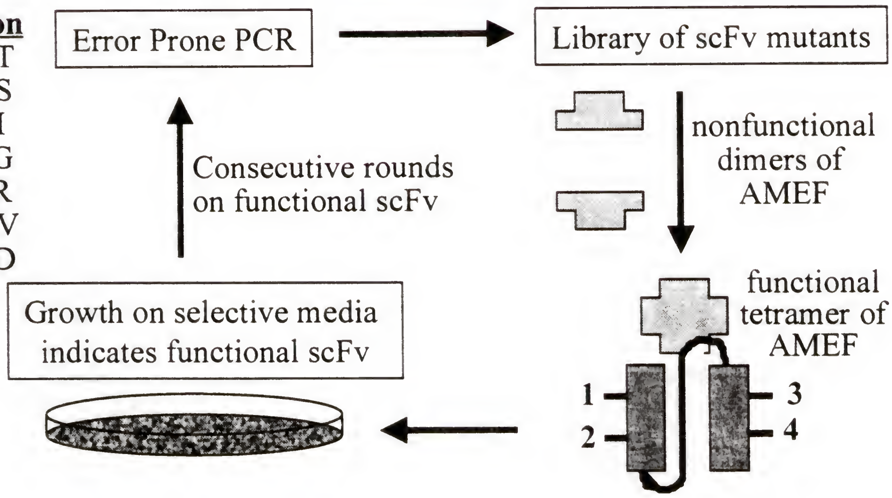
Error Prone PCR
Library of scFv mutants
nonfunctional dimers of AMEF
Consecutive rounds on functional scFv
functional tetramer of AMEF
Growth on selective media indicates functional scFv
1
2
3
4

Figure 1-7. Mutagenesis of scFv13, and selection of functional disulfide-less mutants expressed inside bacteria.

Antibody 03/01/01

Mutagenesis. Plückthun has also examined the effects of additional mutations within scFv 03/01/01 as a means of improving folding stability. The scFv of the mAb 03/01/01 recognizes a musk odorant, 6-acetyl-1-isopropyl-2,3,3,4-tetramethyl-indane.[53] This antibody naturally contains a serine at position H92 in the V_H chain and therefore lacks the disulfide bridge in this chain. A rational prediction from sequence alignments targeted the Q-H6-E mutation as a potentially stabilizing substitution. The presence of glutamine or glutamate at this position is represented equally in both human and mouse sequences. This is striking because the burial of the charged glutamate in the core of a protein tends to be destabilizing. The effects of this alteration as well as the reintroduction of a disulfide bond in the heavy chain of the scFv were explored. Results in Table 1-3 indicate that either reconstruction of the disulfide bond or introducing the glutamate led to an increase in stability and a ten-fold increase *in vitro* refolding yields. On the other hand, combining both changes brought little additional stabilization. This result was explained by the authors in terms of a hydrogen bonding network. Serine at H92 is predicted to be integrated into a conserved hydrogen bonding network spanning the core of the variable domain. The two different side chains at H6 are suggested to assume different conformations in order to satisfy their individual hydrogen bonding requirements. This hypothesis explains the benefits of introducing a glutamate at H6. Furthermore, the amino acid residing at this position also dictates the amino acid requirements for positions H7-H10. This study, therefore, shows the crucial role the positions within framework-1 possess in stabilizing this scFv by interacting with the buried serine residue.

Guidelines to Increase Stability in Engineered Antibodies

Insight into Folding Pathway from Denaturation Curves

Efforts to remove the folding requirement for disulfide bonds to stabilize antibody structures and to understand the changes produced by specific mutations have contributed some guidelines for antibody engineering. Denaturation curves have been used to develop a classification system for the stability of protein domains as they occur in antibody fragments. The effects of some mutations have also yielded insight towards the understanding of the kinetics of folding. These particular advancements are the focus of the following section.

Models derived from stability data

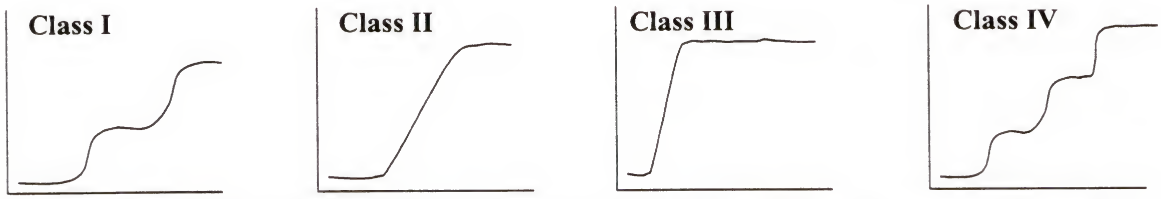

Figure 1-8. Depictions of the denaturing curves expected from scFv fragments of each class. The Y-axis is the fraction of denatured protein and the X-axis is the concentration of denaturant.

Wörn and Plückthun discussed the stabilities of numerous mutants (presented in Table 1-3) of scFv ABPC48 (A48), scFv hu4D5-8 (4D5) and hybrids of the two proteins.[47] Data from these studies gave rise to a classification system for identifying the folding pathway of scFv fragments by examining the pattern of denaturation curves. Once an scFv is classified, predictions can be made as to the most logical route to stabilizing the scFv. The authors used the mutants to organize three of the four classes described above for stability and unfolding pattern predictions. Denaturation curves typical of scFv fragments for each class are illustrated in Figure 1-8.

Class I scFv's have one domain with significantly higher stability than the partner. The denaturation curve of this protein will have a visible step in the unfolding curve (two transitions). Those scFv's in class II have a stable interface between the domains which increases the overall stability of the weaker domain so that it equals that of the stronger domain. This curve will contain a single transition but it will appear gradual due to the two domains unfolding sequentially. Class III consists of two domains of relatively low intrinsic stability linked together by a very stable interface. This curve appears as a steep single transition and the scFv construct would denature at a much higher denaturant than the independent domains. A fourth class, not observed in this study, could include an scFv with two intrinsically stable domains connected by a relatively weak interface. It is predicted that this curve would have multiple steps for the interface unfolding followed by each domain, with the relative stability dictating the appearance of each transition. After classifying an scFv, knowledge about the areas of structural weakness helps to engineer more stable derivatives.

One particular mutant illustrates how valuable this classification system can be in antibody design. The scFv ABPC48 that was included in Table 1-2 (ABPC43 A-H22, V-H92, A-L23 and V-L88) and in Table 1-3 scFv ABPC43 with the stabilizing mutations K-H66-R, N-H32-S and Y-H92-V produced two transitions in the denaturation curve.[47] This type of curve placed the scFv in Class I and indicated that one domain was intrinsically more stable than the other. It was known that the V_L domain of this antibody was less stable than the V_H domain and an increase in stabilization occurred when T-L8-P mutation was introduced into the scFv. Adding this mutation produced an scFv that exhibited a single transition in chemical denaturation experiments and the midpoint of the transition curve was shifted to a higher denaturant concentration. Including the T-L8-P mutation in the scFv (--) K-H66-R, N-H32-S also affected the denaturation curve by increasing the denaturant midpoint.

General Considerations to Increase Proper Folding

Interface interactions between domains

Antibody research has contributed insight into the folding behavior of multimeric proteins by exploring the folding of antibody domains, the association of the chains at the interface and the folding of various covalently linked forms. A better interaction at the interface between the two variable domains helps stabilize the scFv fragment and encourages correctly folded protein.

Proline cis/trans-isomerization

McPC603. A recent study has used antibody McPC603 as a model and looked at the folding and assembly of the F_v McPC603 and compared it to the scFv form.[59] The F_v fragments used in this study contained eight stabilizing mutations dispersed over both chains, and the folding pathway of each chain of the F_v was investigated. While the data were not conclusive, they suggested that two parallel folding pathways existed for the V_H domain and that the V_L domain did not affect the refolding kinetics of the V_H domain. The V_L also refolds through a mutiphasic path that is slowed by the proline *cis/trans*-isomerization of the seven proline residues in this chain. Moreover, the *cis/trans*-isomerization at P-L95 is rate-limiting for the assembly of the Fv fragment. This was confirmed by the effect of peptidyl-proly *cis/trans*-isomerase (PPIase) which produced the *cis*-ProL95 and accelerated the assembly of the heterodimer. While the overall folding behavior of the Fv and scFv fragments is similar, refolding of the scFv includes an added kinetic trap from forcing the domains to close together with a linker during refolding. Prematurely associated V_L and V_H domains can form an intermediate before the *cis*-ProL95 has formed; however, this kinetic trap is reversible and only rate-limiting for fast folding of short-term denatured protein (long-term refolding of scFv's fragments was unaffected).

ScFv hu4D5-8. The folding abilities of four disulfide bridge mutants of scFv 4D5 having either no disulfide bridges, one in either chain, or one in both chains were determined.[60] In all four scFv's, the refolding was limited by the slow isomerization of P-L95 to the *cis*-conformation. The dependence of folding on the stability of the scFv domain interface was also explored by mass spectrometry. Domains retaining the disulfide bridge were able to fold in a stable form independent of interface stability, but the disulfide-less scFv required a stable, native interface between the two domains.

The Need for a General Method

Prior efforts to transform antibodies into intracellular proteins, while successful in some cases, have not led to a generally-applicable method. Many of the studies required uncommon starting antibodies with natural deletions of disulfide bonds or exceptionally high stability. Other studies relied on selection methods for disulfide-less mutants that cannot be generalized. The need for a general method to convert any antibody into a disulfide-less folded protein remains an important issue and an undeveloped field.

Introduction to Research Goal

The long-term goal of this project is to develop a general strategy that will allow engineered antibodies to fold without disulfide bonds and then to use these variants in reducing environments. A model system using the catalytic antibody scFv 43C9 was used initially to develop this strategy. In the future, it should be possible to apply this strategy to an antibody that binds the intracellular domain of p185 (the oncoprotein produced by erbB-2). This would broaden the applicability of antibodies as chemotherapeutic agents in this case by targeting the mitogenic signaling cascade found in breast tumor cell proliferation.

The Model System scFv 43C9

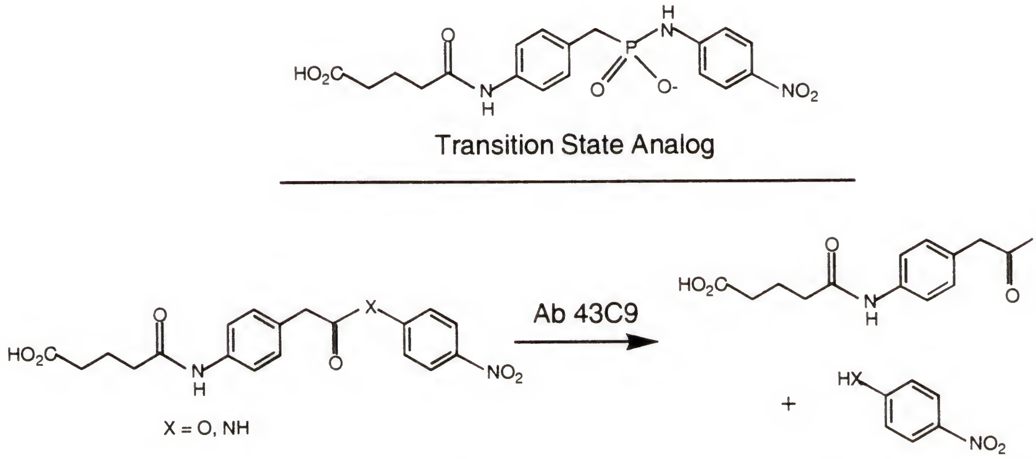

Figure 1-9. The transition state analog (TSA) against which mAb 43C9 was raised. Antibody 43C9 catalyzes the ester and amide hydrolysis by lowering the energy barriers of transition states.

The catalytic antibody scFv 43C9 is an excellent candidate for reengineering.[61] This scFv has been well characterized with regard to binding behavior for a large series of ligands.[14,15,16,62-65] This antibody recognizes a phosphonate antigen that is a transition state analog of ester and amide hydrolysis (Figure 1-9). Mutagenesis studies have mapped the binding pocket and key residues participating in the catalytic mechanism.[15,62,66-68] Ester and amide hydrolysis involves nucleophilic attack of an antibody-bound substrate by histidine-L91[67], and the mechanism is shown below (Figure 1-10). In addition, a number of site-directed mutants have been created and their binding behavior has been probed by fluorescence techniques. A computer model of the scFv structure was created and the x-ray crystal structure was published recently.[14,68] Finally, this antibody does not possess exceptional natural stability and both of the normal intrachain disulfide bonds are present. Taken together, these attributes make 43C9 an excellent starting point for trying to develop a general method of converting any antibody into a stable derivative that is active under reducing conditions.

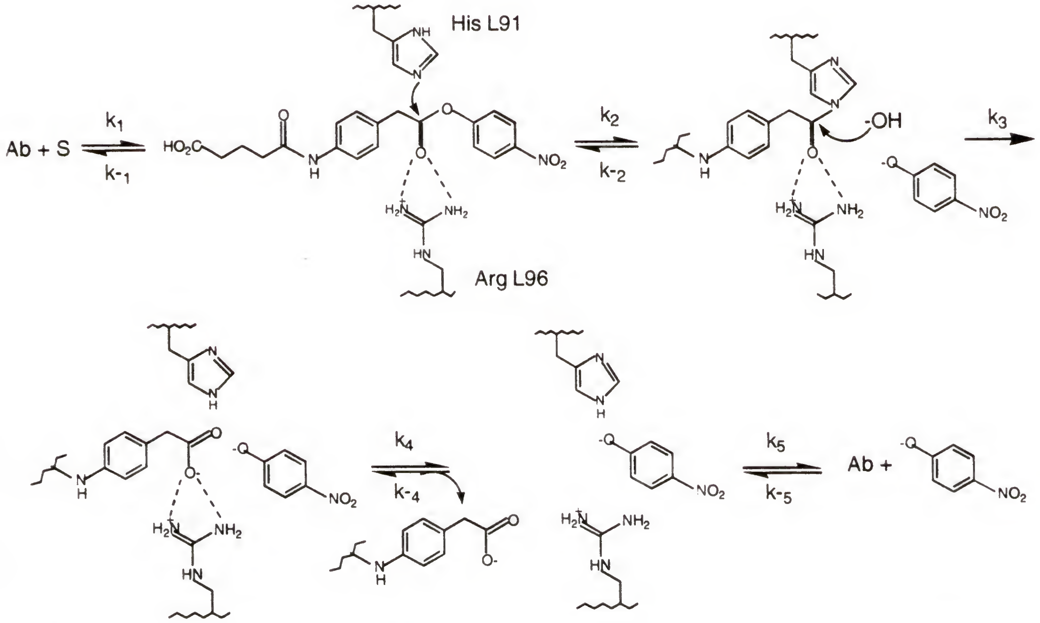

Figure 1-10. The Ab 43C9 catalyzed ester hydrolysis mechanism from mutagenesis studies on active site residues.

Plan for Reengineering

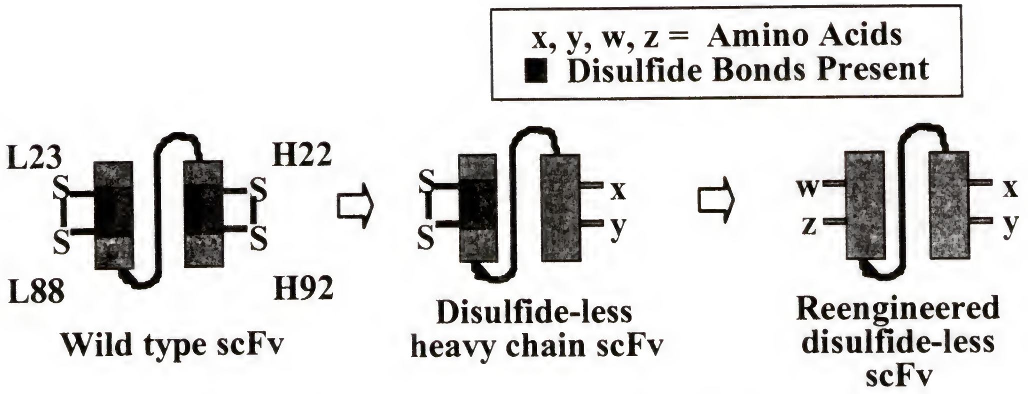
x, y, w, z = Amino Acids
■ Disulfide Bonds Present
L23
H22
S
S
S
S
L88
H92
Wild type scFv
S
S
x
y
Disulfide-less heavy chain scFv
w
z
x
y
Reengineered disulfide-less scFv

Figure 1-11. Strategy for removing the disulfide bonds.

As in other antibodies, two intrachain disulfide bonds exist in the conserved framework region of scFv 43C9. Replacing the cysteines in this conserved region would not be expected to affect the binding ability if the overall structure of the scFv is maintained. Figure 1-11 illustrates the plan for removing both disulfide bridges from scFv 43C9, although this method has only been successful for the removal of the V_H disulfide bond. Each disulfide bond was targeted individually in scFv 43C9, resulting in a pool of mutant domains that were paired with a wild-type partner. The process used to produce and screen for disulfide mutants that retained native structure is presented in Figure 1-12. Dr. Jon Stewart performed this work. A PCR strategy was used to randomly replace all three bases of the cysteine codons (H22 and H92 or L23 and L88) to yield a library of random amino acid substitutions at these positions (Figure 1-12, step 1). Complete scFv genes were reconstructed from the library, then this pool was cloned into bacteriophage λ vectors designed to express functional scFv's in λ plaques (Figure 1-12, step 2).[69] Each plaque expressed only a single scFv variant, and the final library size was efficient to cover all possible amino acid combinations at the positions initially occupied by the two cysteines. One important improvement to the published method was to perform the PCR amplification from a template in which the cysteine codons of in the scFv were replaced with alanines since an F_v fragment with these mutants were shown to be nonfunctional by Plückthun and co-workers.[3] It was predicted that using this gene as the template would make the unavoidable "carryover" from the template DNA into the library expressed in λ plaques (*ca.* 5% of the total) non-functional mutants. If this carryover had been the wild-type scFv, a large number of positives would overwhelm the subsequent screening.

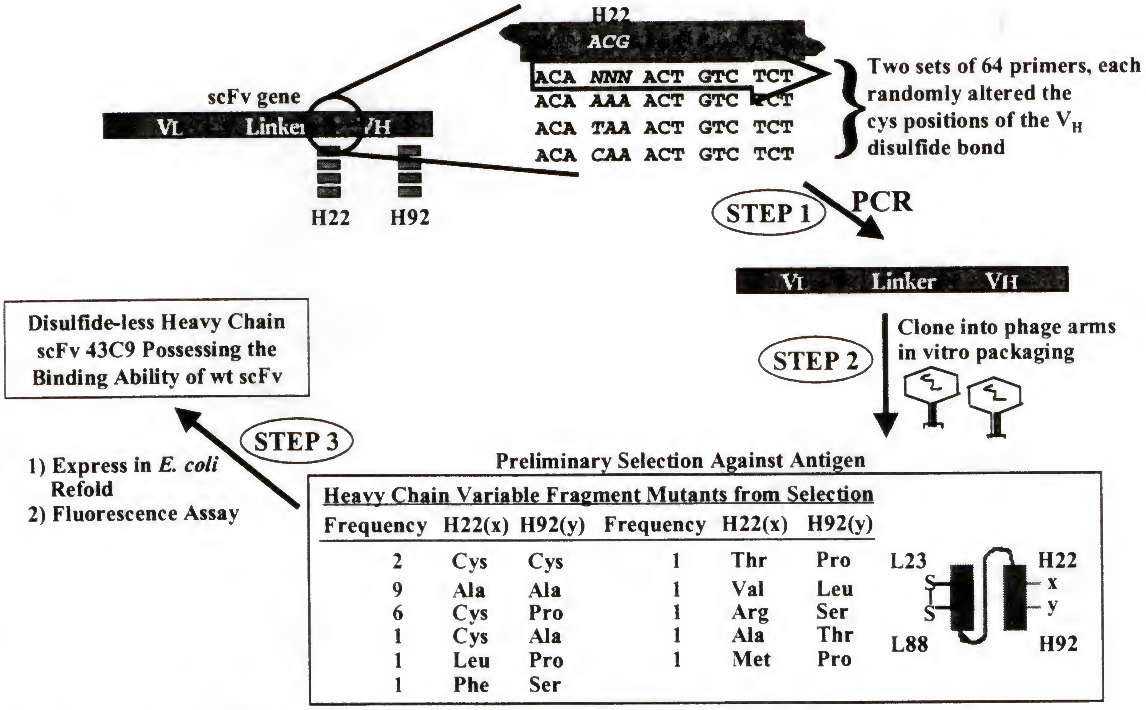
H22
ACG
ACA NNN ACT GTC TCT
ACA AAA ACT GTC TCT
ACA TAA ACT GTC TCT
ACA CAA ACT GTC TCT
Two sets of 64 primers, each randomly altered the cys positions of the VH disulfide bond
scFv gene
VL Linker VH
H22 H92
STEP 1
PCR
VL Linker VH
STEP 2
Clone into phage arms in vitro packaging
Disulfide-less Heavy Chain scFv 43C9 Possessing the Binding Ability of wt scFv
STEP 3
1) Express in E. coli Refold
2) Fluorescence Assay
Preliminary Selection Against Antigen
L23
S
S
L88
H22
x
y
H92

Heavy Chain Variable Fragment Mutants from Selection

Frequency	H22(x)	H92(y)	Frequency	H22(x)	H92(y)
2	Cys	Cys	1	Thr	Pro
9	Ala	Ala	1	Val	Leu
6	Cys	Pro	1	Arg	Ser
1	Cys	Ala	1	Ala	Thr
1	Leu	Pro	1	Met	Pro
1	Phe	Ser			

Figure 1-12. Procedure for site-directed mutagenesis of each scFv domain.

Table 1-4. Primers used to mutate scFv 43C9.

Primer	**Sequence (5' to 3')**
H22 Mutation	AGC CTA TCG ATC ACA NNN ACT GTC TCT GGG
H92 Mutation	GTA ACC ATA TGA GAC NNN GTA ATA CAT GGC

Once the library of λ plaques had been created, it was plated on a lawn of *E. coli* cells. A nitrocellulose filter soaked with isopropylthiogalactoside was overlaid, and scFv's expressed in each plaque adhered to the nitrocellulose in a spatial pattern that reproduced the locations of the plaques. The scFv's bound to nitrocellulose were exposed to the phosphonate antigen covalently linked to bovine serum albumin that was also labeled with digoxigenin. Those scFv's capable of binding antigen localized the labeled BSA to their locations, and this material was detected by a chemiluminescent assay.[69] Plaques showing a positive signal were purified (two rounds), and the scFv genes were recovered in plasmids by superinfection with M13 helper phage R408. The relevant portions of the scFv gene were sequenced to determine the amino acids that had replaced cysteine positions. Dr. Jon Stewart applied this process to both the V_H and V_L disulfide bonds of scFv 43C9. These experiments yielded eleven unique V_H mutants, all but one of which lacked a disulfide bond; however, the V_L library consisted of scFv's that maintained the disulfide bond.

These preliminary experiments demonstrated that the removal of the V_L disulfide bond from scFv 43C9 will be a challenging prospect. However, mutation of the V_H cysteines produced many interesting mutants that appeared to have some affinity to the antigen. Unfortunately, preliminary attempts by Dr. Jon Stewart to express the V_H disulfide mutants using a procedure that was successful for wt scFv 43C9 produced only misfolded aggregates of protein called inclusion bodies. This required an investigation of other possible expression and isolation methods.

Discussion of Methods for Antibody Production

The search for a new expression and isolation system to produce the V_H mutants as soluble scFv's for binding and stability assays encompassed most of the methods presented in the following sections.

In Vivo Protein Folding

Researchers have hunted for valuable artificial expression systems to produce antibodies at low cost and in few steps.[70-75] Numerous Fab and scFv fragments have been expressed from *E. coli* in good yields of active protein.[7] Expression of a leader sequence with the antibody allows proteins to be channeled from the cytoplasm to the periplasm of *E. coli*. Upon passing into the periplasm the leader peptide sequence is specifically cleaved by inner-membrane-bound signal peptidase. The correctly folded antibody is then secreted from the bacteria through the outer cell membrane. Expression systems such as these are highly dependent on the promoter strength of the expression plasmid. Strong expression systems producing high concentrations of antibodies can lead to aggregation into inclusion bodies during folding in the periplasm. A balance between the need for an efficient over-expression system and the synthesis of correctly folded protein prompted efforts to modify the cellular mechanics of *E. coli*.

The complex cellular machinery involved in native disulfide bond formation in the periplasmic space of *E. coli* has recently been unveiled. The discovery of six genes encoding for cell envelope proteins has prompted a search to characterize the function of these proteins.[76] A thioredoxin-like enzyme (DsbA) is the major catalyst for disulfide bond formation and possesses some isomerase activity.[77] DsbA is re-oxidized by a cytoplasmic inner-membrane protein (DsbB) and is recycled for catalysis. Intermediates with non-native disulfide bonds formed along the folding pathway are isomerized by an oxidoreductase (DsbC). This system includes other redox proteins (DipZ and thioredoxin) that maintain a reduced state in the oxidative environment of the periplasm needed for DsbC activity.[78] DsbA and DsbC play a balanced role where the efficient DsbA forms disulfide bonds efficiently and DsbC reorganizes the mismatched bonds.[79]

The machinery of the periplasm produces an environment similar to those found in the secretory pathways of eukaryotic cells. Georgiou and co-workers explored the possibility of introducing eukaryotic protein disulfide isomerases (PDI) into the periplasm of *E. coil* to improve the processing of misfolded protein.[77] PDI possesses cysteine oxidoreductase activity and behaves as a chaperone and an antichaperone in eukaryotic cells. Incorporation of PDI into *E. coli* devoid of DsbA resulted in catalysis of disulfide bond formation; however, this strain did not show increased ability in isomerization of misfolded intermediates.

Bacterial strains conducive to intracellular disulfide bond formation have also been produced by manipulating the levels of thioredoxin reductase (trx) levels in the cytoplasm. The mechanism preventing cytoplasmic disulfide bonds has been shown to involve trx.[80] Mutant *E. coli* strains not carrying the gene for this enzyme were shown to express cytoplasmic proteins stabilized by disulfide bonds. Winter and coworkers have incorporated strains with *trx* deletions in the expression of cytoplasmic antibody mutants as described earlier in Chapter 1.

In Vitro Refolding Methods for Antibody Fragments

While native secretion systems or *in vivo* folding are of unparalleled convenience, many antibody mutants require specific folding conditions supplied best by *in vitro* folding methods. Typically the protein is over-expressed as a non-functional aggregate which is processed into functional protein by first completely unfolding inclusion bodies in a reducing and denaturing environment. The unfolded antibody fragments can then be refolded by introducing a redox reaction for disulfide bond formation and a renaturation buffer. Conditions favoring the correct pairing of cysteine residues and complete folding have been intensively explored.[48,57,58,81,82] Specific redox reagents, detergents, folding temperature, protein concentrations and reaction times have been optimized for various antibody fragments. Research in these areas has offered guidelines for agents or conditions helpful in protein folding; however, each antibody construct requires optimization of these parameters. Expensive redox reagents and stabilizing agents also complicate the use of *in vitro* folding for repetitive protein production.

Ohtsuka and coworkers demonstrated an alternative method to alleviate the expense of refolding inclusion bodies.[83] They developed a procedure to refold inclusion bodies using a his-tagged scFv anchored on a Ni(II) solid support. The immobilized unfolded scFv can be refolded by passing renaturation buffers through the column. The small (1-2 mL) column volume allows for refolding with minimum use of expensive reagents.

Tailoring a procedure for folding antibody fragments *in vivo* or *in vitro* is a common task for most researchers using antibody constructs. Choosing the appropriate host and induction conditions or the optimized conditions for *in vitro* refolding is a process that was investigated for the antibody constructs used in this project.

Identification of Functional and Stable V_H Disulfide-less Mutants

After the appropriate method for producing the V_H disulfide-less mutants was established, the eleven 43C9 V_H mutants isolated from the preliminary screening were tested for binding ability and stability. Identification of the V_H mutants that most closely resemble wt scFv 43C9 binding and stability will provide a guide into successful mutations that produce a disulfide-less V_H domain.

Biological Application

Role of ErbB-2 in Cancer

The long-term goal of this project is to develop an intracellular antibody that interferes with mitogenic signaling in breast and ovarian cancers. To begin this process, the monoclonal antibody PN2A was selected. This antibody was raised against the peptide antigen, KTAENPE-pY-LGLDVPV.[84,85] This tyrosine-phosphorylated peptide is derived from the C-terminal tail of the intracellular domain of p185 that undergoes autophosphorylation.

p185 is an oncoprotein produced from the overexpression and/or amplification of erbB-2 in tumor cells.[84] This transmembrane protein has sequence identity to the epidermal growth factor receptor (EGFR) present in normal cells. EGFR is a transmembrane protein with an extracellular binding site for the epidermal growth factor (EGF). Binding of the hormone triggers the activation of the intracellular domain housing a receptor tyrosine kinase (RTK) core. This intracellular domain possesses a kinase core homologous to other proteins of the tyrosine kinase family.[86] This core contains the binding site for an ATP and a phosphate acceptor protein.[87,88] Extending from the C-terminal end of this domain is a peptide tail containing four tyrosine sites involved in self phosphorylation with the kinase core.[86] The tyrosine autophosphorylation site at position 1248 (Y(p)1248) participates in the mitogenic mechanism for cell proliferation.[84,89]

The 185 kDa oncoprotein, p185, is a truncated version of the EGFR. p185 is found in much larger populations than the EGFR, and EGF binding to the extracellular domain is not required for activation.[90,91] The intracellular domain of p185 contains the phosphorylated tyrosine (Y(p)1248) involved in the mitogenic cascade, and thereby, retains the intrinsic tyrosine kinase activity frequently found in human cancer.[92] A monoclonal antibody that specifically recognizes Y(p)1248 has been isolated by Stern and DiGiovanna et *al.*[84,85,90,92-94] Introduction of the disulfide-less derivative of PN2A into cancer cell may allow selective binding to the intracellular Y(p)1248 of p185 and the disruption of mitogenic signaling in the tumor cells.

CHAPTER 2
EXPRESSION AND ISOLATION OF ANTIBODY FRAGMENTS

The benefits of using antibody fragments in biological systems brought a need for methods to produce these proteins in high concentrations and in active folded forms. Bacterial and yeast systems are common sources for antibody fragment over-expression; however, the ability to express active protein depends heavily on stability. Antibody fragments and mutants of antibodies typically lack the stabilizing forces and physical constraints provided by the complete, wild type monoclonal antibodies. Research in re-engineering antibody structure has generated a need for reliable systems to consistently synthesize active proteins.

Strategies to Isolate Correctly Folded and Active scFv 43C9

In Vivo Expression in Bacteria Strains

An expression and isolation procedure for correctly folded scFv fragments of the catalytic antibody 43C9 and disulfide-less mutants was developed. A system was first selected that produced a large amount of soluble protein for the wt scFv. This was necessary because the mutants of scFv 43C9 were predicted to produce significantly less protein using the same isolation procedure due to their instability and lack of disulfide bond rigidity. The first option explored was to secrete active scFv's from bacteria. The wt scFv 43C9 has been produced this way in the laboratory of Dr. Benkovic.[7,61] While this was successful for the wild-type protein, the less stable disulfide-less mutants required a different approach.

Expression of wt scFv 43C9

General procedure for wt 43C9. As a model for scFv 43C9 mutants, the standard procedure for the isolation of wild-type (wt) scFv 43C9 was performed.[7] The scFv 43C9 was expressed in the periplasm of *E. coli* using a *pelB* leader sequence and under the control of a bacteriophage T3 promoter. The *E. coli* strain BL21(DE3) was cotransformed with the expression plamsid pJS118 and a second plasmid (pTG119) supplying the T3 RNA polymerase under control of the *lacUV5* promoter (Figure 2-1). This promoter allowed for modest expression into the periplasm, and the low concentration of scFv avoided aggregation of the antibodies into inclusion bodies. The culture was induced with isoproplythiogalactoside (IPTG, final concentration of 1 mM), and the scFv was secreted from the leaky outer membrane of the periplasm into the culture media. The functional scFv was then obtained from the media by removing the cells and concentrating the media by ultrafiltration. The antibody was then purified by chromatography on a 21 x 250 mm polyaspartic acid cation-exchange column (PolyCAT-A, Nest Group) using an FPLC (Pharmacia) system. This column was pre-equilibrated with 40 mM Na-MOPS, 1 mM calcium acetate, pH 6.3. The antibody was loaded and then eluted with a linear gradient from the equilibration buffer to 40 mM Na-MOPS, 25 mM calcium acetate, pH 7.5 (total volume 750 ml at 4 mL/min). Eluted fractions containing scFv 43C9 were identified by molecular weight (using SDS-PAGE), combined, concentrated to 1 mL and dialyzed into a working buffer (50 mM HEPES-Cl, 75 mM sodium chloride, pH 7.5). The yield of scFv 43C9 was determined from an absorbance measurement at 280 nm ($\varepsilon^{280} = 48{,}500$ L/mol·cm)[7] and was typically 375 µg per liter.

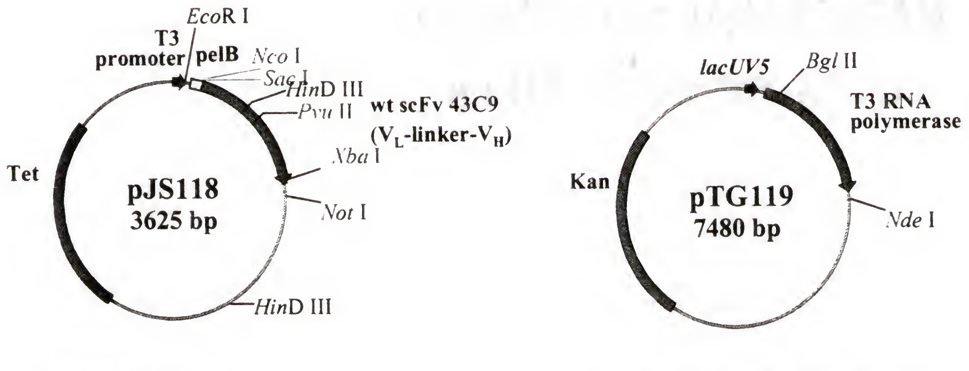

Parent vector: p4.1
Parent insert (pelB+scFv)
pelB leader is not codon optimized
constructed by Dr. J. Stewart

Cotransformed into BL21(DE3) to
provide a T3 RNA polymerase

Figure 2-1. Plasmid constructs of pJS118 and pTG119.

Mutant over-expression. While the methodology described above was successful for the wt scFv 43C9, studies by Dr. Jon Stewart showed that derivatives in which a disulfide-less V_H chain was paired with a wt V_L chain were not secreted into the media. An alternate expression and purification system therefore had to be designed to accommodate these mutants, which were prone to inclusion body formation.

Tools needed to design an alternate synthesis of scFv 43C9

Designing a procedure for expressing and isolating mutant scFv's required a method to track the production of the scFv. Western blots are commonly used to identify protein separated on the basis of molecular weight by SDS-PAGE. While an antiserum against the Fab 43C9 was available, the low titer made it difficult to detect moderate protein expression reliably. A C-terminal *c*-myc peptide (REQKLISEEDLN) was appended to the scFv for detection by a commercially available antibody (Figure 2-4). It is generally observed that the *c*-myc tag has little effect on scFv fragments.[55] Attempts to express scFv 43C9 with the *c*-myc tag were also completed in order to use a BIACORE Optical Biosensor to determine scFv ligand binding. However, the success of fluorescence quenching experiments to determine scFv ligand binding eventually led us to abandon efforts to optimize the expression of scFv 43C9 with a *c*-myc tag.

Searching for an *In Vivo* Protocol for scFv 43C9 Mutants

The lack of mutant protein secretion into the media suggested an accumulation of the protein in the periplasm or cytoplasm as either soluble protein or insoluble inclusion bodies. The location and solubility of wt scFv 43C9 under various promoter strengths was therefore explored.

Attempts to directly produce soluble wt 43C9 scFv/*c*-myc and scFv/*c*-myc/his$_6$.

The first expression system tried was one that used a modest T3 promoter to express the scFv in low levels in hopes of yielding soluble protein in the periplasm. Plasmid pJAT3 was constructed to express the scFv with a *c*-myc tag (Figure 2-2), and pJAT5 was created to express the scFv with a c-myc-his$_6$ tag under the control of a T3 promoter (Figure 2-3). Plasmid pJAT5 was constructed by replacing the *c*-myc tag of pJAT3 with the *c*-myc-his$_6$ tag insert. Annealing the four fragments of single stranded DNA shown in Figure 2-3 produced the *c*-myc-his$_6$ insert that contained cohesive *Xba*I and *Not*I ends.

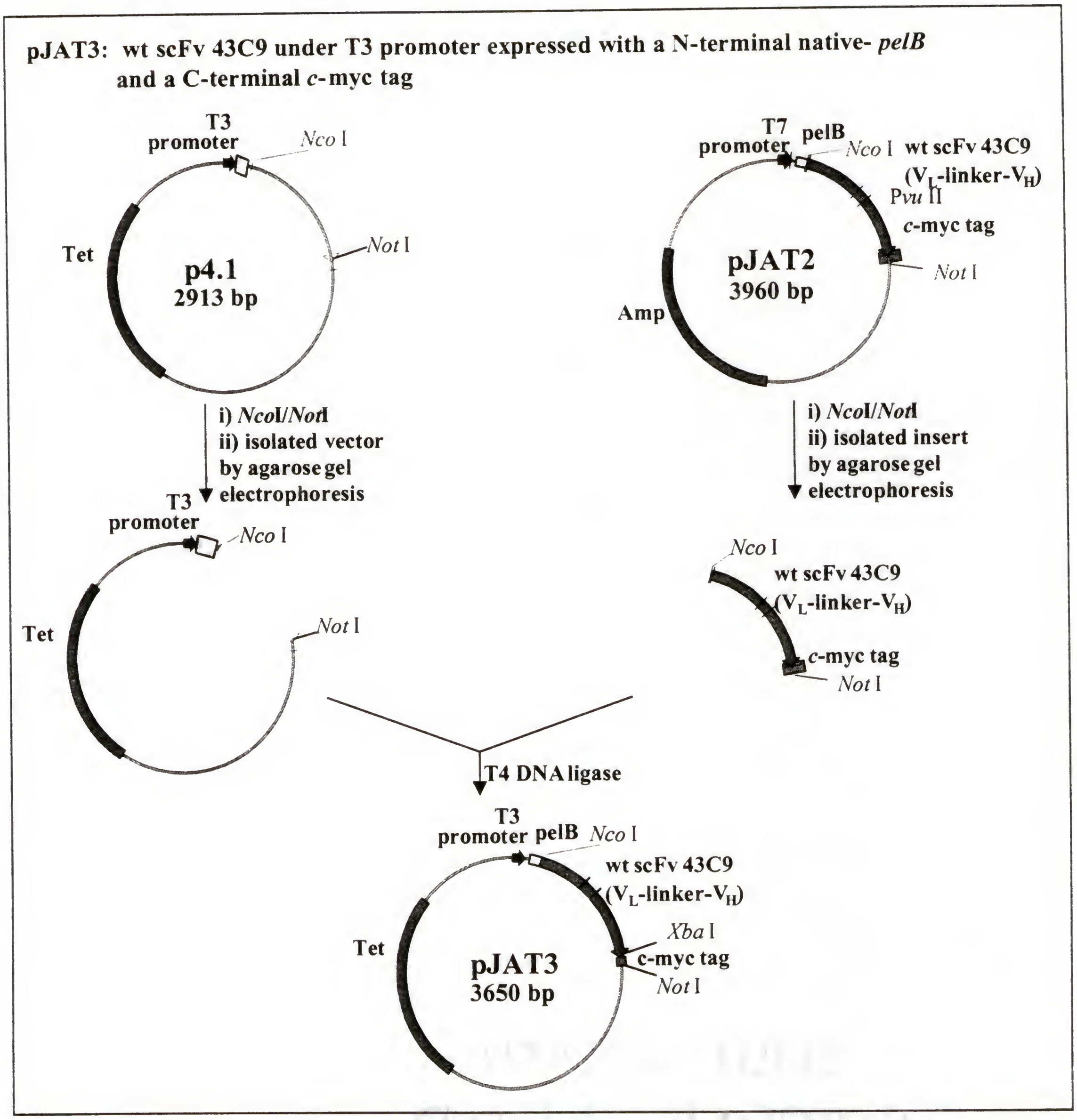
pJAT3: wt scFv 43C9 under T3 promoter expressed with a N-terminal native- pelB and a C-terminal c-myc tag
T3 promoter
Nco I
Tet
Not I
p4.1
2913 bp
T7 promoter
pelB
Nco I
wt scFv 43C9 (V_L-linker-V_H)
Pvu II
c-myc tag
Not I
pJAT2
3960 bp
Amp
i) NcoI/NotI
ii) isolated vector by agarose gel electrophoresis
i) NcoI/NotI
ii) isolated insert by agarose gel electrophoresis
T3 promoter
Nco I
Tet
Not I
Nco I
wt scFv 43C9 (V_L-linker-V_H)
c-myc tag
Not I
T4 DNA ligase
T3 promoter
pelB
Nco I
wt scFv 43C9 (V_L-linker-V_H)
Xba I
c-myc tag
Not I
Tet
pJAT3
3650 bp

Figure 2-2. Construction of pJAT3.

pJAT5: wt scFv 43C9 under T3 promoter expressed with a N-terminal native-*pelB* and C-terminal *c*- myc and his$_6$ tags

```
5'-GTT GTT CAG GTC TTC TTC AGA GAT CAG TTT CTG TTC T-
5'-CTA GAG AAC AGA AAC TGA TCT CTG AAGAAG ACC TGA ACA ACA GAT CTG GGC CC-
5'-GGC CGC CTA GTG GTG GTG GTG GTG GTG GGG CCC AGA TCT-
5'-CAC CAC CAC CAC CAC CAC TAG GC-3'
```

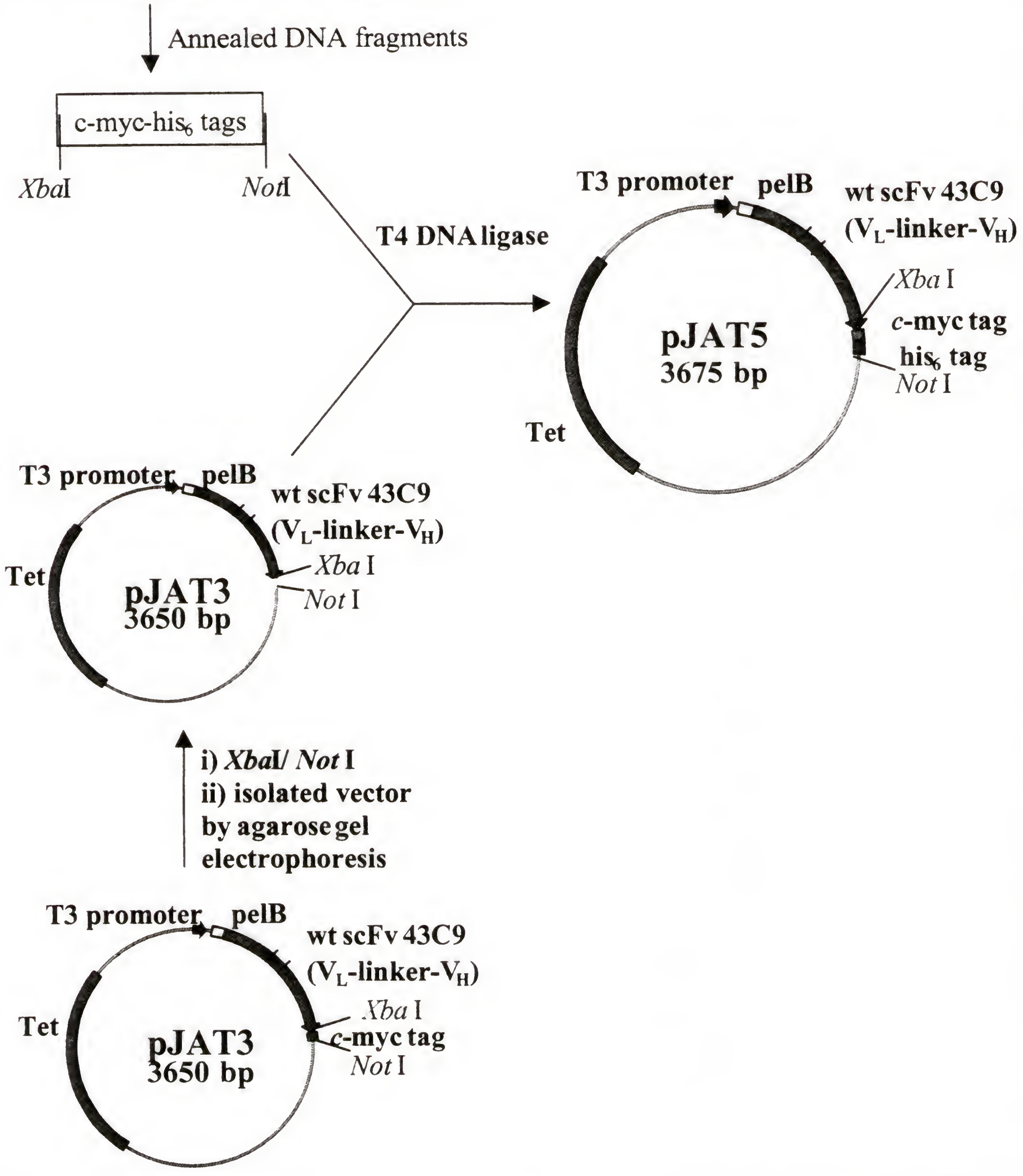

Figure 2-3. Construction of pJAT5.

Test inductions were done on BL21(pTG119) cells carrying pJAT3, and expression in the periplasm was tested. To determine if soluble protein existed in the periplasmic space, the outer-membrane was weakened with chloroform to release the periplasm contents.[102] Western blots using the anti *c*-myc monoclonal antibody (Figure 2-4) showed a negligible amount of soluble scFv in the periplasmic fraction. Despite this discouraging result, periplasmic proteins were isolated from 1g of induced BL21(pTG119, pJAT5) cells by osmotic shock.[95] The protein expressed from pJAT5 differs from that expressed from pJAT3 by the presence of a hexahistidine sequence following the *c*-myc tag. The his_6 tag was expressed with scFv 43C9 in order to explore possible refolding of inclusion bodies on a solid support as described later in this chapter. SDS-PAGE analysis revealed that this strain also failed to produce adequate amounts of properly folded scFv in the periplasm (data not shown).

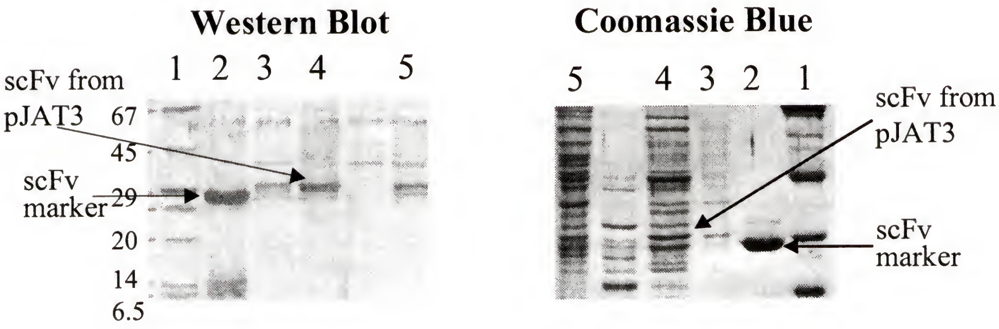

Lane	Sample
1	Molecular weight marker (kDa)
2	wt scFv 43C9 (positive control)
3	BL21(pTG119, pJAT3) growth medium
4	BL21(pTG119, pJAT3) periplasm fraction
5	BL21(pTG119, pJAT3) boiled cells

Figure 2-4. Western Blots and SDS-PAGE of IPTG induction of BL21(DE3)pJAT3.

The inability to isolate significant amounts of wt scFv 43C9 with the *c*-myc or *c*-myc/his6 tags in the periplasm of *E. coli* using a modest promoter designed to avoid inclusion body formation prompted a search for a different expression system.

Construction of alternative expression systems carrying a strong T7 promoter.

The genes for the wt scFv 43C9 with a *c*-myc tag and a *c*-myc/his$_6$ tag were cloned under control of a T7 promoter and fused to a bacterial codon optimized *pelB* leader sequence. The plasmid pJAT2 was constructed to expresses the scFv with a *c*-myc tag (Figure 2-5), and pJAT11 was created to express the scFv with a *c*-myc/his$_6$ (Figure 2-6). The construction of pJAT2 required an intermediate step that removed a stop codon before the *c*-myc tag using PCR. The primers used to complete this step are included in Table 2-1.

Table 2-1. Primers used to construct pJAT2.

Primer	**Sequence**
H97E For	5′-TTC TGT CAG CAA GAA TAT AGG GCT CCT-3′
JT43C9Rev	5′-GCG TCT AGA GAC AGT GAC CAG AGT CCC TTG-3′

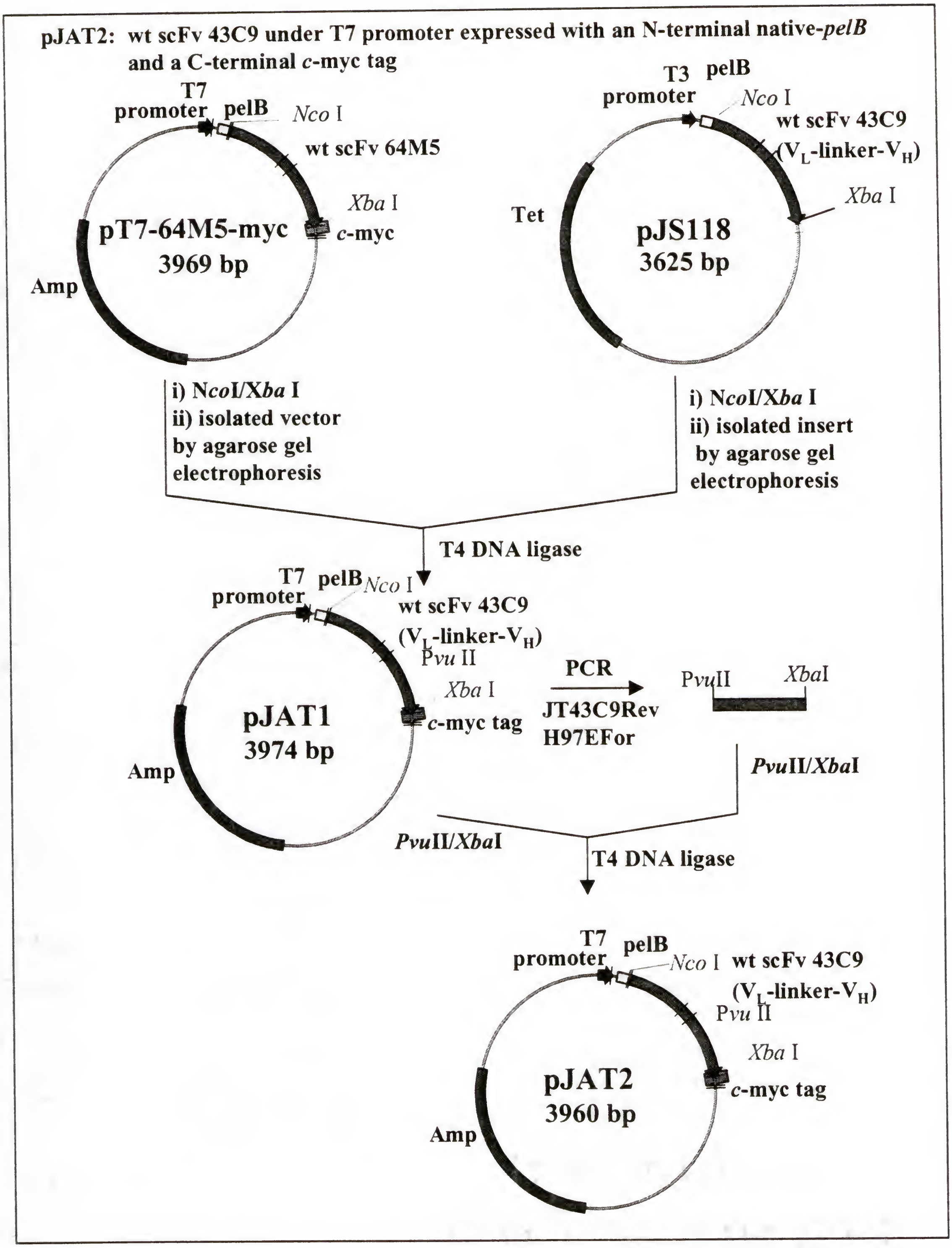

Figure 2-5. Construction of pJAT2.

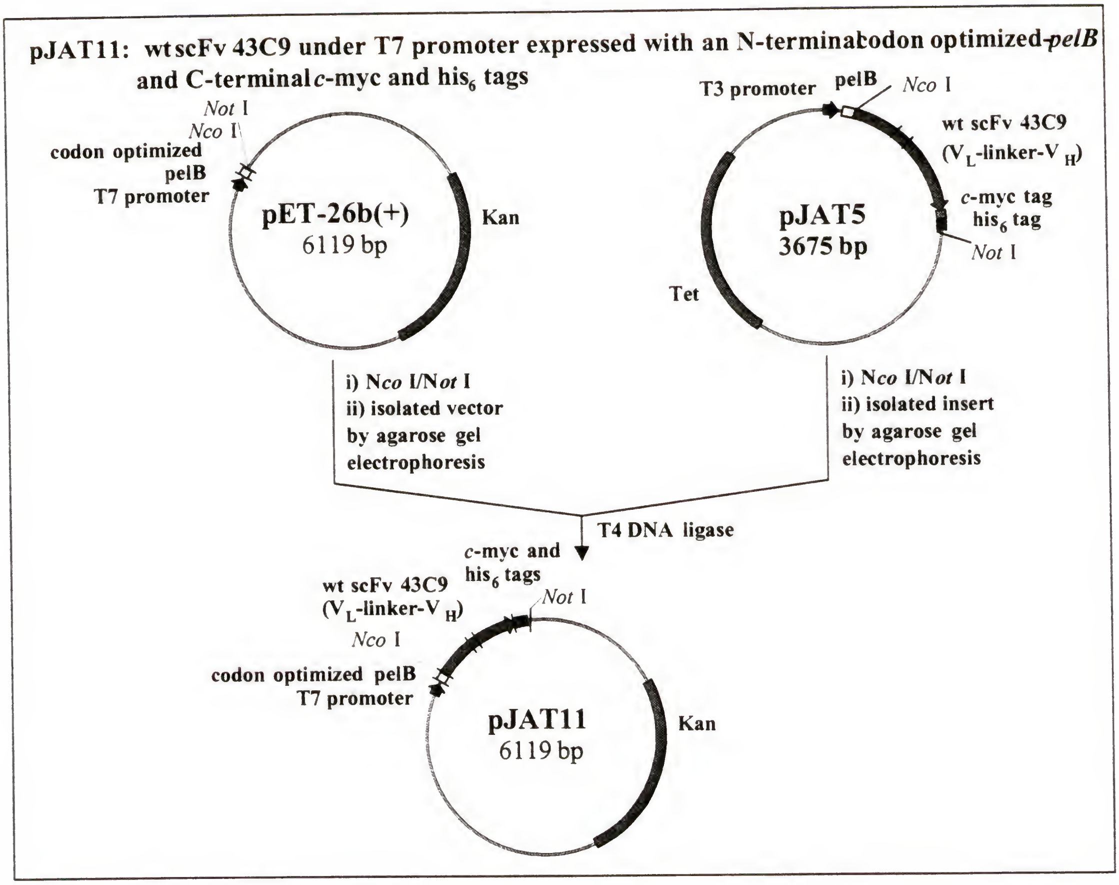
pJAT11: wt scFv 43C9 under T7 promoter expressed with an N-terminal codon optimized *pelB* and C-terminal *c*-myc and his$_6$ tags
Not I
Nco I
codon optimized pelB
T7 promoter
pET-26b(+)
6119 bp
Kan
T3 promoter
pelB
Nco I
wt scFv 43C9 (V$_L$-linker-V$_H$)
c-myc tag
his$_6$ tag
Not I
pJAT5
3675 bp
Tet
i) *Nco* I/*Not* I
ii) isolated vector by agarose gel electrophoresis
i) *Nco* I/*Not* I
ii) isolated insert by agarose gel electrophoresis
T4 DNA ligase
c-myc and his$_6$ tags
Not I
wt scFv 43C9 (V$_L$-linker-V$_H$)
Nco I
codon optimized pelB
T7 promoter
pJAT11
6119 bp
Kan

Figure 2-6. Construction of pJAT11.

Attempt to express wt 43C9 scFv in an engineered TrxB$^-$ *E. coli* host. The previous results suggested that high expression levels of scFv 43C9 would be necessary, and these conditions tend to produce aggregated protein. Since disulfide bond formation appears to play an important role in stabilizing soluble scFv's, an *E. coli* host that allows disulfide bond formation in the cytoplasm due to inactivation of thioredoxin reductase was investigated.[80] The potential of this strain (AD494(DE3)pLysS) in scFv production has also been explored by Georgiou and co-workers.[77]

The wt scFv under control of a T7 promoter (pJAT11) was used to transform AD494(DE3)pLysS (Novagen). The time course of scFv production using four IPTG concentrations ranging from 0.01 to 0.2 mM was determined by SDS-PAGE. Unfortunately these gels did not show the presence of the scFv clearly and this strategy was not pursued further.

High-level expression of wt scFv 43C9 as inclusion bodies. Since the previous attempts were unsuccessful at producing large amounts of the wt scFv 43C9, the T7 plasmids pJAT2 and pJAT11 were used to transform *E. coli* Bl21(DE3). The two strains were tested for scFv production in the growth media, the periplasmic space and the whole cell. Test inductions of pT7-64M5-myc and pJAT2 did not yield scFv overexpression. On the other hand, overexpression from *E. coil* BL21(DE3)(pJAT11) was observed. SDS-PAGE indicated that approximately 85% of the scFv accumulated as inclusion bodies. Unfortunately, while the yield of protein was acceptable, this experiment proved that the only procedure allowing for acceptable yields of scFv would be *in vitro* refolding of the aggregated protein.

In Vitro Refolding from Inclusion Bodies

Once expression systems capable of large-scale production of wt scFv 43C9/*c*-myc/his$_6$ had been developed, it was necessary to refold the inclusion bodies that were produced by the *E. coli* strains. A major concern with refolding protein in a redox buffer is the expense of the reagents and the large quantities needed.

Immobilized refolding of over-expressed scFv 43C9

Several groups have reported the use of immobilized-metal affinity columns to capture denatured protein by the polyhistidine tail. Once captured, the proteins are refolded *in situ* by a descending gradient of denaturant.[109] This method has been applied to scFv's by Ohtsuka and co-workers.[83,110] This single-step approach to refolding and purification avoids the costly use of high dilution conditions since the immobilized proteins are effectively isolated from one another. The expensive and standard refolding protocols involve unfolding proteins in a small volume of a denaturant (6M guanidine or urea) and a reducing agent (dithiothreitol (DTT) or reduced glutathione) if needed. Proper refolding requires that the denaturant be removed and the appropriate redox state maintained to allow the native disulfide bonds to form. The refolding is normally carried out by diluting the unfolded protein solution into a large volume of a non-denaturing buffer with redox reagents.

Refolding wt 43C9 scFv/*c*-myc/his$_6$ according to Ohtsuka *et. al.*[83] Wt scFv 43C9 was refolded from inclusion bodies overexpressed by a T7 promoter using *E. coli* BL21(DE3)(pJAT11). A 1 L culture was induced overnight at room temperature with 0.1 mM IPTG, then the cells were harvested and lysed in 50 mM Tris-HCl, 5 mM magnesium chloride, 0.5 mM EDTA, 0.1 M sodium chloride, 1 mM PMSF, pH 8.0 using sonication (12 x 30 s). SDS-PAGE analysis showed that the scFv was insoluble. The pellet containing inclusion bodies was dissolved in a minimum volume (typically 20 mL) of a solubilization buffer consisting of 6 M guanidine-HCl, 0.1 M Tris-HCl, 0.5 M sodium chloride, pH 8.0 overnight at room temperature. A Hi-trap® Chelating Resin (1 x 5 mL, Pharmacia Biotech) was charged with 0.1M nickel sulfate according to manufacture's directions. The denatured protein solution was then centrifuged (23,000 x g, 20 min) to remove insoluble debris and the supernatant was loaded onto the column over 3 hours. Two linear gradients: 6 to 1 M guanidine-HCl in 0.1 M Tris-HCl, 0.5 M sodium chloride, pH 8.0 (200 mL) over 2 hrs and 1 to 0 M guanidine-HCl in 0.1 M Tris-HCl, 0.5 M sodium chloride, pH 8.0 (200 mL) over 2 hrs were used to refold the protein.

Weakly bound species were then removed with 20 mL of a wash buffer composed of 0.1 M Tris-HCl, 20 mM imidazole, pH 8.0 and the refolded scFv was eluted in 0.1 M Tris-HCl, 500 mM imidazole, pH 8.0 as 1 mL fractions. Bradford assays were used to indicate fractions containing the eluted scFv and the appropriate fractions were concentrated to 2 mL by ultrafiltration and dialyzed into 50 mM HEPES-Cl, 75 mM sodium chloride, pH 7.5. Fluorescence quenching assays using the antigen (K_D <1 nM) were used to determine the yield of active scFv after this procedure. This assay indicated that only 22% of the protein eluted from the column was active scFv (97.2 μg of active scFv was present in the 442 μg of isolated protein). On the other hand, SDS-PAGE analysis showed that the scFv was 80% pure. The refolding procedure was repeated and this resulted in only 7.4% of the eluted protein being active scFv 43C9. It was clear that if this method were to be useful for scFv 43C9, it would have to be improved significantly.

Attempt to optimize *in situ* refolding. The results described above suggested that either the protein was not unfolded completely prior to binding to the column or it was misfolded during *in situ* refolding. Reducing agents were not used in the literature procedure. Optimization of this procedure was attempted in order to create a reproducible and efficient refolding system for scFv 43C9, and these efforts are summarized in Table 2-2. The scFv was unfolded completely by adding DTT (300 mM) to the buffer used to denature the inclusion bodies (entry 3, Table 2-2). Attempts to load the crude scFv on the Ni(II)Hi-Trap® column were unsuccessful; however, this can be attributed to the preferential binding of the reducing agent to the immobilized Ni(II). Lower concentrations of DTT including 0, 2, 2.5, 5, 10 and 15 mM DTT were used in the denaturant buffer in order to find a level sufficient to dissolve the scFv without affecting the solid support. SDS-PAGE assays indicated that 2.5 mM DTT was the lowest concentration that dissolved the inclusion bodies (entry 4, Table 2-2). In addition, other chelating columns capable of withstanding higher concentrations of reducing agents were tried with the dissolved scFv mixture (entry 5-7, Table 2-2). The effectiveness of guanidine versus urea as a denaturant was also tested, and studies indicated that 6 M guanidine dissolved the scFv slightly better. Elution buffers other than those containing imidizole were also explored. These elution buffers included 1 M ammonium chloride, 0.1 M Tris-HCl, pH 7.3, 6.9, 6.6 and 6.4, 2 M ammonium chloride, 0.1 M Tris-Cl, pH 7.3, 6.9, 6.6 and 6.4; 50 mM EDTA, 100 mM Tris, pH 8.0 and 100 mM EDTA, 100 mM Tris pH 8.0 (entry 8, Table 2-2). Analysis of the eluant and resin from these experiments led to the final conclusion that the scFv was not properly bound to the column and became an insoluble aggregate during the refolding procedure. Difficulties were also experienced when attempting to further purify the refolded protein. Attempted chromatography on PolyCAT-A cation, monoQ cation and monoS anion exchange resins were all unsuccessful, despite the fact that the properly folded scFv 43C9 has been successfully chromatographed on all three resins (Stewart, J. D. and Benkovic, S. J.; unpublished results).

All attempts at *in situ* refolding the 43C9 scFv/*c*-myc/his$_6$ protein were unsuccessful and resulted in either poor or no binding to the immobilized metal columns. Moreover, since the refolding process proceeded with very poor efficiency, it was suspected that the his$_6$ tag was destabilizing the protein. This procedure was therefore abandoned, and instead, batch refolding of scFv 43C9 was explored.

Table 2-2. Conditions explored to optimize the refolding of immobilized scFv's 43C9. Two scFv (43C9 and PN2A) were tested. The percent of eluted scFv that was active was determine by fluorescence assays when a significant amount of scFv was isolated.

Entry	scFv	Conditions	scFv eluted	Percent Active scFv
1	43C9	Literature procedure[7] without DTT in solubilization buffer	Yes	22%
2	43C9	Repeat of conditions in entry 1	Yes	7.4%
3	43C9	300 mM DTT in solubilization buffer	No	-
4	43C9	Optimized concentration of reducing agent used in solubilization buffer (2.4 mM DTT)	No	-
5	43C9	FreeZyme Conjugate Purification Kit (Pierce) chelating column using 2.5 mM DTT in solubilization buffer	Yes	8.4%
6	43C9 PN2A	FreeZyme column with various DTT concentrations	No	-
7	PN2A	Chelating Sepharose® Fast Flow resin (Pharmacia Biotech) with 230 mM DTT	Yes	not tested
8	43C9	Chelating Sepharose® Fast Flow resin with 230 mM DTT in solubilization buffer	No	-
9	43C9	Chelating Sepharose® Fast Flow with various DTT concentrations.	Yes	<7%
10	43C9	Varying elution buffer	No	-

Design of batch refolding procedure for wt scFv 43C9

The instability of the his$_6$ tagged scFv and the difficulties associated with *in situ* refolding prompted the search for an alternative strategy for reliably refolding inclusion bodies. Several laboratories, including that led by Plückthun, have explored batch refolding methods for scFv's.[48,51,58,81,82] Methods suitable for isolating wt scFv 43C9 as well as mutants lacking a V$_H$ disulfide bond were developed after reviewing these procedures.

Batch refolding of wt scFv 43C9. Because of the possibility that C-terminal *c*-myc and hexahistidine tags might affect the refolding of scFv 43C9, a new expression plasmid was constructed in which these sequences were removed (Figure 2-7). This expression plasmid also eliminated an extraneous Met-Ala N-terminal extension left after signal peptide cleavage in earlier generation plasmids. In the final construct, the wt scFv 43C9 gene under the control of a T7 promoter was fused to an *E. coli* codon optimized *pelB* leader sequence.

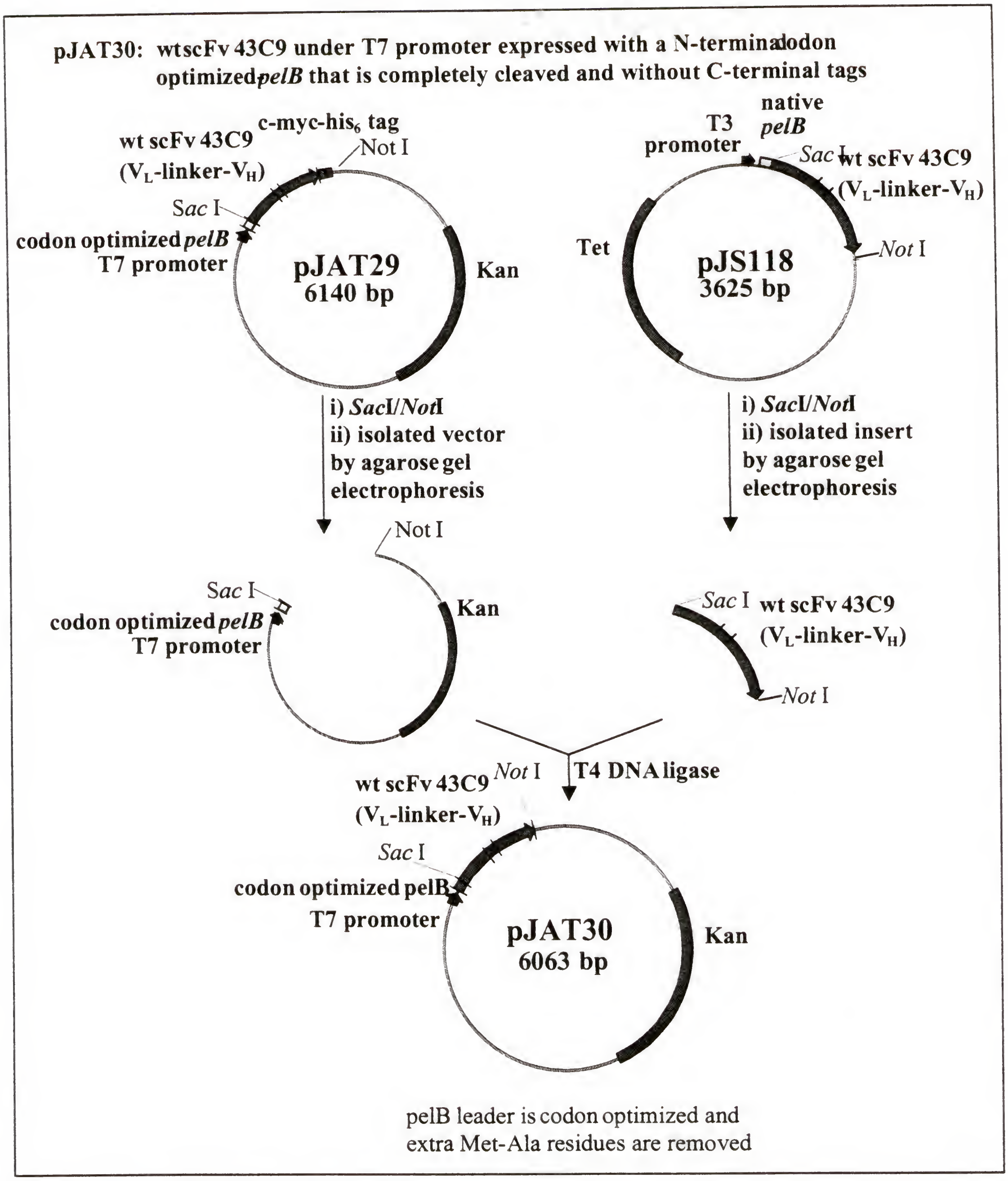

Figure 2-7. Construction of the expression plasmid pJAT30.

After construction, pJAT30 was used to transform *E. coli* BL21(DE3). ScFv expression was induced with 0.1 mM IPTG at room temperature overnight. The cells containing inclusion bodies of scFv 43C9 were pelleted, suspended in 20 mL of 50 mM Tris-HCl, 1 mM EDTA, 1 mM DTT, 1 mM PMSF, pH 7.5, and then lysed by two passages through a French Pressure Cell at 10,000 to 12,000 psi. The crude lysate was centrifuged for 20 min at 7,000 x *g*, then the pellet was resuspended in 20 mL of the previous buffer supplemented with 0.5% Triton X-100. After centrifuging at 7,000 x *g* for 20 min, the supernatant was discarded. This washing process was repeated an additional time without the use of Triton X-100. The insoluble material containing scFv 43C9 was dissolved overnight at room temperature in 10 mL of solubilization buffer (100 mM Tris-HCl, 6 M guanidine-HCl, 2 mM EDTA, 10 mM DTT, pH 8.0). Bradford assays were performed to determine the soluble protein concentrations and the values are presented in Table 2-3. The dissolved protein mixture was then refolded by adding 3 mL aliquots to 1 L of renaturation buffer (100 mM Tris-HCl , 0.5 M L-arginine, 2 mM EDTA, 0.267 mM oxidized glutathione, pH 8.0). Following each addition, the mixture was allowed to equilibrate for 100 min at 10°C, and after the final addition, the mixture was left stirring overnight. This protocol is a modification of that reported by Buchner and co-workers.[81,82] It was shown by these authors that the optimum concentration of the refolding protein is approximately 80 μg/mL. The final composition of the refolding mixture corresponds to that published previously except for the optimized concentration of oxidized glutathione needed to establish a redox ratio of 0.17:0.2 oxidized glutathione:reduced glutathione.

After refolding, the volume of the scFv solution was reduced to less than 10 mL by ultrafiltration, then the proteins were dialyzed into 20 mM MOPS, 0.4 mM calcium acetate, 5% glycerol, pH 6.3. The scFv was purified on a 200 x 4.6 mm PolyCAT-A column as described earlier.[7] The amount of protein refolded and the final isolated yield of scFv was determined by Bradford Assays (Table 2-3). Interestingly, the elution patterns obtained from PolyCAT-A chromatography differed between the refolded scFv 43C9 and that obtained from protein secreted from *E. coli* as shown in Figure 2-8 (the dashed line in the figure indicates the linear gradient to 100% 25 mM calcium acetate buffer). The refolded wt scFv 43C9 was eluted in three peaks while the secreted protein was observed in one peak. SDS-PAGE analysis indicated that the three peaks (labeled as A, B and C) isolated from *in vitro* refolding all appeared to contain scFv. Moreover, peak B of the refolded scFv eluted at a similar buffer composition as the single peak observed for the secreted scFv expression. Fluorescence titrations described in Chapter 3 proved that the three peaks contained active scFv's. The concentrations of purified scFv's were determined by absorbance at 280 nm (ε^{280} = 48,500 L/mol·cm) and these values were compared to the active protein concentrations as determined by fluorescence titrations. Table 2-3 includes this comparison for the wt scFv obtained from three independent experiments. This data indicates that peak A and B contained the majority of active scFv. Clearly, the percent of active scFv is much greater than that observed for the on-column refolding protocol investigated previously.

Table 2-3. This table organizes information from three *in vitro* refolding experiments for wt scFv 43C9. Concentrations of protein samples refolded and separated by polyCAT-A chromatography are listed. The eluted peaks from chromatography were assayed for scFv concentration by absorbance at 280 nm and by fluorescence titration.

Pre-refolding protein concentration (mg/mL)	**pre-refolding total protein (mg)**	**pre-column total protein (mg)**	**Eluted Peak**	**[scFv]$_{ABS}$ (μM)**	**[scFv]$_{Titration}$ (μM)**	**Percent active protein**
4.1	41	2.0	A	6.7	4.8	72
			B	4.1	2.9	71
4.2	42	0.39	A	N/D	0.098	-
			B	1.43	1.59	>100
			C	0.31	0.314	~100
2.9	29	4.8	A	13.2	15.6	>100
			B	~7	2.66	~40
			C	6.2	1.492	24

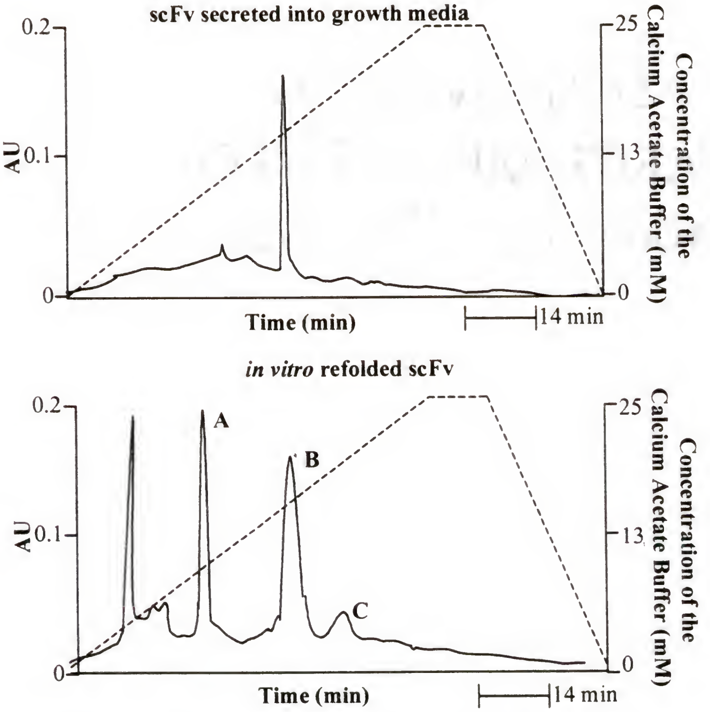

Figure 2-8. Elution pattern of wt scFv 43C9 secreted from BL21(DE3) and of the *in vitro* batch refolded wt scFv 43C9. The dotted line represents the linear gradient increase to 25 mM calcium acetate buffer.

Characterization of chromatograph elution pattern

The peak pattern observed in the PolyCAT-A chromatogram suggested that different forms of functional scFv 43C9 were produced from batch refolding. While the various forms were capable of antigen binding, this observation was troubling. Ample literature precedent suggested that dimerization or polymerization of isolated scFv fragments might occur and potentially give rise to the multiple forms of scFv observed. This phenomena would alter the native molecular weight of the scFv's. Whether this putative aggregation occurred during the refolding procedure or after isolation was not clear.

Determination of the molecular weights of isolated scFv's. The native molecular weights of the isolated scFv fractions were assigned by gel filtration chromatography. A 1.5 x 30 cm G-75 Superfine Sephadex column with an exclusion limit of 80 kDa and a fractionation range of 2 to 70 kDa was used to separate scFv oligomers. The column was first calibrated by four protein standards: bovine serum albumin (66 kDa), carbonic anhydrase (29 kDa), myoglobin (18 kDa) and cytochrome C (12 kDa). The void volume (V_o) was determined by the elution volume of blue dextran. Protein standards of varying molecular weight were isolated on the column and the V_e/V_o (volume eluted/column void volume) for each protein was recorded. A plot of the V_e/V_o versus molecular weight of eluted protein is shown in Figure 2-9 and the line of best fit was used as a calibration curve to identify the apparent antibody sizes.

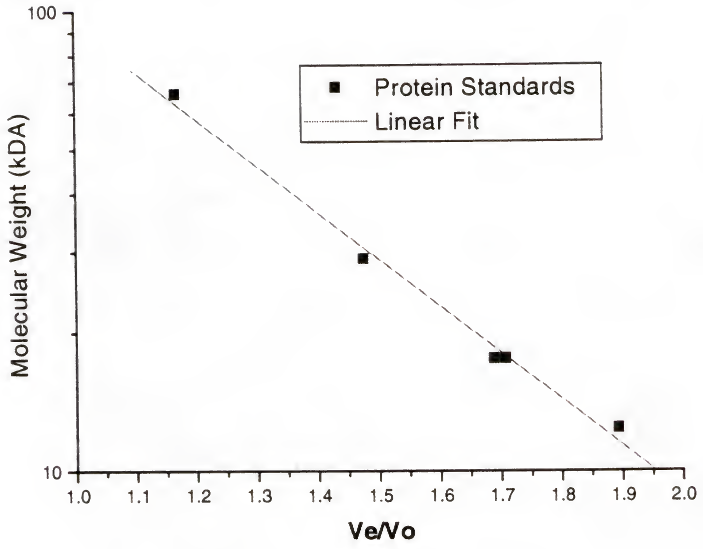

Figure 2-9. Protein standards for molecular weight determination.

Table 2-4. Molecular weight determination of the three peaks isolated by the PolyCAT-A column for wt scFv 43C9.

Peak	Time (hrs)	Molecular Weight (kDa)	Protein Fraction (%)
A	0	28	100
	48	28	63
	48	89	34
B	0	29	96
	0	73	4
	48	22	91
	48	65	9
C	0	30	61
	0	69	39
	48	33	45
	48	>75	55

Table 2-4 shows the molecular weights determined for each peak isolated by PolyCAT-A chromatography (A, B and C; Figure 2-10). Each PolyCAT-A peak was analyzed both immediately after isolation (0 hrs) and 48 hours after isolation. Peak A initially contained monomeric scFv; however, the protein aggregated over time and only 63% remained monomeric after 48 hours. Peaks B and C were eluted from PolyCAT-A as mixtures of scFv oligomers. Peak B seemed to possess the most stable scFv form, retaining >91% of the monomeric protein after 48 hours. Peak C initially contained a large amount of scFv oligomer and the monomeric scFv initially present aggregated to very high molecular weight species.

The stock scFv samples were assayed for antigen binding by fluorescence quenching after 48 hours as described later in Chapter 3. Table 2-5 shows both the total protein and active scFv concentrations as a function of time after isolation by PolyCAT-A chromatography. The change in proportion of functional scFv before and after 48 hours was compared with the gel filtration data to determine whether the retention of monomeric scFv correlated with antigen binding. This appeared to be the case, although errors associated with these measurements prevented a quantitative analysis. Only peak A was tested for molecular weight and for functional scFv immediately after eluting from the polyCAT-A due to the availability of only a single calibrated gel filtration column. Fluorescence quenching data indicated that all samples bound antigen as tightly as the parent monoclonal antibody, and the values reported in Table 2-5 reflect the assayed antibody concentration. The antibody concentration used in each experiment set the upper limit for the K_D estimates from the assays ($K_D < 1$ nM).[67]

Table 2-5. Active protein present for wt scFv 43C9 eluted in peak A and B and scFv binding ability from fluorescence hapten quenching. (N/D represents data that was not determined).

Eluted Peak	Time (hrs)	$[\mathrm{scFv}]_{\mathrm{Abs}}$ (μM)	$[\mathrm{scFv}]_{\mathrm{Titration}}$ (μM)	Percent Active Protein	Hapten K_D (nM)
A	0	13.2	15.6	>100	≤12.9
A	48	13.2	6.68	51	≤6.68
B	0	~7	2.66	~40	≤9.95
B	48	4.7	1.82	38	≤9.01
C	48	6.2	1.49	24	N/D

From these studies, it was clear that both peaks A and B contained significant fractions of monomeric scFv, although that in peak B resisted subsequent aggregation more effectively. This data also underscored the importance of obtaining characterization data for the scFv's as soon as possible following isolation. The instability of scFv's, even with a normal complement of disulfide bonds, is a general problem with these engineered proteins. This issue must be overcome for scFv's if they are to become as useful as native monoclonal antibodies. The second important conclusion from these preliminary studies was that the batch refolding procedure was acceptable for the wt scFv 43C9, which paved the way for studying derivatives lacking the V_H disulfide bond.

Expression of scFv 43C9 V_H disulfide mutants

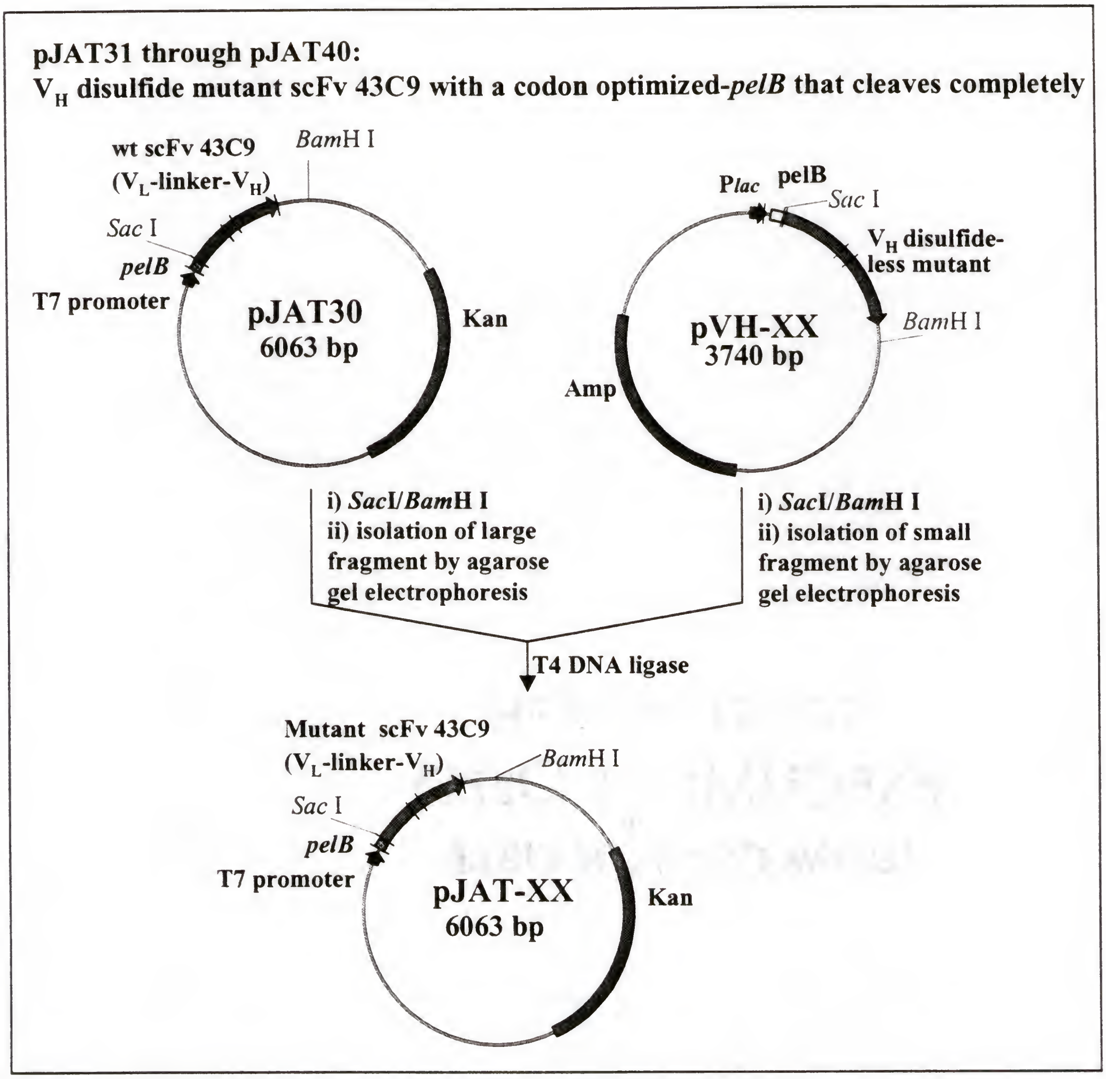
pJAT31 through pJAT40:
V_H disulfide mutant scFv 43C9 with a codon optimized-*pelB* that cleaves completely

Figure 2-10. Construction of mutant expression vectors pJAT31-pJAT40.

The V_H disulfide mutants were expressed from the plasmids constructed as shown in Figure 2-10 from plasmids (pVH-XX) containing the mutated heavy chains identified previously (Chapter 1). After the expression plasmids had been constructed, the correct V_H cysteine substitutions were verified by DNA sequencing, then the plasmids were used to transform *E. coli* BL21(DE3). Following cell growth and scFv production, inclusion bodies were obtained and the scFv was renatured using the batch refolding procedure described above. Table 2-6 describes each of these purifications. The concentration of protein prior to refolding correlates with the expression level of each mutant compared to the wt protein. This expression level can result from codon influences on protein synthesis. The protein concentration prior to polyCAT-A chromatography is also included in Table 2-6 and this provides a rough indication of refolding efficiency.

The chromatograms patterns presented in Figure 2-11 seem to be correlated to scFv stability. Elution profiles similar to the wt scFv and large peak areas reflect good stability and ligand binding as will be discussed in Chapter 3. For each protein, the scFv concentrations determined from absorbance measurements at 280 nm and fluorescence quenching titrations are compared in Table 2-6. The fraction of active antibody from the comparisons of peak A and B in the mutants tested reinforced the results from the wt scFv experiments. The scFv obtained from peak B was consistently the most stable and functional form.

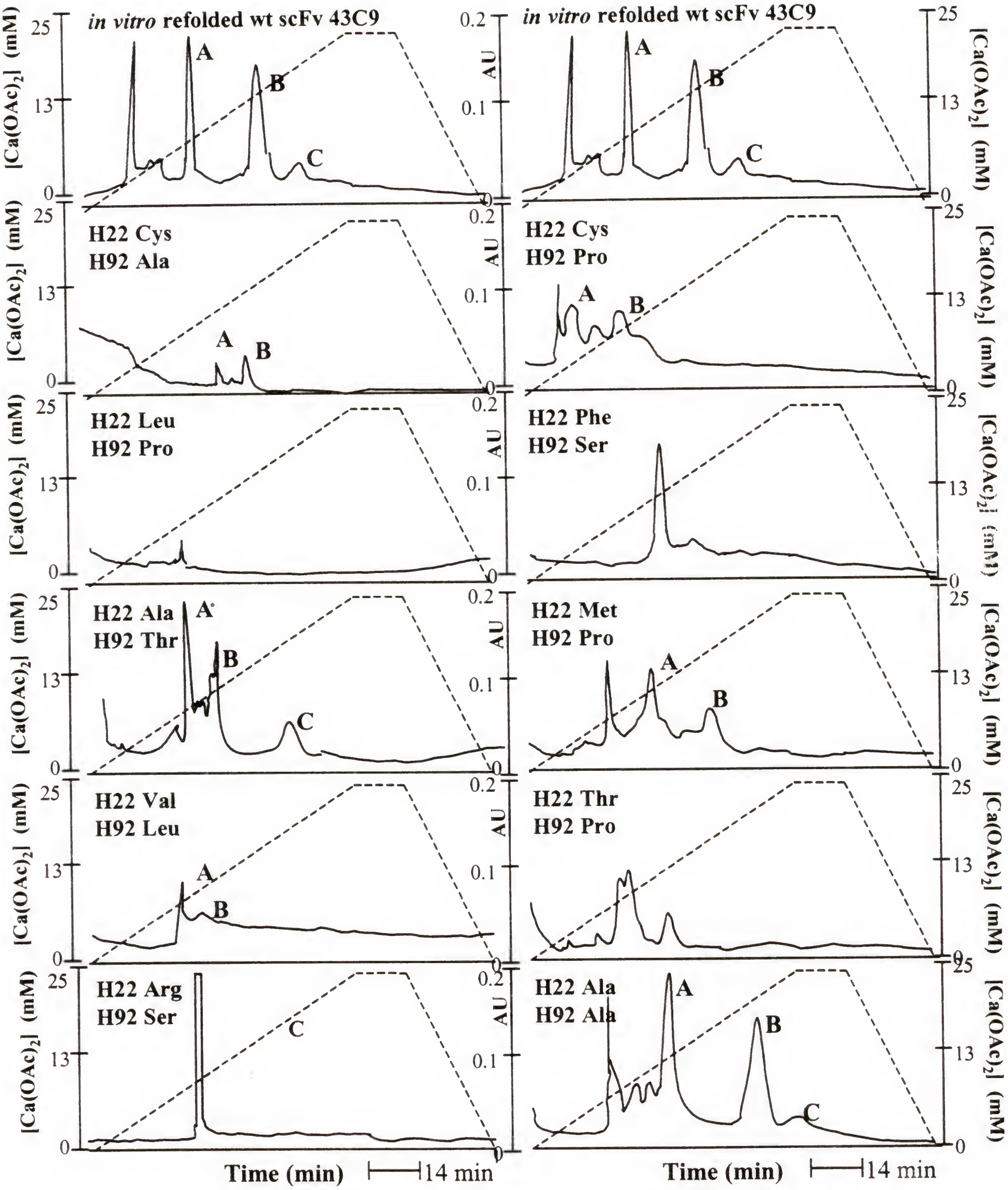

Figure 2-11. Chromatograms from the separation of scFv fragments by polyCAT-A chromatography. The dotted line represents the increasing buffer gradient.

Table 2-6. Summary of protein isolation for the VH disulfide mutants. Protein concentrations during the isolation are listed. The purified scFv stock contrations are included, and the percent of active scFv present in each stock. N/D = not determined. The highlighted entries are the scFv stocks that were used to characterize binding and stability.

H22	H92	previous plasmid	plasmid	pre-refolding protein concentration (mg/mL)	pre-refolding total protein (mg)	post-refolding total protein (mg)	eluted peaks	A^{280}, [scFv](μM)	titration, [scFv](μM)	percent active protein
Cys	Cys	pJS118	pJAT30	2.9	29	4.8	A	13.2	15.6	**>100**
							B	~7	2.66	40
Ala	Ala	pVH-5	pJAT40	6.8	68	10.7	A	4.63	N/D	-
							B	6.29	6.53	**>100**
Cys	Pro	pVH-15	pJAT36	7.1	70.6	3.2	A	4.60	0.284	6.2
							B	2.76	2.23	**80**
Cys	Ala	pVH-7	pJAT31	6.8	68	6.6	A	1.8	0.936	-
							B	9.8	9.76	**99**
Leu	Pro	pVH-11	pJAT32	0.52	5	1.7	single	1.4	0.153	**11**
Phe	Ser	pVH-22	pJAT37	3.8	38	N/D	single	3.03	0.1015	**3.4**
Thr	Pro	pVH-19	pJAT39	17	165	2.9	single	0.74	no quenching	**N/D**
Val	Leu	pVH-13	pJAT34	5.7	57	~2	A	0.5	0.523	-
							B	4.44	1.311	**30**
Arg	Ser	pVH-8	pJAT35	N/D	N/D	6	single	2.40	0.064	**2.7**
Ala	Thr	pVH-9	pJAT33	5.5	55	1.8	A	4.13	N/D	-
							B	6.38	5.09	**80**
Met	Pro	pVH-23	pJAT38	14	137	2.7	A	0.638	0.064	10
							B	0.6380	0.0644	**10**

CHAPTER 3
BINDING AND STABILITY STUDIES OF WILD-TYPE AND V_H DISULFIDE MUTANT SCFV 43C9 PROTEINS

The effect of removing the V_H disulfide bond on the stability and binding affinity of an scFv was unknown at the time this project was begun. One reason for choosing scFv 43C9 as the basis for this work was that the parent monoclonal antibody contains a normal complement of disulfide bonds and it does not possess unusual structural stability, both of which would complicate this study. Finally, the parent antibody is a catalyst for ester and amide hydrolysis and the mechanism involves nucleophilic catalysis by the protein.[15,16] Because catalysis is highly sensitive to antibody structure and because binding to high-energy species is a critical part of catalysis, these properties were explored to characterized the V_H mutants. When this strategy proved unsuccessful, fluorescence assays that take advantage of the high intrinsic fluorescence of the scFv's used instead.

Methods Investigated for the Binding Activity of scFv 43C9

Ester Hydrolysis Kinetics

While the antigen design of mAb 43C9 was aimed at producing an antibody capable of hydrolyzing a *p*-nitroanilide, it was discovered that the same antibody also catalyzed the hydrolysis of related phenyl esters (Figure 3-1).[62] Since Benkovic and co-workers had recently demonstrated that commercially available *p*-nitrophenyl acetate was a substrate for scFv 43C9, this ester was first examined.

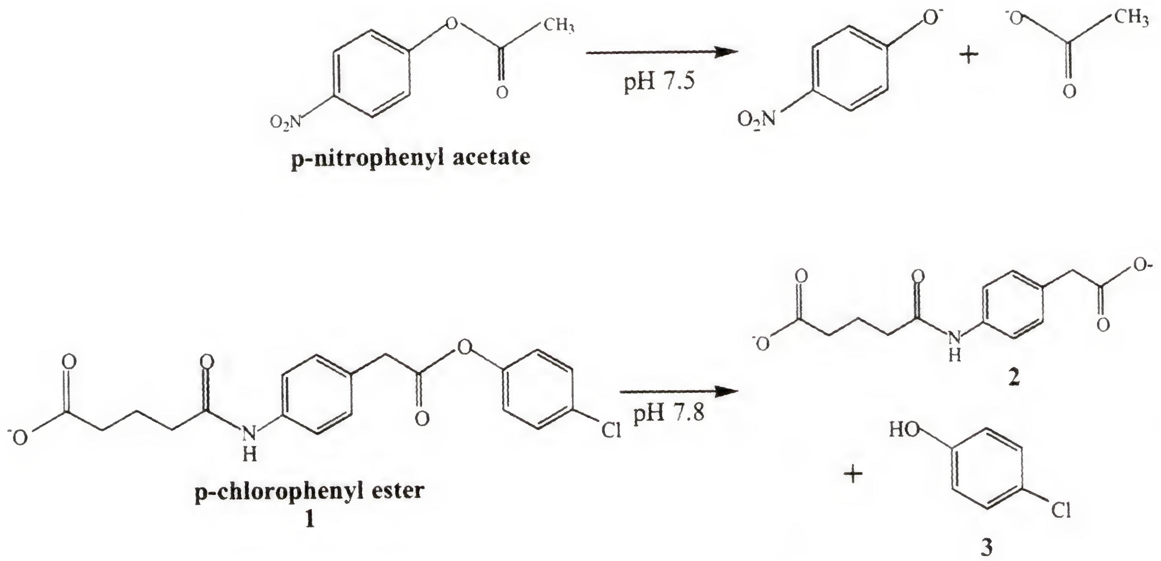

p-nitrophenyl acetate

p-chlorophenyl ester
1

2

3

Figure 3-1. Hydrolysis reactions followed by kinetic assays.

Hydrolysis of *p*-nitrophenyl acetate

Ester hydrolysis was followed at *p*-nitrophenyl concentrations of 0.1, 0.5, 1.0, 1.5 and 3.0 mM using 5% v/v dioxane to maintain a homogeneous reaction mixture. Product formation in the presence and absence of 0.1 μM wt scFv 43C9 was monitored at 404 nm for 30 min at 32°C. Unfortunately, a number of experimental problems (mainly due to the insolubility of the substrate in aqueous buffers) complicated these measurements and this approach was abandoned.

Synthesis of *p*-chlorophenyl ester

p-Chlorophenyl ester **1** was investigated next since the carboxylate-containing side chain was expected to confer greater aqueous solubility and the less-activated ester would slow the rate of spontaneous hydrolysis. The ester was synthesized by a known route (Figure 3-2).[62] The amino group of 4-aminophenylacetic acid **4** was first protected with BOC in 65% yield. A carbodiimide-mediated coupling with *p*-chlorophenol afforded ester **6** in 23% yield. The nitrogen protecting group was removed under acidic conditions, then the liberated amine **7** was reacted with glutaric anhydride. The *p*-chlorophenyl ester **1** was purified by column chromatography on silica gel, then subjected to reversed phase chromatography by HPLC. The final yield of *p*-chlorophenyl ester **1** was 7.5%.

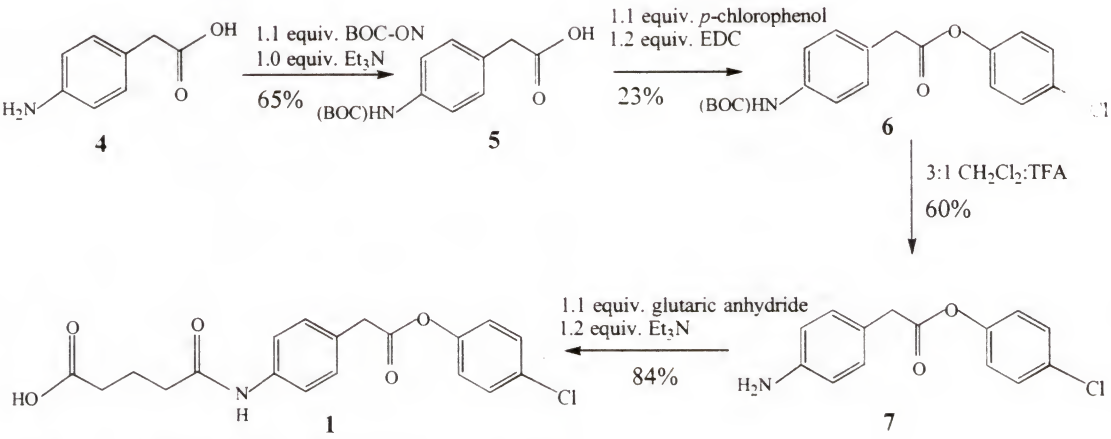

Figure 3-2. Synthesis of *p*-chlorophenyl ester

Hydrolysis of *p*-chlorophenyl ester

Prior to kinetic studies, the stock concentration of ester **1** was determined by adding 2 M sodium hydroxide to an aliquot, then measuring the absorbance at the isosbestic point for *p*-chlorophenol (282 nm, $\varepsilon^{282} = 1540$ L/mol·cm). The rates of hydrolysis of 0.1, 0.25, 0.5, 0.75 and 1.0 mM concentrations of *p*-chlorophenyl ester in the presence and absence of 0.1 μM wt scFv 43C9 were monitored at 282 nm for 300 min at 32°C.[96, 66,64] Initial rates were gathered before 5% hydrolysis. As with the *p*-nitrophenylacetate, precipitation introduced error into the observed rates for substrate concentrations ≥1 mM. These problems affected both the antibody-catalyzed and the background reactions. To determine whether these problems were due to salts introduced during HPLC purification, the silica purified *p*-chlorophenyl ester was assayed. Data from substrates purified by both methods were combined in the plot of Figure 3-3. While the general shape of the velocity versus substrate concentration curve is approximately correct, the large scatter in the data made this method unsuitable for distinguishing between scFv mutants with similar, but not identical, properties. This approach was therefore also abandoned.

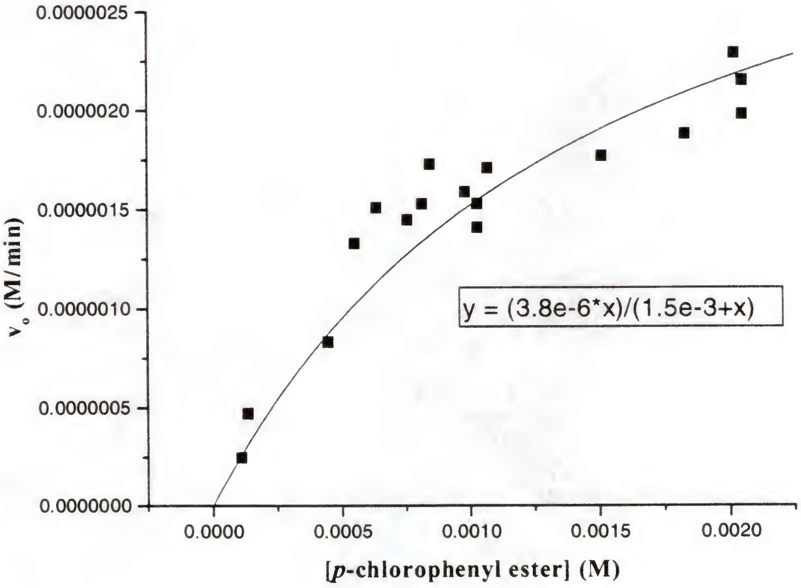

Figure 3-3. Observed catalyzed hydrolysis of p-chlorophenyl ester with scFv 43C9 corrected for background hydrolysis is in the absence of scFv 43C9.

Electrospray Mass Spectroscopy

One way to avoid problems with the poorly-soluble substrates used in the kinetic studies would be to instead examine ligand binding directly. Ligands bound by scFv 43C9 have K_D values in the nanomolar and micromolar range. Electrospray mass spectroscopy has been used previously to probe ligand binding by scFv 43C9.[65,97] The behavior of wt scFv 43C9 during electrospray FT-ICR was analyzed by Lisa Lang of the Eyler group at the University of Florida. Three sets of experimental conditions were examined: 8 μM scFv 43C9 dissolved in 1:1 50 mM HEPES, 75 mM sodium chloride, pH 7.5:methanol, 16 μM scFv 43C9 in 50 mM HEPES, 75 mM sodium chloride, pH 7.5 and 8 μM scFv 43C9 in 50 mM HEPES, 75 mM sodium chloride, pH 7.5 plus 50 μL 0.1 M HCl. The first two samples showed no signals corresponding to the scFv, and instead only showed the polymers that were introduced into the sample from the ultrafiltration membrane used to concentrate the protein solution. The third experiment produced a spectrum with three peaks at +17, +16 and +15; however, the corresponding molecular weights were not consistent with the scFv. While it may have been possible to identify conditions suitable for obtaining useful mass spectroscopy data from the scFv, assays of ligand binding introduced the further requirement that the protein also retain its native conformation under the conditions of the measurements. Given the limitations of solvent requirements for this technique, we sought a different approach for probing ligand binding

Binding Studies Using Fluorescence Spectroscopy

Fluorescence quenching upon ligand binding has been recognized as a useful strategy since the pioneering work by Velick in 1960.[98] Antibodies contain a relatively high proportion of tryptophan residues and thus display large intrinsic fluorescence at around 340 nm when excited near 280 nm. Moreover, the fluorescence quantum yield and/or emission maximum are often sensitive to the presence of bound ligands. The precise mechanism of this modulation is not defined for antibodies and may be due to a combination of protein conformational changes, contact quenching, and/or energy transfer. Regardless of its origin, such changes can be used to determine thermodynamic K_D values. This technique has been applied extensively to scFv 43C9 during studies of its catalytic mechanism.[7,62,64,67,96] While a variety of ligands can be examined by this technique, three of the most useful are depicted in Figure 3-4. The antigen analog **8** differs from the actual inducing antigen used in immunization by substitution of an acetyl side chain for the glutaryl side-chain. While this change has no affect on the K_D value, it dramatically simplifies the synthesis of the compound. The hydrolysis products, acid product **10** and alcohol product **11** are also useful in probing specific portions of the antigen binding pocket.[67]

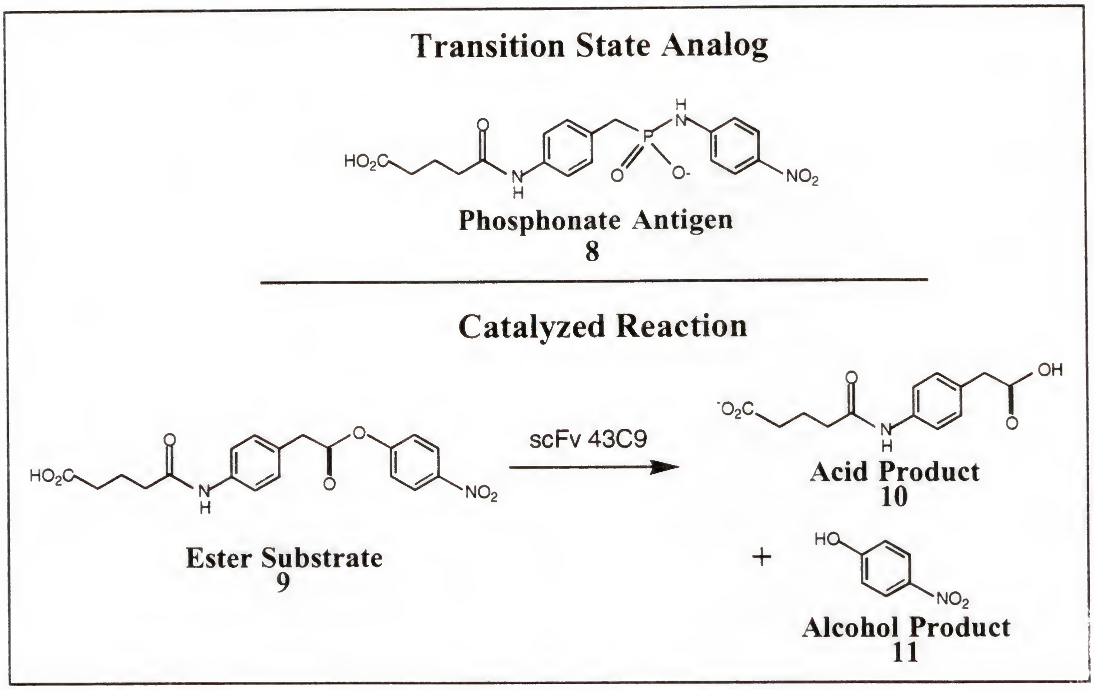

Figure 3-4. Ligands used in binding assays of scFv 43C9.

Fluorescence Spectroscopy of scFv 43C9

The scFv 43C9 possesses five tryptophans that emit strongly around 340 nm and overlap in the 300-400 nm region with strong absorption bands of the antigen analog **8** and ligands **10** and **11**. The plot presented on the left of Figure 3-5 is an emission scan of 6.93 μM scFv 43C9 excited at 270 nm. Saturating the scFv with the phosphonate antigen quenched the intrinsic fluorescence. The small residual fluorescence reflects emission by small levels of contaminants in buffer and the quantum yield for the scFv with bound antigen.

Quantitative Binding Measurements

Active antibody concentrations

The plot presented on the right of Figure 3-5 shows the decrease in fluorescence emission at 340 nm when the scFv is titrated with additions of antigen analog **8**. The initial decrease of fluorescence is linear with respect to the antigen concentration; however, once the antigen concentration is equal the antibody concentration, the binding pocket is saturated and further addition of this antigen does not affect the level of fluorescence emission. Such an active site titration is possible when the scFv concentration significantly exceeds the K_D value for ligand binding. This can be achieved easily for antigen analog **8** since the K_D value is <1 nM.[67] This titration is used to determine the concentration of active antibody. This experiment is extremely reliable when a large change of fluorescence is seen before saturation and when a sufficient number of data points define the region just prior to antibody-antigen saturation. This value can be compared to the antibody concentration determined by UV absorbance at 280 nm using Beer's Law. The relationship between the two concentrations quantifies the amount of active scFv in the isolated protein stock. This method was used throughout these studies to define the working concentrations of scFv stocks.

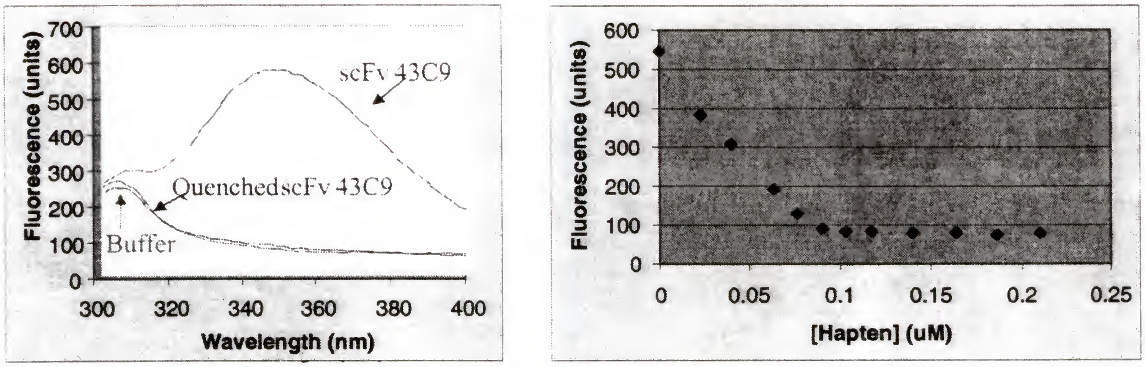

Figure 3-5. Quenching of scFv 43C9 fluorescence by the phosphonate antigen.

Measurement of thermodynamic dissociation constants

In contrast to the situation described above, titration experiments carried out under conditions where the antibody concentration is significantly below the K_D value of the ligand under study allows measurement of the K_D for the antibody-ligand complex. For such measurements, the working concentration is usually 10 to 20-fold more dilute compared to concentrations used to determine active antibody concentration.[98] Once measurements of fluorescence as a function of added ligand are complete, the data are fit to a quadratic equation that can be derived from the definition of K_D with no additional assumptions.[99] The initial fluorescence (F_o), the total change in fluorescence (ΔF), the working concentration of the scFv 43C9 ([Ab]) and the total concentration of ligand added ([L]) are all known and these are used to calculate the K_D for the ligand.

Binding Equilibrium

$$\mathrm{Ab\bullet\ L} \xrightleftharpoons{K_D} \mathrm{Ab} + \mathrm{L} \qquad K_D = \left(\frac{k_{\mathrm{off}}}{k_{\mathrm{on}}}\right)$$

Fluorescence Dependence on Antibody Complex Fluorescence

$$\mathrm{F([L])} = \mathrm{F_o} + \Delta\mathrm{F}\left(\frac{[\mathrm{Ab\bullet\ L}]}{[\mathrm{Ab}]}\right)$$

Quadratic Equation Fit for Fluorescence Quenching

$$\mathrm{F([L])} = \mathrm{F_o} + \frac{\Delta\mathrm{F}}{[\mathrm{Ab}]}\left(\frac{(K_D + [\mathrm{Ab}] + [\mathrm{L}]) - (\,(K_D + [\mathrm{Ab}] + [\mathrm{L}])^2 - (4[\mathrm{Ab}][\mathrm{L}])^{1/2}}{2}\right)$$

Figure 3-6. Fit used to determine K_D of the quenching ligand.

Before the raw fluorescence data can be fit to the quadratic equation, the data must be corrected to minimize two artifacts: photobleaching and inner filter effects.

Photobleaching. Constant irradiation of the scFv at the excitation wavelength results in irreversible damage to tryptophan indoles, which decreases the observed fluorescence emission. Antibody denaturation can also contribute to this problem, and the intrinsic stability of the scFv determines the severity of this problem. Each isolated scFv was assayed for rates of photobleaching and denaturation by exposing the scFv in buffer to the excitation wavelength for a time period typically used in the quenching assay. The fluorescence measurements over these sample points mimic the exposure of the scFv to photobleaching during ligand additions. The linear decrease of fluorescence over the sample points is fit to a line whose slope is used to correct the collected fluorescence quenching values.

Inner filter effect. Another artifact that also complicates fluorescence quenching titrations is the absorption of the excitation light by the ligand, thereby decreasing its intensity. This lowers the tryptophan emission by a binding independent mechanism. Since inner filter effects influence the fluorescence of free tryptophan to a similar extent, parallel titrations were performed on 0.83 μM tryptophan under the same conditions (this concentration gave a fluorescence emission comparable in intensity to the scFv). Fluorescence experiments using ligands exhibiting slight inner filter effects were corrected by plotting the observed fluorescence as a function of added ligand. The plot was then fit to a linear relationship that resulted in a slope that was used to calculate the correction factor at each ligand concentration. Inner filter effects were insignificant for the antigen analog **8**; however, the acid product **10** and the alcohol product **11** required correction.

Fluorescence Assays of scFv 43C9

Experimental procedures for fluorescence titrations were standardized for the wt scFv 43C9 before analyzing the V_H disulfide mutants. As discussed in the previous chapter, the scFv isolated from *in vitro* batch refolding yielded several peaks containing scFv 43C9. The fractions containing the most stable scFv species in peak B were assayed for binding. Those mutants whose elution patterns resembled the wt scFv were treated in the same manner.

Titration of scFv 43C9 with the Phosphonate Antigen

Titrations of the scFv fragments with the phosphonate antigen were first completed to determine the concentrations of active antibodies. Table 2-5 in Chapter 2 contains the results from these titrations for the wt scFv 43C9 and the library of V_H disulfide mutants produced from the initial chemiluminescent immunoassay. Table 3-1 summarizes the specific refolded wt scFv 43C9 and V_H mutants that produced the acceptable percentages of active protein presented in Table 2-5. The high portion of functional protein in these cases gives insight into the stability of these specific V_H disulfide mutants and suggests the presence of correctly folded and stable fragments.

Table 3-1. Summary of percent of active refolded scFv comparing the isolated scFv concentration determined from fluorescence titration experiments *versus* protein absorbance at 280 nm.

H22	**H92**	**Percent Active Protein**
Cys	Cys	~100
Ala	Ala	~100
Cys	Pro	80
Cys	Ala	99
Ala	Thr	80

Quantitating Dissociation Constants for scFv 43C9

All of the scFv's were investigated by fluorescence titrations to determine dissociation constants for the phosphonate antigen **8** and the two products **10** and **11** resulting from the ester hydrolysis catalyzed by scFv 43C9 (Figure 3-4). The wt scFv 43C9 was initially tested to determine baseline values for these dissociation constants which have also been reported in literature.[61,64,67] Table 3-2 includes this data for the refolded wt scFv as well as for all the V_H disulfide mutants. The refolded wt scFv 43C9 maintained the expected K_D for antigen binding, although these measurements can only place an upper limit on a K_D value since concentrations of scFv is greater than the calculated K_D value were required in order to detect the scFv fluorescence. The tight binding of the antigen makes it impossible to arrive at a true K_D value because the fluorescence changes cannot be detected at the required scFv concentrations. Therefore, the assays were performed at the lowest practical scFv concentrations and the K_D value that is presented in Table 3-2 for the antigen analog is set by the antibody concentration used in the assay. Even with this limitation, antigen analog binding is instrumental in comparing the binding properties of the wt with those mutants lacking a V_H disulfide bond.

In contrast, the K_D value for *p*-nitrophenol binding can be measured very accurately since the ligand quenches scFv fluorescence efficiently and the required scFv concentrations are easily achievable. The lower K_D value obtained for the refolded wt scFv *versus* the previously-published value is not significant in terms of free energy. There was relatively little change in affinity for *p*-nitrophenol **11** across the spectrum of V_H disulfide mutants examined, except for the two that contained serine at position H92, both of which had significantly greater affinity for this ligand.

The K_D values determined for the acid product **10** contained significant error due to its poor quenching ability and inner filter effects associated with this ligand. These values are therefore considered less reliable than those for the antigen analog **8** or *p*-nitrophenol **11**.

Table 3-2. K_D Values for the Fluorescence Quenching for scFv 43C9. [a]Benkovic *et al.*, 1990, *Science*, **250**, 1135-1139. [b] Gibbs *et al.*, 1991, *Proc. Natl. Acad. Sci. USA*, **88**, 4001-4004 and Stewart *et al.*, 1994, *Biochemistry*, **33**, 1994-2003. Plots are included in Appendix B and plots showing poor fits to the quadratic relationship is indicated with (poor). If a quadratic relationship did not fit data at all (no quenching) was entered in the table.

H22	H92	Antigen **8** K_D (nM)	Alcohol Product **11** K_D (μM)	Acid Product **10** K_D (μM)
Published wt scFv 43C9		<1 (nM)[b]	1.0(±0.2)[a]	28(±5)[a]
Cys	Cys	not tested	0.35(±0.04)	63(±42)
Ala	Ala	≤21.2	0.29(±0.02)	3(±4)
Cys	Pro	≤22.2	0.14(±0.10)	18(±6)
Cys	Ala	≤13.0	0.20(±0.02)	not tested
Leu	Pro	8.14(poor)	0.20(±0.05)	not tested
Phe	Ser	6.44(poor)	no quenching	no quenching
Thr	Pro	no quenching	not tested	not tested
Val	Leu	87.4(poor)	0.16(±0.03)	14(±3)
Arg	Ser	2.57(poor)	no quenching	1(±3.9)
Ala	Thr	≤4.24	0.37(±0.03)	not tested
Met	Pro	3.85(poor)	No quenching	not tested

Stabilities of scFv Fragments

Antibody stability is highly dependent on interchain disulfide bonds between the light and heavy chains and intrachain bonds residing within the domains themselves. A few robust antibodies have been identified that naturally lack intrachain conserved disulfide bonds and these retain their folded structures with other folding forces.[52,56] Several studies have yielded stable fragments of antibodies such as F_v's and scFv's without interchain disulfide bonds linking the domains by protein engineering techniques. This study has attempted to achieve these results by removing an intrachain disulfide bond of the V_H domain in a scFv that does not contain enhanced stabilizing forces in the starting protein. The success in creating V_H disulfide mutants having binding constants similar to the wild type scFv prompted further investigations into the relative stability of these scFv fragments. Examining the resistance to protein unfolding can provide important information on the consequences of removing the V_H disulfide bond from the scFv 43C9.

Guanidine Denaturation Studies

Protein folding can be affected by both chemical and conformation stability.[100] While chemical stability is based on covalent structure that is essentially irreversible, under the experimental conditions used in this project, conformational stability depends on the maintenance of a specific folded state. The folding states of a scFv can be described most simply as a two-state equilibrium (Figure 3-7). It is recognized by this study and others[100] that this simple model may not adequately describe the unfolding of a non-natural protein such as an scFv, particularly since the V_L and V_H domains can fold independently under certain conditions.

The methods available to observe the changes of folded states include spectroscopic techniques such as UV difference spectroscopy, fluorescence and circular dichroism. Fluorescence assays were chosen for scFv 43C9 because this technique produced large differences in emission for the two folding states, and this data was not influenced by non-specific protein interactions. Once a system for measuring protein folding was established, the manner used to denature the protein between folding states was chosen. Protein folding can be influenced by temperature, pH or guanidine and urea concentrations. Guanidine denaturation was chosen to examine scFv 43C9 since many researchers investigating scFv folding commonly use guanidine or urea as a denaturant as discussed in Chapter 1.

Denaturation of scFv 43C9

Guanidine induced denaturation studies must be performed under conditions that strictly control other parameters that may influence protein stability. For example, guanidine-mediated unfolding requires a temperature below the protein melting temperature to avoid the influence of thermal unfolding.[101] The incubation time for denaturation must also allow for complete equilibration at each denaturant concentration. The denaturation mixtures used in this study were incubated at 10°C for 18 hours and the pH was maintained at 5.8.[51] ScFv concentrations that afforded appropriate fluorescence signal changes were used, and these ranged from 25 to 32 nM.

Data Interpretation

Denaturation curves consist of three regions: a pre-transition region, the transition region and a post-transition region. The pre- and post-transitions regions reflect denaturant concentrations that do not affect folding to a great extent and ideally have no slopes. However, experimentally it is common to have slight slopes in these regions and data points that reflect error due to difficulties in reaching true equilibrium at the extreme denaturant concentrations. To correct for this deviance and create curves that can be easily compared between multiple proteins, a linear fit (represented by y_N and y_D) for these regions is used to determine the fraction of denatured protein based on the formula shown in Figure 3-7. This fit is then used to convert the raw data gathered from the spectroscopic assays to determine the fraction of protein denatured at each denaturant concentration.[100] Note that this analysis is only applicable in a two-state process. To avoid complications that result from deviations from this model, the denaturant concentration at the midpoint of the curve can be used as an index of protein stability, although these values are not directly related to the free energy of folding.

Natured State (N) $\rightleftharpoons$ **Denatured State (D)**

Fraction Natured (f_N) and the Fraction Denatured (f_D) scFv:
$f_N + f_D = 1$

The Observed Fluorescence (y) at Any Guanidine Concentration:
$y = y_N f_N + y_D f_D$

Combining the Two Expressions gives the fit for the denaturation:
$F_D = (y_N - y)/(y_N - y_D)$

Figure 3-7. Model used to fit guanidine denaturation data.

Wt scFv 43C9 Denaturation Curves

The denaturation of the refolded wt scFv 43C9 was first studied to compare the stability of the three elution peaks from the polyCAT-A column containing scFv 43C9 after *in vitro* batch refolding. The results shown in Figure 3-8 indicated that peak B was the most stable form of the scFv, which confirmed the results obtained previously (Chapter 2). A comparison between the denaturation of the refolded and secreted wt scFv is also shown in Figure 3-9, and the data indicate that the refolded scFv may be slightly more stable than the scFv secreted into media.

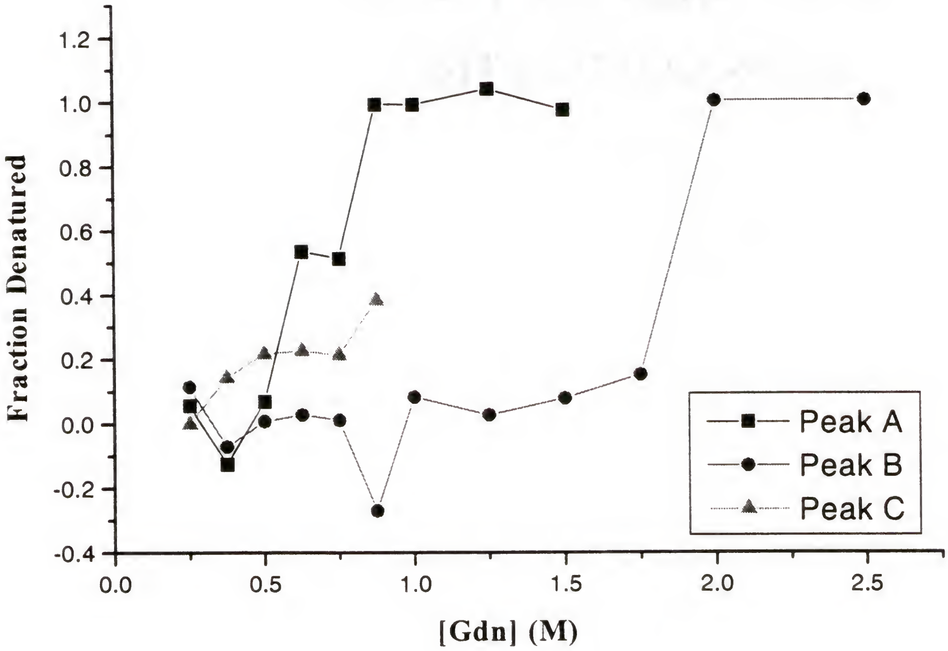

Figure 3-8. Guanidine denaturation of three stocks of refolded wild type scFv 43C9 isolated from polyCAT-A column chromatography.

Denaturation Studies of the V_H Mutant Library

The four mutants demonstrating wt-binding behavior were assayed for denaturation stability (Figure 3-9 and 3-10). As mentioned previously, the midpoint of the transition region is the most reliable means to compare the relative stabilities of the V_H disulfide mutants and the starting scFv. As expected, the disulfide-less V_H mutants are less stable than the wt scFv 43C9. Figure 3-9 also includes a mutant constructed by Brian Kyte that contains an additional salt bridge to increase the stability of the light chain of scFv 43C9. This Q-L27-E mutation introduces an electrostatic interaction between the mutated glutamate and an arginine at the top of one β-strand that also contains the disulfide bond. As expected, the denaturation of this stabilized mutant showed a shift in the denaturation curve to a more stable folded protein.

Table 3-3. Results from Denaturation of scFv with Guanidine.

Preparation	**H22**	**H92**	**$[\mathrm{Gdn}]_{1/2}$(M)**
Secreted	Cys	Cys	1.31
Refolded	Cys	Cys	1.84
	Cys	Pro	1.13
	Ala	Ala	0.86
	Cys	Ala	0.78
	Ala	Thr	0.50

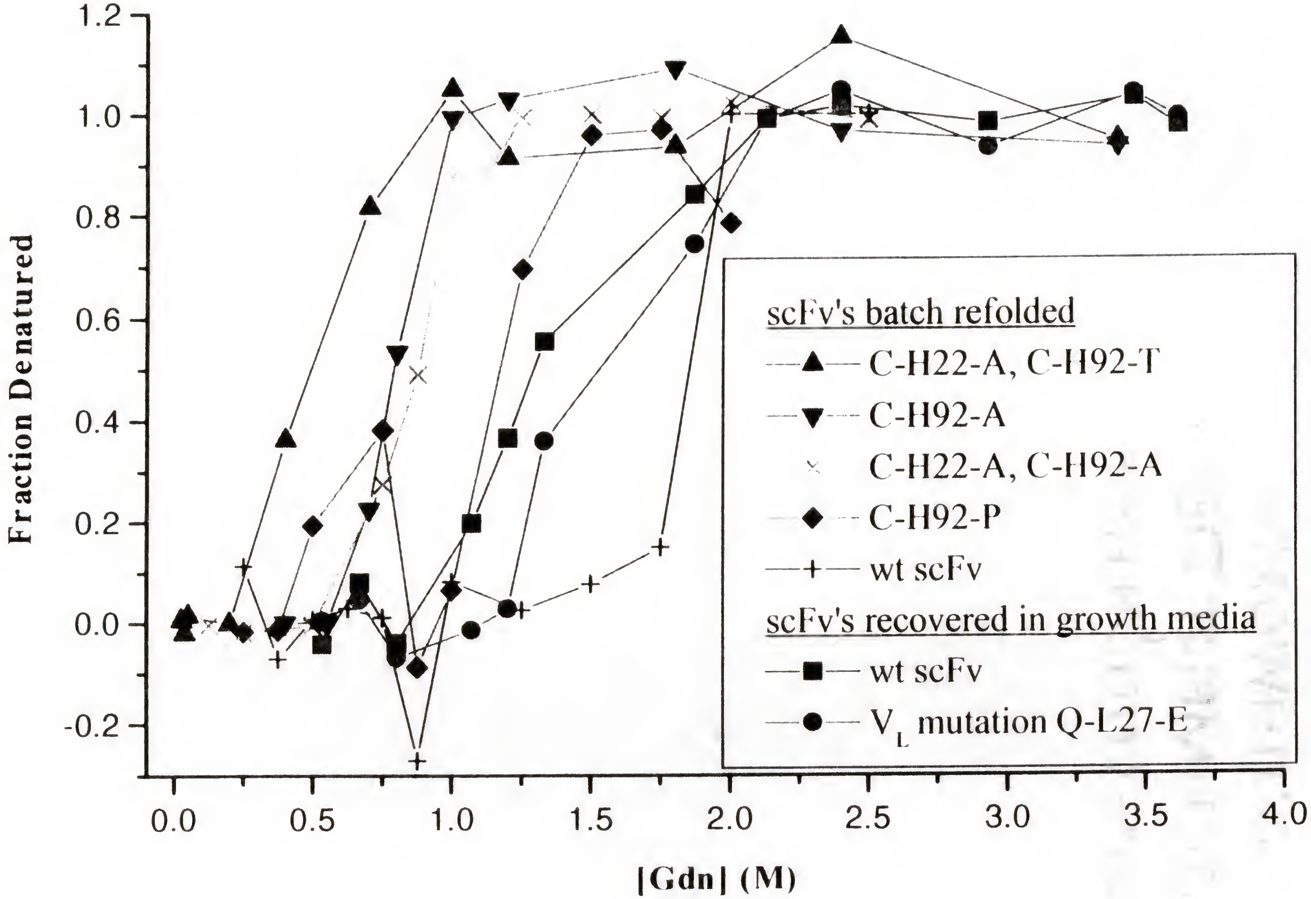

Figure 3-9. Guanidine denaturation of wt scFv 43C9 isolated from secretion into the media and from *in vitro* batch refolding compared to the V_H mutants of scFv 43C9 isolated from *in vitro* batch refolding.

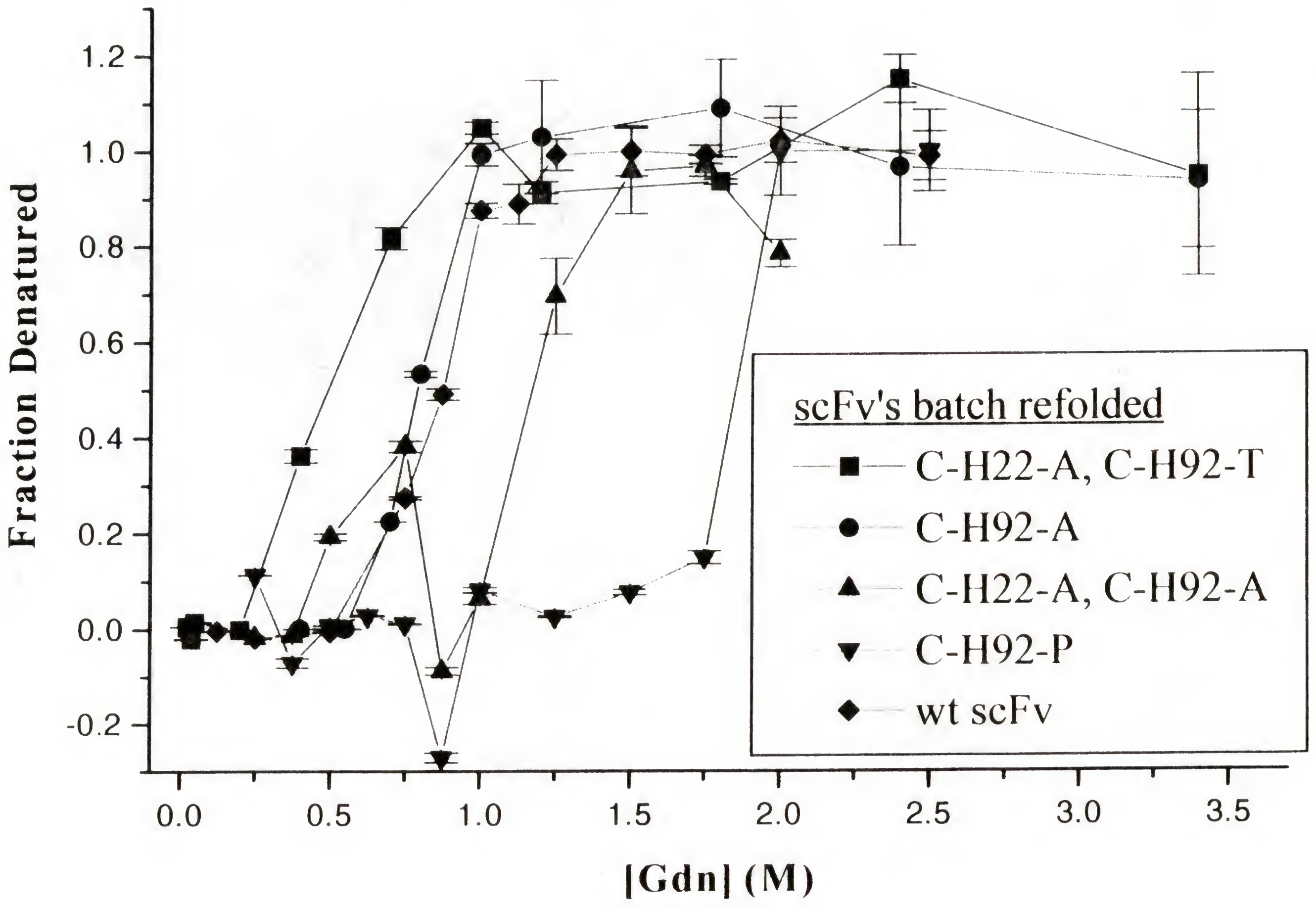

Figure 3-10. Guanidine denaturation curves with the calculated experimental error of *in vitro* batch refolded wt and V_H mutant scFv 43C9 presented in Figure 3-9.

Predicted Folding Pathway of the wt scFv and V_H Mutants

The folding pathway of scFv 43C9 can be predicted by comparing it to the stability model proposed by Wörn and Plückthun as discussed in Chapter 1.[47] From the denaturation curves in Figure 3-9, the refolded scFv mutants tend to demonstrate a steeper transition region than the wt scFv's or the Q-L27-E mutant. According to Wörn and Pluckthün, this steep curve identifies the refolded mutants as class III scFv's. This group is characteristic of two domains of relatively low intrinsic stability linked together by a very stable interface. This suggests that the mutations in the heavy domain are destabilizing the light chain somewhat. If the V_H chain were the only destabilized domain, a visible step would appear in the transition region of the denaturation curve. The wt and V_L stabilized mutant exhibit a curve that has an apparent step at a guanidine concentration of about 1.3 M. This categorizes these scFv's into Class I that is characterized as having one domain of higher stability than the partner chain. The positioning of the active site residues in the light chain suggests that this domain is more rigid than the heavy chain. This rigidity may also be responsible for a higher stability in the light chain. The heavy chain of the wt scFv and the Q-L27-E mutant may initially denature followed by the unfolding of the more stable light chain. Insight into the folding stability from these predictions can only be used as a guide to predict the benefits of additional mutations.

CHAPTER 4
CONSTRUCTION OF SCFV PN2A

Biological Application of Reengineered Antibody Fragments

Restructured antibodies that are able to fold into active forms under the reducing conditions that prevail in living cells might find many biological applications. For example, a treatment for breast and ovarian cancer could be designed by introducing a disulfide-less antibody that interrupts the mitogenic cascade associated with the oncoprotein p185. Stern and DiGiovanna have isolated the monoclonal antibody (mAb) PN2A that binds to a major autophosphorylation site, Y(p)1248, at the C-terminal end of p185$^{neu/\mathrm{erbB\text{-}2}}$.[84,85,93] High levels of this oncoprotein are produced by the *neu* and erbB-2 genes in mice and humans, respectively, and there is ample evidence that disrupting the signaling by this protein will prevent cell proliferation.[92] The antigen used to create mAb PN2A was the synthetic phosphopeptide KTAENPE-(p)Y-LGLDVPV, which corresponds to the major autophosphorylation site. The high selectivity of this antibody enables distinction between the phosphorylated and non-phosphorylated states of p185 and between activated p185 and activated EGFR. This antibody has been instrumental in detecting activated p185 in immunohistoblots.[84] The long-term goal of this study is to expand the utility of mAb PN2A by creating an scFv derivative lacking disulfide bonds. Such an antibody could be used for *in situ* detection of activated p185 in living cells or possibly as a therapeutic agent that blocks the signaling of Y(p)1248 of p185. The first step in reaching this goal was to create an scFv derivative from the existing monoclonal antibody and this goal has been reached.

Creating a scFv Fragment from a Monoclonal Antibody

A two-step procedure was used to isolate the DNA encoding the V_H and V_L portions of the PN2A antibody. Amplification protocols for obtaining DNA sequences encoding antibody Fab fragments are relatively reliable and were used to isolate the antibody Fab genes. The isolation of the heavy chain sequences from hybridoma cDNA by the polymerase chain reaction (PCR) was first reported by Winter and coworkers.[103] The procedure was expanded to include the isolation of light chain sequences in the laboratory of Lerner.[104,105] These scientists designed a series of primers that annealed to the 3' and 5' ends of the Fab heavy and light chains for each antibody subgroup. Combinations of these forward and reverse primers (Kang Primers) can be used in separate reactions to attempt to amplify the chains of a Fab fragment. Once the Fab gene was cloned and sequenced, the sequences corresponding to the F_v fragment were isolated and joined to create the scFv PN2A. Preliminary characterization data have been obtained for this scFv.

Construction of ScFv PN2A

Isolation of Fab chains of mAb PN2A

The cDNA isolated from the PN2A hybridoma was provided by DiGiovanna and Stern. The heavy and light chain genes of the Fab fragment of mAb PN2A were amplified from this cDNA as illustrated in Figure 4-1. The light chain was first amplified by using the forward primers 3-7 and the reverse primer 9 included in Table 4-1. All five

PCR reactions showed an amplified DNA band of approximately 700 base pairs (bp), and one of the reactions was arbitrarily picked and the DNA was sequenced. The sequenced light chain of the Fab fragment aligned with the κ Light Chain VI mouse variable region. Sixteen residues of the amplified gene did not align with the consensus sequence of this subgroup; however, all of these positions corresponded to variable residues within this subgroup.

The heavy chain of the Fab fragment was then amplified in the same manner. Kang Primers corresponding to the Kabat Subgroup IgG-I were chosen to amplify the PN2A gene. This subgroup was previously identified by isotyping tests on mAb PN2A by DiGiovanna and coworkers (unpublished results). Two PCR reactions containing forward primers 2 and 5 and the reverse primer 12 indicated in Table 4-1 were performed. PCR product was obtained from both reactions, and the forward primer 2 produced the greatest amplification. Sequence alignment of this amplified heavy chain with the Kabat Subgroups closely matched subgroup IgG-II and retained all invariant residues.

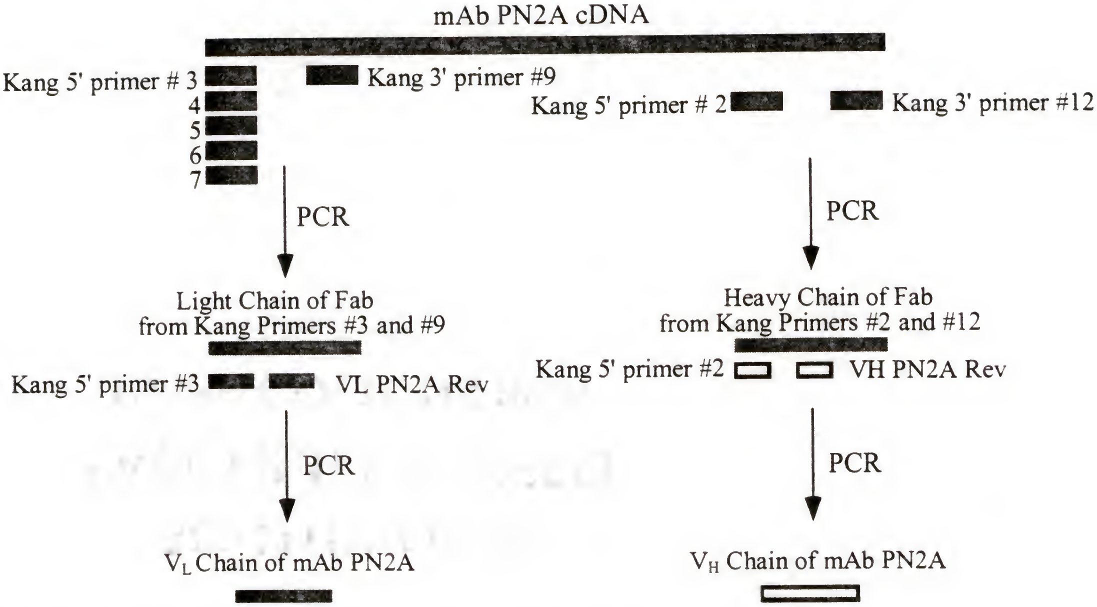

Figure 4-1. Scheme for isolation of V_L and V_H domains of scFv PN2A.

Table 4-1. Collection of primers used for PCR amplification of Fab Fragment.

	Light Chain Primers
For	SacI
3	5'-CC AG**T** T**CC** GAG CTC **GTG** **CTC** ACC CAG TCT CCA-3'
4	5'-CC AG**T** T**CC** GAG CTC **CAG** **ATG** ACC CAG TCT CCA-3'
5	5'-CC AG**A** T**GT** GAG CTC **GTG** **ATG** ACC GAG ACT CCA-3'
6	5'-CC AG**A** T**GT** GAG CTC **GTC** **ATG** ACC CAG TCT CCA-3'
7	5'-CC AG**T** T**CC** GAG CTC **GTG** **ATG** ACC CAG TCT CCA-3'
Rev	Xba I
9	5'-GCG CCG TCT AGA ATT AAC ACT CAT TCC TGT TGA A-3'
	Heavy Chain Primers
For	Xho I
1	5'-AG GTC CA**G** CT**G** CTC GCG TCT GG-3'
2	5'-AG GTC CA**G** CT**G** CTC GCG TCT GG-3'
3	5'-AG GTC CA**G** CT**T** CTC GCG TCT GG-3'
4	5'-AG GTC CA**G** CT**T** CTC GCG TCT GG-3'
5	5'-AG GTC CA**A** CT**G** CTC GCG TCT GG-3'
6	5'-AG GTC CA**A** CT**G** CTC GCG TCT GG-3'
7	5'-AG GTC CA**A** CT**T** CTC GCG TCT GG-3'
8	5'-AG GTC CA**A** CT**T** CTC GCG TCT GG-3'
Rev	Spe I
12	5'-AGG CTT ACT AGT ACA ATC CCT GGG CAC AAT-3'

Isolation of the light and heavy chains of the variable domain

The DNA encoding the light and heavy chain portions of F_v PN2A were amplified by PCR. Primers for F_v amplification used the same Kang Forward Primers to anneal to the 5' end of each gene fragment but different reverse primers that annealed to 3' end of the V_L or V_H chains. Following amplification (Figure 4-2), the PCR products were separately cloned into "TOPO TA" vectors and sequenced.

Table 4-2. Summary of primers used to amplify the variable fragment of each chain.

	Primers	Sequence (5' to 3')
V_L fragment	Forward Kang LC#	CC AGT TCC GAG CTC GTG CTC ACC CAG TCT CCA
	Reverse VLPN2AREV	GCG AAG CTT GGA TGG TGG AAG ATG GAT ACA GTT
V_H fragment	Forward Kang HC#2	AG GTC CAG CTG CTC GCG TCT GG
	Reverse VHPN2AREV	GCG CTC TAG ATG CAG ACA GTG ACC GAG TCC

Construction of scFv PN2A

Components of the scFv PN2A construct. Connecting the variable domains of the F_v fragment with a polypeptide linker creates a scFv fragment. Various linkers have been used in literature, and choice of an appropriate linker is still a matter of debate.[106] The scFv PN2A fragment was initially constructed with the linker used in scFv 43C9 which consists of 14 amino acids with a repeat of glycine and serine. The effectiveness of this linker in maintaining the two chains of PN2A as a functional F_v dimer was determined by binding studies discussed later in this chapter. scFv PN2A was also expressed with the *pelB* leader sequence that has been used successfully with 43C9. The initial expression vectors contained the codon-optimized *pelB* leader sequence that retained an extraneous Met-Ala at the N-terminal end of the V_L chain after signal peptidase cleavage. Preliminary studies were used to determine the ability of the Met-Ala modified scFv PN2A to bind the peptide antigen. Various tags were also expressed with the scFv. A version in which the scFv PN2A was followed by a *c*-myc peptide that was created for binding studies by ELISA. A version in which C-terminal *c*-myc and hexahistidine tags were both present was also created to explore the immobilized *in vitro* refolding of this antibody.

ScFv construction. The complete scFv PN2A gene was created by replacing the V_L and V_H portions of the scFv 43C9 gene with those for PN2A (Figure 4-2). The PN2A V_L and V_H F_v genes contained flanking restriction sites created by the primers used during amplification that matched those required in the expression vector. *Sac*I and *Hind*III sites flanked the V_L chain and *Pvu*II and *Xba*I flanked the V_H portion. The presence of a naturally occurring *Sac*I site within the PN2A V_H gene required the insertion of the V_L chain into the expression vector prior to introducing the V_H gene. C-terminal appended tags were transferred from expression plasmids as described in Chapter 2 using *Xba*I and *Not*I sites at the 3' end of the cassette. Figure 4-2 and 4-3 contain two expression plasmids pJAT21 and pJAT22, respectively, that were initially synthesized with the *pelB* codon-optimized leader sequence and combinations of *c*-myc and his_6 tags.

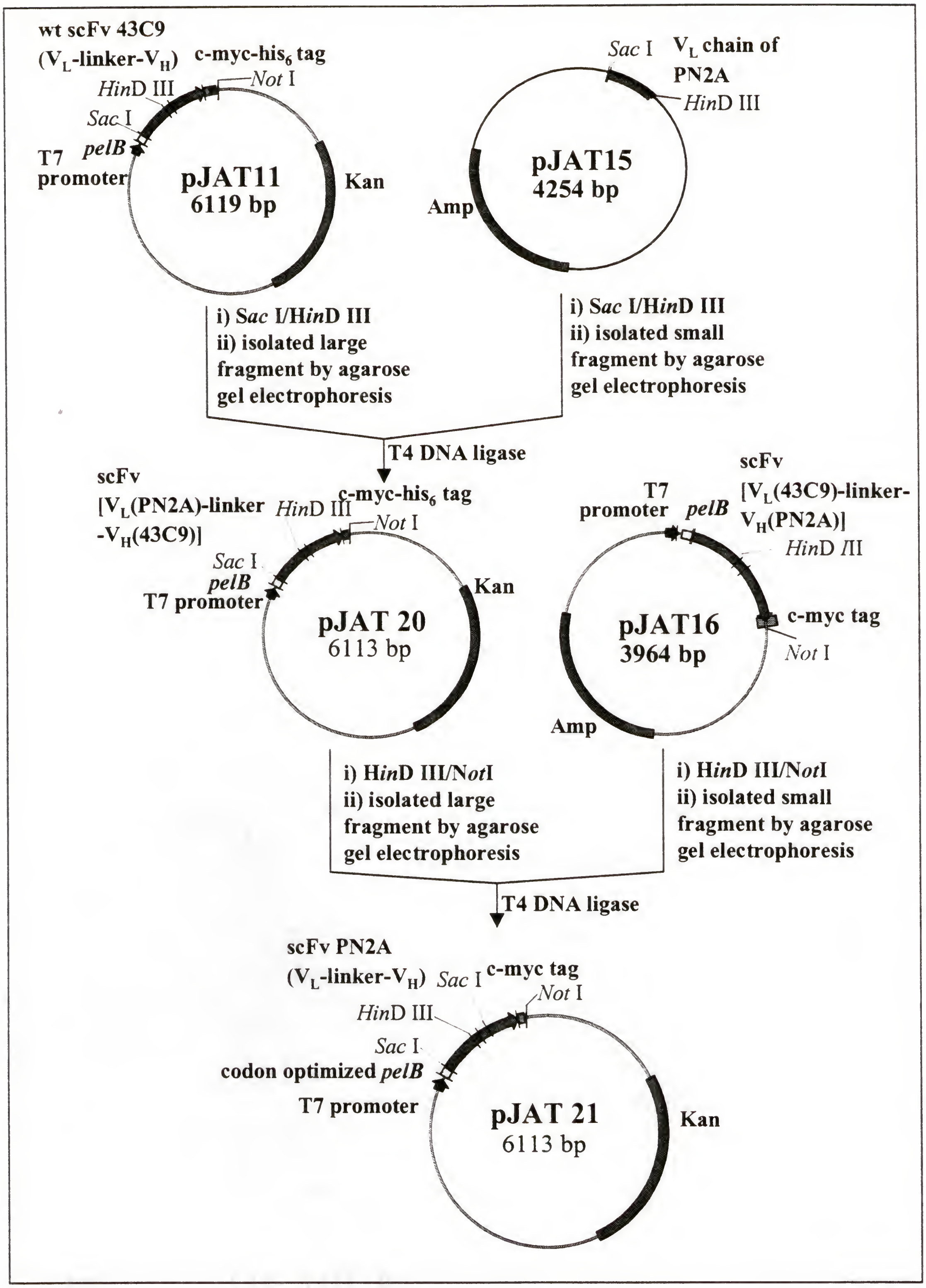

Figure 4-2. Construction of pJAT21.

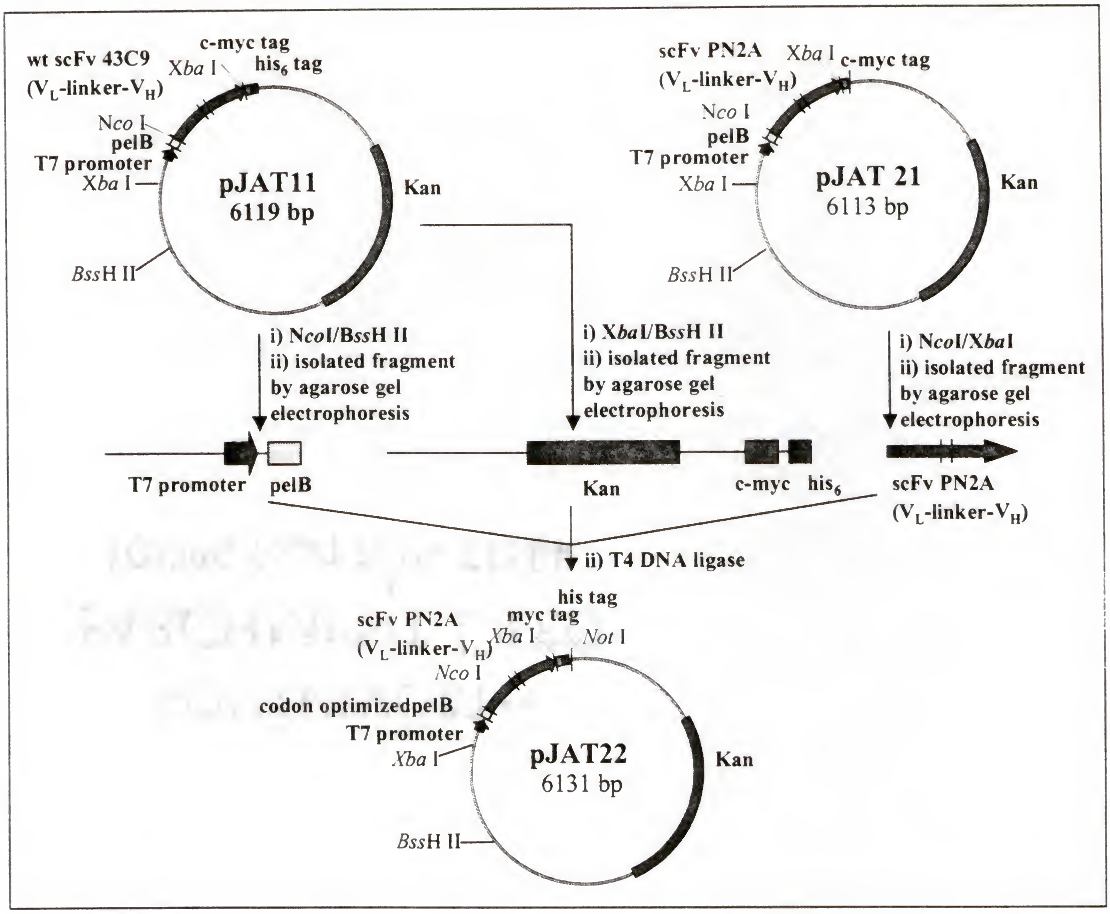

Figure 4-3. Construction of pJAT22.

Expression of scFv PN2A

scFv PN2A Expressed with a c-Myc Tag from pJAT21

Test inductions

Expression of scFv PN2A with a C-terminal tag using pJAT21 was examined in the growth media, the periplasm and total protein from cells boiled in loading buffer. SDS-PAGE analysis and western blots using an anti-*c*-myc monoclonal antibody in Figure 4-3 (lanes 1-3) showed that intracellular scFv represented the most significant amount of the scFv. Experience with the scFv 43C9 encouraged the isolation of scFv PN2A from *in vitro* refolding.

Lane	Sample
1	pJAT21 media
2	pJAT21 periplasm
3	pJAT21 cellular
4	myc and is tagged scFv marker
5	crude isolation from pJAT21
6	concen. crude isolation from pJAT21
7	open lane
8	concen. Crude isolation from pJAT21 non-reducing loading buffer

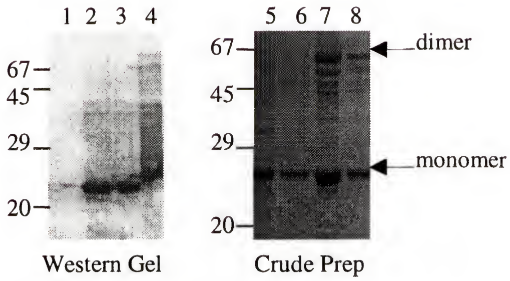

Western Gel
Test Inducitons

Crude Prep

Figure 4-4. Test inductions and isolation of the myc tagged scFv PN2A.

Batch refolding

ScFv PN2A with a C-terminal *c*-myc tag was batch refolded using conditions previously used as a standard procedure in the laboratory (Chapter 6, Experimental). This protocol was used because the optimization of the *in vitro* refolding of model scFv 43C9 was still in progress at the time. The crude protein obtained from the refolding process was chromatographed on a 4.6 x 200 mm PolyCAT-A column as described in Chapter 2. Unfortunately, little protein was retained and the scFv could not be isolated by this method.

The experiment was then repeated and the PolyCAT-A purification step was omitted in order to produce a crude sample of scFv PN2A to be tested by ELISA. The crude scFv PN2A was produced from batch refolding in a 14.2 mg yield (determined by a Bradford Assay) and is shown in lanes 5 and 6 of Figure 4-4. The crude preparation appeared to contain oligomers of the scFv as shown by the lack of monomeric scFv in lane 8 of Figure 4-4 under non-reducing conditions. Western bloting of the sample loaded in lane 8 indicated that under reducing conditions only monomeric scFv is present. This experiment indicates that the refolded crude scFv PN2A contains covalently-linked oligomers of scFv PN2A.

Expression of scFv PN2A with a *c*-Myc and His_6 Tag

Test inductions and isolation from *in vivo* isolation methods

Expression of the scFv PN2A with a C-terminal *c*-myc and hexahistidine tag was detected in the periplasm and within the whole cell; however, the protein was not recovered from the growth media (Figure 4-5, lanes 1 and 2). This indicated that scFv PN2A with a *c*-myc-his_6 tag was also expressed as insoluble aggregates in *E. coli* BL21(DE3).

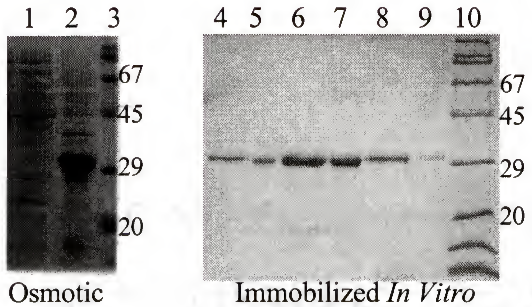

Osmotic Shock Prep

Immobilized *In Vitro* Refolding

Lane	Sample
1	pJAT22 soluble periplasmic scFv
2	pJAT22 insoluble periplasmic scFv
3	molecular weight marker
4-8	eluted myc and his tagged scFv PN2A
9	myc and his tagged scFv marker
10	molecular weight marker

Figure 4-5. Accumulation of scFv PN2A with c-myc and his_6 tag as inclusion bodies in BL21(DE3) cells and the eluted fractions of the immobilized *in vitro* refolding..

In vitro batch refolding

Attempts to isolate periplasmic scFv PN2A with a *c*-myc-his_6 tag using osmotic shock were unsuccessful. SDS-PAGE analysis of the insoluble debris produced from this method indicated that the scFv existed as an inclusion body (Figure 4-5, lane 2). These inclusion bodies were then refolded by immobilization on Chelating Sepharose® Fast Flow resin (Pharmacia Biotech) as described in Chapter 2 and Table 2-2. The insoluble scFv was dissolved in 6mL of 6 M guanidine-HCl, 0.1 M Tris-HCl, 0.5 M sodium chloride, 0.23 mM DTT, pH 8.0. The scFv loaded on the Fast Flow resin was refolded by passing two linear renaturation and oxidizing buffers as described previously. The scFv was eluted in 0.1 M Tris-HCl, 500 mM imidazole, pH 8.0, and the fractions containing the scFv were concentrated to 1 mL using ultrafiltration and introduced into 50 mM HEPES, 75 mM sodium chloride, pH 7.5 (Figure 4-5, lanes 4-8). The scFv stock was then centrifuged at 100,000 x *g* to remove insoluble precipitated material that appeared during dialysis, then the scFv PN2A with a c-myc-his$_6$ tag was tested using ELISA.

Binding Studies of scFv PN2A

ELISA screening

Ligand binding by the refolding scFv PN2A was studied by ELISA experiments completed by Michael DiGiovanna (Yale University). Various antigens listed in Table 4-3 carried by bovine serum albumin (BSA) were immobilized on plastic ELISA plates. The antigens were mixed with the refolded scFv PN2A and non-binding protein was subsequently removed by washing. Addition of an anti-*c*-myc antibody that bound immobilized scFv PN2A and colorimetric detection of the anti-*c*-myc antibody gave a qualitative indication of binding by the refolded scFv PN2A (Table 4-3).

Table 4-3. Binding study of scFv PN2A with c-myc-his$_6$ tag.

Ligand	Structure	ELISA
(phospho)-*neu*-erbB2 peptide	KTAENPE-(p)Y-LGLDVPV	YES
(phospho)-EGFR		YES
(phospho)-tyrosine	(p)Y	YES
(nonphospho)-*neu*-erbB2 peptide	KTAENPEYLGLDVPV	YES
BSA		NO

These results showed that the engineered scFv PN2A bound to several of the ligands tested. This promiscuity is unfortunate since the unique selectivity of the mAb for the phosphorylated *neu*-erbB2 peptide was one of the key attractions of this antibody.

Fluorescence studies

Fluorescence studies were also explored as a possible method to test ligand binding by the scFv PN2A. Evidence from ELISA that the scFv PN2A bound to free phospho-tyrosine suggested this commercially available compound might be a suitable ligand for fluorescence quenching. Unfortunately, excitation and emission UV scans showed that phospho-*O*-tyrosine at low concentrations exhibited a large fluorescence. Phospho-*O*-tyrosine concentrations less than 1% of the amount needed for scFv saturation had a nine fold larger emission than either the mAb or scFv itself. This ligand was not studied further.

The synthetic polypeptide antigen was next investigated for the ability to quench the intrinsic tryptophan fluorescence of mAb PN2A. Experiments in which 0.22 μM antibody was mixed with 3.7 μM phosphopeptide did not substantially reduce the antibody intrinsic fluorescence. The experiment was also reversed, and it was shown that the fluorescence of 3.5 μM of antigen was not quenched by several additions of mAb PN2A. These assays indicated that fluorescence quenching was not a reliable method for quantifying ligand binding by scFv PN2A, and alternative methods would have to be used in future studies.

Future Work to Increase the Binding Selectivity of scFv PN2A

Correcting the *pelB* Leader Sequence

The results from the ELISA experiments proved the binding selectivity the scFv PN2A with a *c*-myc-his$_6$ tag expressed from pJAT22 was broadened relative to the parent monoclonal antibody. This scFv construct contained an extra Met-Ala sequence at the N-terminal end of the V_L chain of the scFv. The N-terminus of this domain in the scFv construct ends at the face of the binding pocket, and extra amino acids in this area may disrupt the antigen-binding site. Constructing the scFv PN2A without these two residues could improve the selectivity of the scFv PN2A.

CHAPTER 5
CONCLUSIONS

Project Goal

Efforts to use antibodies for cancer prognosis and treatment have developed into areas of increasing interest. Tailored antibodies have the ability to target specific mechanisms of tumor cells for either diagnostic studies or therapeutic applications. This study has presented a model that can be used to guide these efforts to construct functional V_H disulfide-less scFv's.

Engineering the Model System scFv 43C9

An intracellular antibody can fold into an active structure in a reducing environment if the traditional stabilizing forces of disulfide bonds are replaced with other folding interactions. The model system scFv 43C9 was used in an attempt to produce a disulfide-less scFv by site-directed random mutatagenesis on the two pairs of cysteine residues involved in the disulfide bonds. The mutated chains were then paired with a wild-type domain. Chemiluminescent screening of the mutated V_H chain library produced ten engineered scFv's that retained antigen affinity. However, the mutated V_L domain library produced from this screening contained only scFv's with the two native disulfide bonds. Construction of a disulfide-less V_L chain requires additional mutations to increase the stability of this domain and to allow the removal of the disulfide bond.

Production of Disulfide-less Heavy Chain Mutants

In order to characterize the V_H disulfide mutant scFv's, a reliable method to produce and isolate the ten mutants was developed. Considering the number of scFv's in the V_H library and the modest amount of protein required for the binding and stability assays, *in vitro* refolding was chosen as an appropriate procedure. This method was optimized for the wt scFv 43C9 to produce functional protein in acceptable yields and at 1.5% of the cost for typical procedures found in literature.[48,57,58]

Characterization of the V_H Disulfide-less Mutants of scFv 43C9

Proportion of Functional Protein

The expression and isolation of the V_H mutant library was performed according to the refolding protocol that was optimized for the wt scFv 43C9. The concentration of each isolated mutant scFv was characterized by absorbance at 280 nm. This value of total protein was then compared to the concentration of scFv determined by fluorescence titration with the antigen. This relationship gave insight into the proportion of functional protein and corresponded to the stabilities of the mutants. The percentage of active protein can be used to divide the V_H mutants into three groups: Group 1, in which an acceptable portion of the total protein was active, ($\geq$80%); Group 2, in which a modest amount of the protein was functional (>30%) and Group 3, in which only a minimal amount of the scFv was functional ($\leq$15%).

Table 5-1. Grouping of V_H mutants on the basis of percentage of active scFv produced from refolding.

Group 1		**Percent Active Protein**	**Group 2**		**Percent Active Protein**	**Group 3**		**Percent Active Protein**
H22	H92		H22	H92		H22	H92	
Ala	Ala	100	Val	Leu	30	Leu	Pro	11
Cys	Pro	81				Phe	Ser	3.4
Cys	Ala	99				Thr	Pro	-
Ala	Thr	80				Arg	Ser	2.7
						Met	Pro	10

Binding Assays

The binding affinities of members of the V_H mutant library were characterized by dissociation constants (K_D) for the phosphonate antigen and the alcohol and acid products produced from the catalysis of ester hydrolysis by scFv 43C9.[67] These values were obtained from the quenching of the intrinsic fluorescence of each scFv by adding ligands. The plots of fluorescence quenching experiments are included in Appendix B. The quenching data obtained for the phosphonate antigen and *p*-nitrophenol were the most effective in comparing the binding affinities to the wt scFv 43C9 (Table 3-2). Fluorescence quenching behavior most resembling that of the wt scFv was observed for the Group 1 V_H mutants. The K_D values of the four mutants also proved that these scFv's maintained a binding pocket and ligand affinity similar to that of the wt scFv. The V_H mutants of Group 2 and Group 3 also exhibited fluorescence quenching; however, only two scFv's produced usable data. Both of these V_H mutants contained serine residues at H92. The intrinsic fluorescence of the remaining mutants in Group 2 and Group 3 was not quenched well by the addition of ligand. The characteristic of the fluorescence quenching is helpful in determining the V_H mutants that most closely resemble wild-type binding behavior.

Guanidine Denaturation Experiments

Stability studies

The four V_H mutants of Group 1 were tested for stability by denaturation experiments. As expected, all four disulfide-less V_H mutants were less stable than the wt scFv 43C9 (Figure 3-9). The C-H92-P mutant that represented a large portion of the V_H mutant library from the chemiluminescent screening also possessed the most stable folded structure of the mutants lacking a V_H disulfide bond. The C-H22-A, C-H92-A and C-H22-C, C-H92-T double mutants had similar stabilities and denaturation midpoints (Table 3-3). The least stable mutant in Group 1 was the C-H22-A, C-H92-T double mutant. The three amino acids Ala, Cys and Thr all have similar sizes and seem reasonable residues for the positions of the disulfide bond from a steric standpoint.

Classification of scFv 43C9 V_H mutants

Guanidine denaturation curves contributed to understanding the stability of the scFv's in this study. The steep slopes of the denaturation curves categorize these scFv's as Class I antibodies. The class system that was developed by Wörn and Plückthun indicates that this category contains scFv fragments that have one domain of higher stability than the partner chain.[47] The V_H mutated chain is obviously the less stable partner, but this information also underscores the requirements for a stable light chain in scFv 43C9. This classification further suggests that the scFv can not sustain a destabilized light chain, which is consistent with our inability to produce functional disulfide-less V_L mutants. Therefore, the light chain will require other stabilizing forces to fold in a functional form without disulfide bonds. This need for additional adjustments to produce a disulfide-less scFv 43C9 makes this model scFv a realistic example of the process required to remove the stabilizing forces of disulfide bonds from scFv's.

Engineering Monoclonal Antibody PN2A

Construction of scFv PN2A and Binding Studies

Engineering of the monoclonal antibody (mAb) PN2A began with the construction of the scFv fragment. This was completed by PCR amplification of the DNA's encoding the Fab and F_v fragment from the cDNA of the monoclonal antibody. The F_v genes for the V_H and V_L domains were isolated and introduced into a scFv construct. ELISA studies of the scFv PN2A with a *c*-myc and his_6 tag determined that the scFv not only bound the antigen of mAb PN2A, but also recognized other related antigens. The scFv binding was extended to the (phosho)-*neu*-erbB2 peptide (the antigen), (phospho)-EGFR, (phospho)-tyrosine and *neu*-erbB2 peptide.

Tailoring the Binding of scFv PN2A

Future experiments must attempt to increase the binding specificity of the scFv to that of the monoclonal antibody. Binding selectivity is predicted to improve once the extra Met-Ala residues at the N-terminal end are removed. This will be completed by expressing the scFv with an altered *pelB* sequence that is completely cleaved from the scFv by signal peptidases during expression.

Long-Term Goal of the Project

Once the model system is completed and a disulfide-less scFv 43C9 retains binding and stability, this model will be invaluable in the field of antibody construction.

The process optimized for scFv 43C9 can then be used as a guide to transform any scFv into a disulfide-less antibody. Mutations at residues that favor a disulfide-less scFv include the cysteine positions of the disulfide bonds within the conserved β-sheets and other positions that can increase protein stability and binding. The ability of the model scFv 43C9 to represent the general structure of common antibody fragments will be illustrated by converting scFv PN2A into a cytoplasmic antibody fragment and an intracellular probe.

CHAPTER 6
EXPERIMENTAL

Molecular Biology

Biochemicals and Media

Bacto Tryptone, Bacto Yeast Extract and Bacto Peptone were purchased from Difco. Ampicillin was obtained from Promega. Kanamycin and tetracyclin were purchased from Sigma.

Restriction endonucleases were purchased from New England Biolabs or Promega. T4 DNA ligase was obtained from New England Biolabs. Oligonucleotides were obtained from Integrated DNA technology or Gemini Biotechnology. *Taq* polymerase, PCR and sequencing grade, as well as the DNA Silver Sequencing kit were purchased from Promega. Agarose was obtained from Kodak.

Vectors

E. coli cloning plasmids pUC18, pVH-XX and pVL-XX were from the laboratory collection and pCR2.1TOPO was purchased in a TOPO TA Cloning Kit from Invitrogen. *E. coli* expression vectors pJDS118, pTG119 and p4.1 were obtained from the Benkovic laboratory and pET22b-(+) was purchased from Novagen. The Ohtsuka laboratory donated the *E. coli* expression vector pT7-64M5HL-15myc that provided the scFv construct with a *c*-myc tag.

Primers

Polymerase chain reactions (PCR) using primers designed for specific steps in the project were routinely ordered from Integrated DNA Technologies, Inc. (IDT) or Gemini Biotech. Primers used to amplify the scFv PN2A gene were adopted from the Benkovic laboratory or purchased from IDT.

Conditions for PCR

PCR was carried out with 100 μL mixtures as described in Sambrook *et al.* and contained 1 μg of template DNA and 0.1 μg/μL of each primer. The reactions were subjected to 28 cycles of 94°C for 4 min, 94°C for 1 min, 52°C for 2 min, 72°C for 3 min and 72°C for 10 min and then maintained at 4°C.

E. coli Strain Genotypes

E. coli strains XL1-blue and JM109 were used for routine cloning procedures while BL21(DE3) and AD494(DE3)pLysS were used for protein expression.

Table 6-1. *E. coli* strains used in this work and their genotype.

E. coli strain	Genotype
XL1-blue	F'::Tn*10* *proA*$^{+}$*B*$^{+}$ *lacI*^{q} *Δ(lacZ)M15/ recA1 endA1 gyrA96* (Nal^{r}) *thi hsdR17* (r_K^{-} m_K^{+}) *supE44 relA1 lac*
JM109	F' *traD36 lacI*^{q} *Δ(lacZ)M15 proA*$^{+}$*B*$^{+}$/ e14^{-}(McrA^{-}) *Δ(lac-proAB)* *thi gyrA96* (Nal^{r}) *recA1 endA1 hsdR17* (r_K^{-} m_K^{+}) *supE44 relA1*
AD494(DE3)pLysS	Δara^{-} leu7697 ΔlacX74 ΔphoApvuII phoR ΔmalF3 F'[lac^{+}(lacI^{q})pro] trxB::kan(DE3) pLysS
BL21(DE3)	F^{-} *ompT [Ion] hsdS*$_{B}$ (r_B^{-} m_B^{-}; an *E. coli* B strain) with DE3, a λ prophage carrying the T7 RNA polymerase gene.

Maintenance of *E. coli* Strains

Standard media (LB) and techniques for routine growth and maintenance of *E. coli* strains were used.[107] Recipe per liter: Bacto Tryptone (10 g), Yeast Extract (5 g), and sodium chloride (10 g). For solid media, agar (15 g) was included. When appropriate, antibiotics were added at final concentrations of 200 ug/mL ampicillin, 30 ug/mL kanamycin and 10 ug/mL tetracyclin.

For short term storage, bacterial strains were kept on plates sealed with parafilm at 4°C. For long term storage, strains were stored at –80 °C in media containing 15% glycerol.

Recombinant DNA Techniques

Recombinant DNA procedures were carried out essentially as described by Sambrook *et al.*[107] PCR amplification was carried out using a Perkin-Elmer Geneamp PCR system 2400, and products were purified by agarose gel electrophoresis and digested with appropriate restriction enzymes for cloning into the desired vector. Restriction enzyme digestions were checked by DNA gel electrophoresis. DNA agarose gel electrophoresis was carried out as described by Sambrook *et al.*[107] The desired DNA fragment was isolated from the digestion reaction using DNA gel electrophoresis. The DNA fragment was than excised from agarose gel, and the DNA was extracted from the gel slice according to Sambrook *et al.*[107] *E. coli* transformations were carried out using calcium chloride transformation or electroporation.[107] Purified DNA was obtained by either density gradient ultra-centrifugation with CsCl in presence of ethidium bromide (plasmids pJAT1 and pJAT2) or by means using Clontech, QIAGEN or

Promega midiprep kits (remaining plasmids). DNA sequencing was accomplished using the Silver Sequence kit, according to the manufacturer's instructions, or off-site by the ICBR DNA sequencing core laboratory or The Center for Mammalian Genetics at the University of Florida.

Test inductions of expression plasmids

Materials and Equipment

Media used from expression was the same as described in Molecular Biology. Culture optical densities (OD) were determined at A^{600} using a Cary 118 spectrophotometer. SDS-PAGE gel electrophoresis and western blots were completed using electrophoresis units purchased from Bio-Rad.

General

Test inductions to examine expression of the desired protein were performed to determine the amount and location of the protein. Protein expression was analyzed for secretion into the media, for transport into the periplasm, or for retention within the cell.

Experimental Procedures

Induction

Overnight cultures of BL21(DE3) with the appropriate plasmid(s) were diluted 1:100 and grown to an OD^{600} of 1.0. These cultures were then induced with 0.1 mM IPTG and 1 mL samples were taken at the desired time points. These samples were centrifuged and the media was removed, then both the cell pellet and media were frozen at –20°C until samples were worked up.

Sample preparation

The media samples were centrifuged multiple times to ensure that all cell debris was removed. The proteins were precipitated from the supernatant by adding trichloroacetic acid (TCA) to a final concentration of 5%, incubating on ice for 15 min, and then micro-centrifuging for 15 min at 4°C. The pellet was dissolved in 20 µL 10 mM Tris-HCl, pH 7.0 with loading buffer and titrated to a basic pH, indicated by a blue color, with 1.5 M Tris-HCl, pH 8.8.

Periplasm fractions were analyzed by disruption of the outer membrane by $CHCl_3$ shock.[102] This was carried out by treating the cell pellet from a 1 mL of culture with 20 µL of $CHCl_3$ and incubating at room temperature for 20 min. The proteins were then extracted into 100 µL 10 mM Tris-HCl, pH 7.5 and pelleted by micro-centrifugation for 15 min at 4°C.

Total cellular protein was prepared by resuspending the cells from a 1 mL culture sample in 80 µL of water. SDS-PAGE loading buffer was then added (20 µL) and the cells were lysed by boiling the samples for 5 min.

Samples loaded into the gel for separations were prepared from dilutions of the above stocks to a final volume of 10 µL. The volumes of the stocks used in the dilutions were as follows: growth media (6 µL), periplasmic space (4 µL) and boiled cells (2 µL).

Separation by gel electrophoresis

Samples were separated on 12% SDS-polyacrylamide gels as described by Sambrook *et al.*[107] Loading buffer was added to samples and these were boiled for 1 min to denature the proteins. Gels were stained with Coomassie Brilliant Blue R for 20 min at room temperature and destained overnight.

Western blots

Two identical SDS-PAGE gels were run. One gel was stained with Coomassie Blue to ensure that the samples were resolved. The second gel was used to transfer the proteins to nitrocellulose for Western blotting as described by Sambrook *et al.*[107] Visualization of proteins with a *c*-myc tag was completed by exposing the nitrocellulose to the following agents: 5 ng/μL of *c*-myc (Ab-1) monoclonal mouse IgG (Calbiochem), 8.67 μL of anti-Mouse IgG (Fc specific) alkaline phosphatase conjugate (Sigma) diluted with 10 mL blocking solution and 20 mL of TBS (0.02 M Tris-HCl, 0.5M sodium chloride, pH 7.5), 36.7 mM Nitro BT and 69.2 mM 5-bromo-4-chloro-3-indolyl phosphate *p*-toluidine salt (Fisher Scientific).

Materials and Equipment

Media used for expression of scFv fragments was prepared as described in Molecular Biology except Na-MOPS (10 g/L, pH 7.5) which was added for cultures in which the scFv was secreted into the media. Dilute protein solutions were concentrated using a trangential flow apparatus (Minitan^{TM} Ultrafilitration system, Millipore) equipped with 10,000 NMWL low binding regenerated cellulose membranes or an Amicon system using YM-10 membranes. Preparative (250 x 21.0 mm) and analytical (200 x 4.6 mm, 12 μm, 300 Å) polyCAT-A columns purchased from the Nest Group were used with an FPLC (Pharmacia) system. This same system was also used for the various nickel columns (HiTrap® Chelating resin (Pharmacia), FreeZyme Conjugate Purification Kit (Pierce), or Chelating Sepharose® Fast Flow resin (Pharmacia)). Efforts to purify the scFv's with *c*-myc-his$_6$ tags used MonoS and MonoQ ion exchange columns purchased from Pharmacia. Buffers, salts and glycerol were typically purchased from Fisher Scientific.

General

Wild-type scFv 43C9 was isolated from the growth media of BL21(pTG119, pJS118) cultures as described previously.[7] Protein isolation from the periplasm was also attempted for many strains. ScFv's carrying a *c*-myc or *c*-myc-his$_6$ tags was isolated from the whole cells as inclusion bodies.

Experimental Procedures

Isolation from media. Recovery of scFv fragments from the growth media was carried out according to Stewart, J. D. *et al.*[7]

Isolation from periplasm using osmotic shock.[95] One-liter cultures were induced overnight at room temperature with 0.1 mM IPTG. The cultures were then centrifuged at 7,000 x *g* for 20 min. The cell pellet was resuspended in 40 mL of cold 0.01 M Tris-HCl, pH 8.1 and centrifuged at 7,000 x *g* for 20 min. This process was repeated two more times. The cell pellet was then gently resuspended in 80 mL of 0.03 M Tris-HCl, 0.001 M disodium ethylenediamine tetraacetate (EDTA), 20% sucrose, pH 8 at 24°C per 1 g of cells. The mixture was rotated on a shaker in a 1 L flask at 180 rpm for 10 min at 4°C. The mixture was centrifuged at 13,000 x *g* for 10 min and the supernatant was decanted rapidly. Cold water in the same volume as the sucrose solution above was added to the pellet. The mixture was swirled to suspend and left to rotate on a shaker at 500 rpm for 10 min at 4°C. The solution was then centrifuged at 13,000 x *g* for 10 min at 4°C. The periplasmic protein in the supernatant was then concentrated by ultrafiltration. The protein mixture was placed into the starting buffer for chromatography by dialysis.

Isolation of the scFv was completed on an analytical polyCAT-A column as described by Stewart, J. D. *et al.*[7].

Isolation from the whole cell. Two 1 L cultures were induced for expression with 0.1 mM IPTG overnight at room temperature. The cultures were centrifuged 6,000 x *g* for 20 min. The cell pellet was re-suspended in 20 mL of 50 mM Tris-HCl, 1 mM EDTA, 1 mM DTT, 1 mM PMSF, pH 7.5 and lysed by either sonication or using a French Pressure Cell. To ensure complete lysis of this large culture, lysis using a French Press maintained at 10,000 psi was preferred. The lysed mixture was then centrifuged at 7,000 x *g* for 20 min.

In vitro refolding of the lysed mixture on the Ni(II) solid support is described in Chapter 2 (Immobilized refolding of over-expressed scFv 43C9). The refolded scFv eluted from the Ni(II) column was identified using Bradford assays.[108] These fractions were then concentrated using the Amicon system, and the stocks were analyzed by SDS-PAGE.

In vitro batch refolding of the lysed mixture is presented in Chapter 2 (Design of batch refolding procedure for wt scFv 43C9). Proteins eluted from the PolyCAT-A were detected by an absorbance at 280 nm, and the scFv fractions were identified by SDS-PAGE. These fractions were then concentrated using the Amicon system.

Protein Concentration

Protein concentrations of purified scFv's were determined from A^{280} measurements using an extinction coefficient of 48,500 L/mol·cm.[61] A Bradford assay[108] of the crude protein samples allowed determination of the total protein present during protein purification steps.

Molecular Weight Determination by Size Exclusion

Materials and equipment

Gel filtration chromatography was carried out using Sephadex G-75 Superfine, (Pharmacia) resin in a 60 mL column (30 cm x 1.5 cm). The elution buffer was 50 mM HEPES, 75 mM sodium chloride, 5% (v/v) glycerol, pH 7.5. The void volume was determined from the elution volume of Blue Dextran (1 mg/mL, Pharmacia). The standard curve for the column was generated from the following proteins obtained from Sigma: bovine albumin (5 mg/mL), carbonic anhydrase (2 mg/mL), myoglobin (2 mg/mL) and cytochrome C (2 mg/mL).

Experimental procedure

The resin was prepared according to the manufacture's recommendation. All samples were loaded in volumes <2% of the column volume. The samples were separated at a flow rate of 1 mL/min. The eluted protein was detected by absorbance at 280 nm. The void volume (V_o) was initially determined, and then a mixture of the four standard proteins was analyzed. The elution volumes (V_e) were determined, and the V_e/V_o versus the molecular weight for each standard was plotted. This plot was used to determine the molecular weight for the V_e/V_o of each scFv sample.

The percent of protein present at the each molecular weight was determined by comparing the peak areas. This was carried out by cutting out each peak and weighing it on a micro-balance (Cahn). The values for the protein fraction presented in Table 2-3 of Chapter 2 were calculated by dividing the individual peak weight by the total weight of all the eluted peaks.

Assays for scFv 43C9 Activity and Binding

Kinetic Assays

Materials and equipment

Kinetic experiments were performed on either Cary 118 or Olis Cary-14 spectrophotometers. Assays were conducted in 1 mL quartz cuvettes with a pathlength of 1 cm. The hydrolysis mixtures contained the assay buffer of 40 mM HEPES, 20 mM sodium chloride, pH 7.5, the dissolved substrate, and the isolated wt scFv 43C9. Substrates were dissolved in 1:1 dioxane:1 mM sodium acetate and stored at 4°C. Antibody stocks were maintained in the working buffer and stored at 4°C.

Experimental procedure

Hydrolysis reactions were monitored for initial rates at 25°C.[64,66,96] Catalyzed reactions were corrected for background hydrolysis by monitoring reaction velocities without wt scFv 43C9.

Fluorescence Assays

Materials and equipment

Antibody quenching and denaturation experiments were performed on a Perkin Elmer Luminescence Spectrometer LS50B. Samples were excited at 270 nm and the emission was collected from 300 to 400 nm. The maximum emission was typically observed at 340 to 350 nm. The instrument was set for a slit width of 5 and a scan time of 50. Titration and quenching assays incorporated an assay buffer of 50 mM HEPES, 75 mM sodium chloride, 5% (v/v) glycerol, pH 7.5 that was filtered and degassed under vacuum for 20 min. Ligands were stored at -20°C in the assay buffer. The antibody stocks were kept at 4°C in the assay buffer. Denaturation experiments were completed with 6 M guanidine-HCl diluted to the appropriate working concentration with 40 mM HEPES, 20 mM sodium chloride, pH 5.8. Mixtures were analyzed in 3 mL quartz cuvettes.

Experimental procedure

Titration and quenching assays were completed at 25°C. The background buffer emission was recorded from 300 to 400 nm using 3 mL of buffer. The emission spectrum was then determined for the scFv in a total volume of 3 mL. The amount of antibody used in the fluorescence assay typically produced 100 fluorescence units. After the maximum emission wavelength was determined for the sample, readings were taken at that emission wavelength from an excitation at 270 nm. At this point, the cuvette was not removed from the fluorometer until the assay was complete, and a non-transparent filter was used to eliminate photobleaching when the fluorescence was not recorded. The ligand was added to the assay mixture in minimum volumes not exceeding 10 µL per addition. The assay solution was then mixed gently by paddling and was allowed to equilibrated for 2 min before fluorescence readings were taken. Three fluorescence readings were recorded for each ligand addition. The assay samples were inspected for precipitation before the ligand was added and after the scFv was completely quenched. The emission pattern from 300 to 400 nm for the completed quenched scFv assay mixture was also recorded.

Photobleaching experiments were carried out as described above without ligand addition and sample mixing. Inner filter effects were determined by adding ligand to

0.83 mM tryptophan. This assay was carried out in the same manner as the method described for the quenching experiments.

Guanidine denaturation experiments were performed on mixtures that contained the appropriate amount of scFv to give a fluorescence of 100 units, 6 M guanidine and the assay buffer described above. These samples were kept at 10ºC overnight to reach the unfolding equilibrium. The various guanidine concentrations used to create the unfolding equilibrium were prepared in triplicate. The fluorescence of each sample was measured at an excitation wavelength of 270 nm and an emission wavelength at the maximum determined by the quenching experiment. The samples were introduced into a 3 mL quartz cuvette at 10°C, protected with the non-transparent filter and allowed to equilibrate for 1 min. Samples at each guanidine concentration were then tested for fluorescence, and five readings were taken for each of the three prepared samples. This data was then averaged and plotted against the respective guanidine concentration.

Organic Synthesis

Chemicals and General Procedures

Reagents were purchased from Aldrich and were used as received. Unless otherwise specified, reactions were carried in flame dried glassware, using dry solvents, and under an inert atmosphere of argon. Flash column chromatography was carried out using 60 Å silica gel. Thin layer chromatography was performed on pre-coated plates of silica gel (60 Å) from Aldrich and products were identified using phosphomolybdic acid as an indicator.

Product characterization was completed with ^{1}H NMR and ^{13}C NMR. NMR spectra were taken on a Gemini or VXR300 instruments operating at 300 MHz. Spectra obtained in $CDCl_3$ were referenced to residual $CHCl_3$ (7.26 ppm) for ^{1}H NMR and to $CDCl_3$ (77.0 ppm) for ^{13}C NMR and spectra obtained in DMSO were referenced to residual DMSO-d_6 (2.5 ppm) for ^{1}H NMR, and to DMSO-d_6 (39.52 ppm) for ^{13}C NMR .

Synthesis of Substrate[62]

The p-chlorophenyl ester (compound 1) was synthesized according to Gibbs *et al.*[62]

APPENDIX A
EXPLANATION OF ABBREVIATIONS

Intrabody Antigens

Antigen	Description
ADH I	alcohol dehydrogenase I
HIV-I	human immunodeficiency virus type-1
Interleukin 2	cytokine of central importance to the immune system
NGF	nerve growth factor
ErbB-2	type I oncoprotein/epidermal growth factor receptor
p21^{ras}	oncoprotein involved in meiotic maturation
L-NFMP	N-phenyl methionine ester
Anti-Viral	intracelluar plant virus
Oxabicyclic Hapten	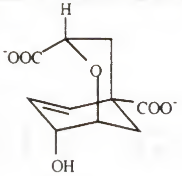

Amino Acid Nomenclature

Name	Symbol	Letter	Name	Symbol	Letter
Alanine	Ala	A	**Methionine**	Met	M
Cysteine	Cys	C	**Asparagine**	Asn	N
Aspartate	Asp	D	**Proline**	Pro	P
Glutamate	Glu	E	**Glutamine**	Gln	Q
Phenylalanine	Phe	F	**Arginine**	Arg	R
Glycine	Gly	G	**Serine**	Ser	S
Histidine	His	H	**Threonine**	Thr	T
Isoleucine	Ile	I	**Valine**	Val	V
Lysine	Lys	K	**Tryptophan**	Trp	W
Leucine	Leu	L	**Tyrosine**	Tyr	Y

APPENDIX B
FLUORESCENCE QUENCHING PLOTS

For the plots presented in this section, the X-Axis is the concentration of ligand added (units are nM for antigen quenching plots, μM for p-nitrophenol quenching plots and μM for acid product quenching plots.) The Y-Axis is fluorescence units. The antigen quenching plots also include the concentration of scFv used for the assay.

Ala-H22 Antigen Quenching [scFv]=0.219 μM
Ala-H92

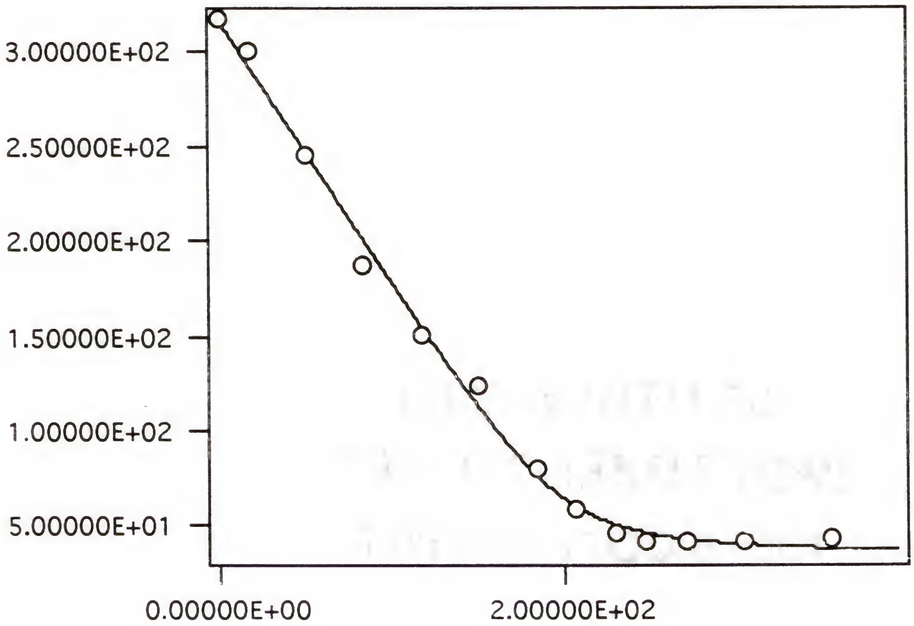

Ala-H22
Ala-H92

Antigen Quenching [scFv]=0.0218 μM

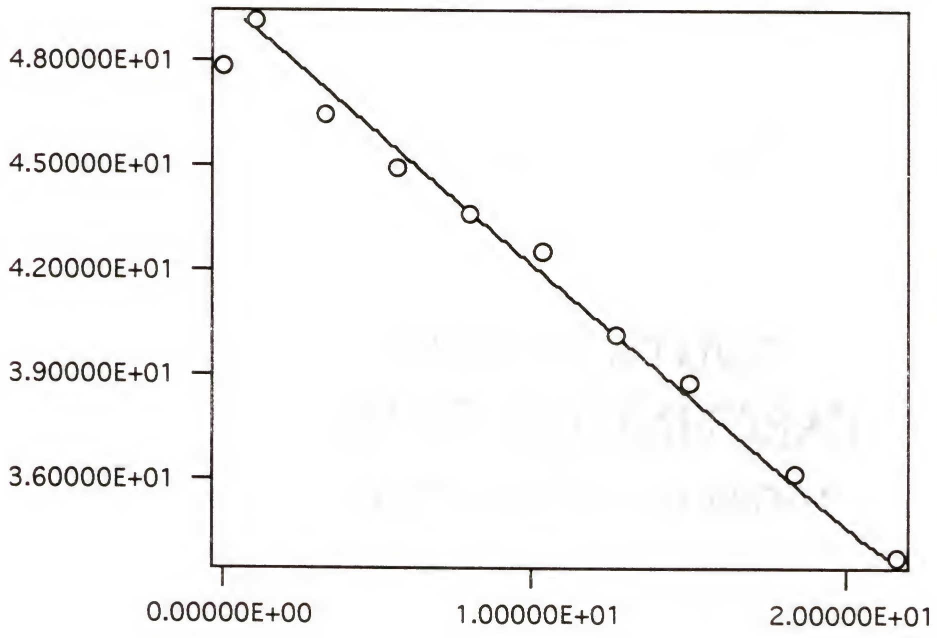

Ala-H22
Ala-H92

p-Nitrophenol Quenching

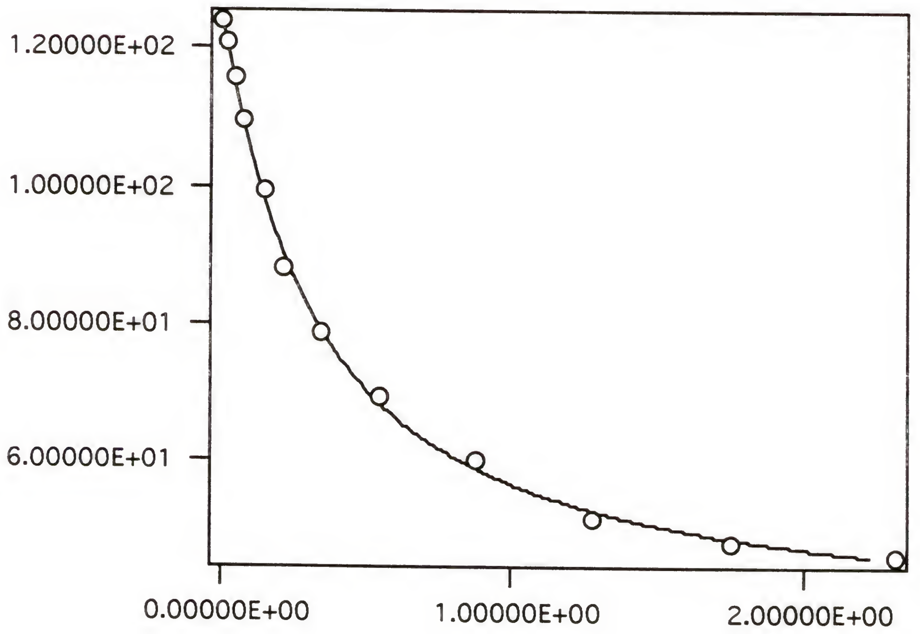

Ala-H22 Acid Product Quenching
Ala-H92

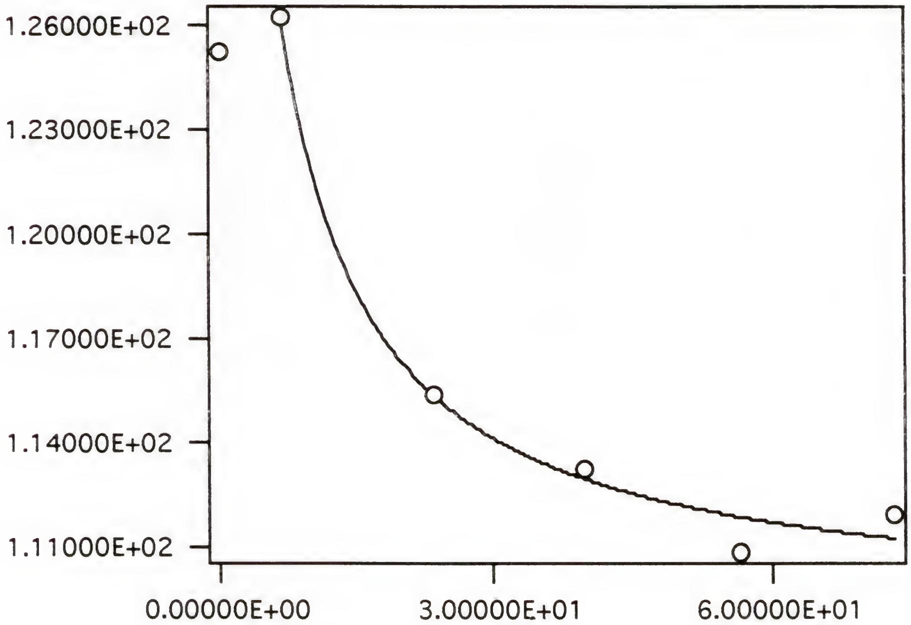

Cys-H22 Antigen Quenching [scFv]=0.0226 μM
Pro-H92

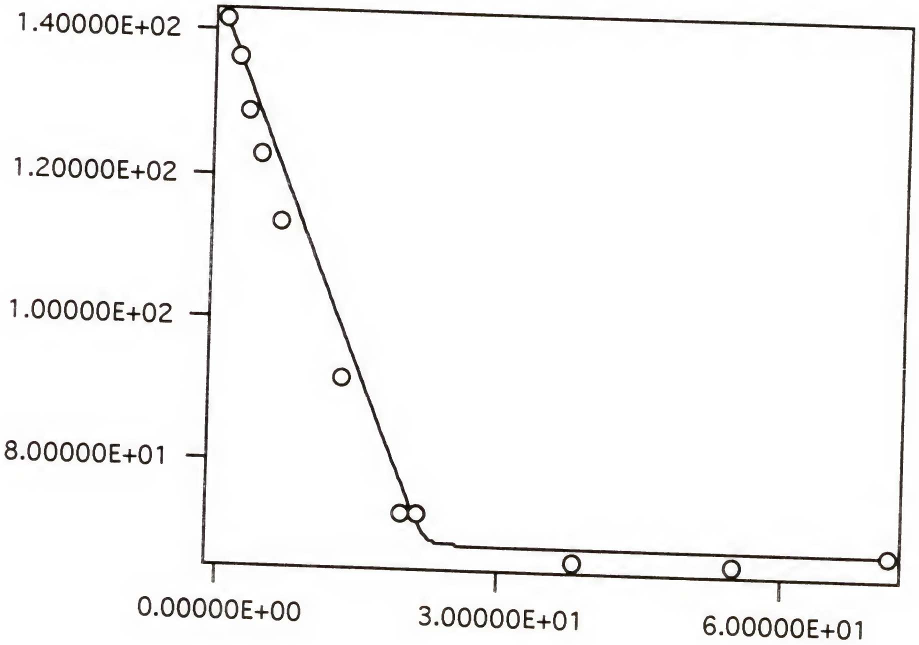

Cys-H22 p-Nitrophenol Quenching
Pro-H92

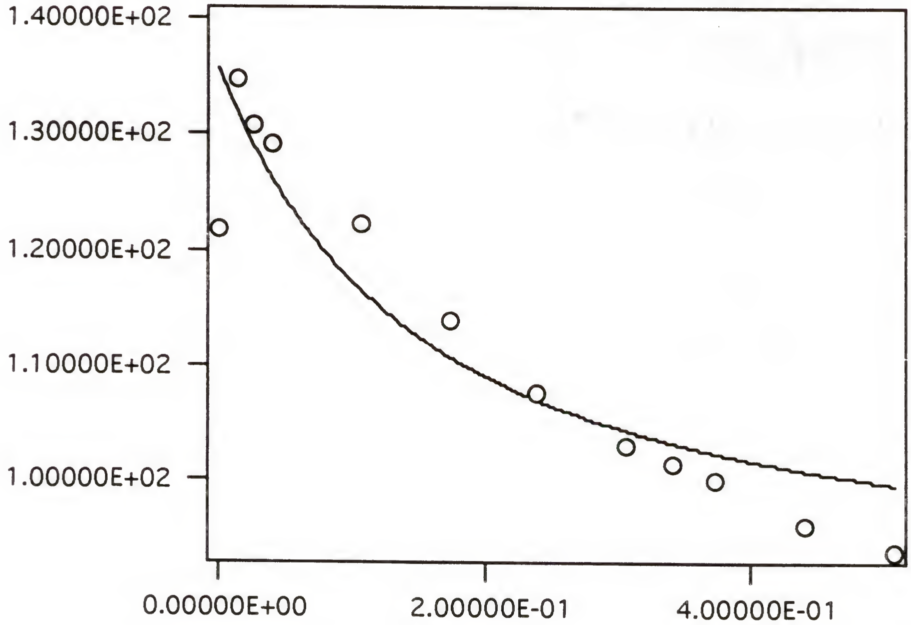

Cys-H22 Acid Product Quenching
Pro-H92

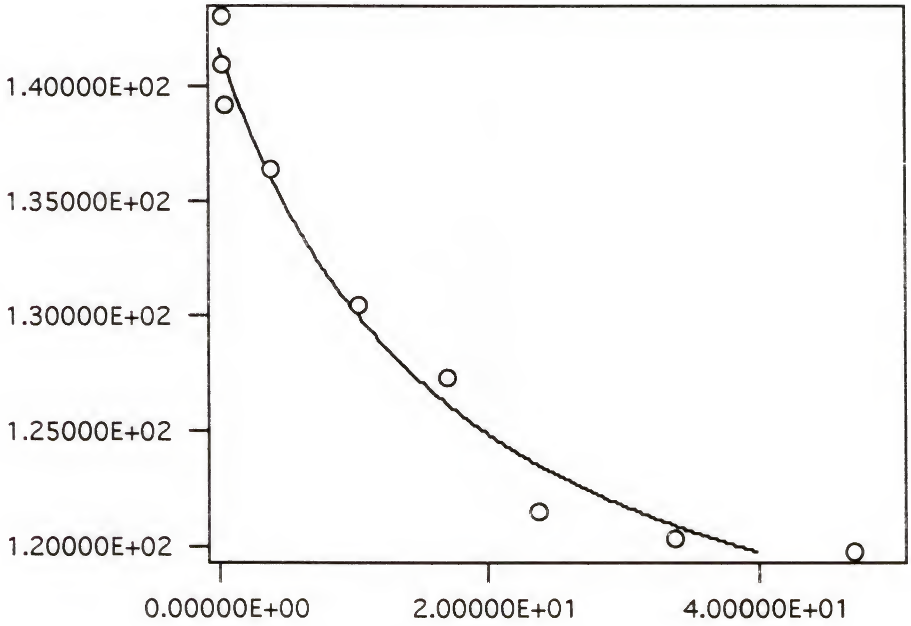

Cys-H22 Antigen Quenching [scFv]=0.0130 μM
Ala-H92

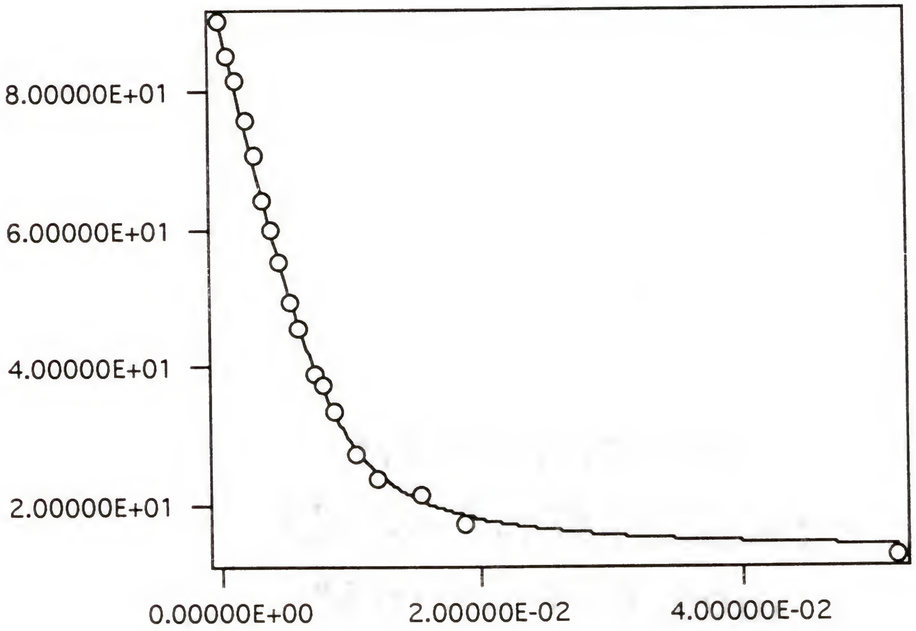

Cys-H22 p-Nitrophenol Quenching
Ala-H92

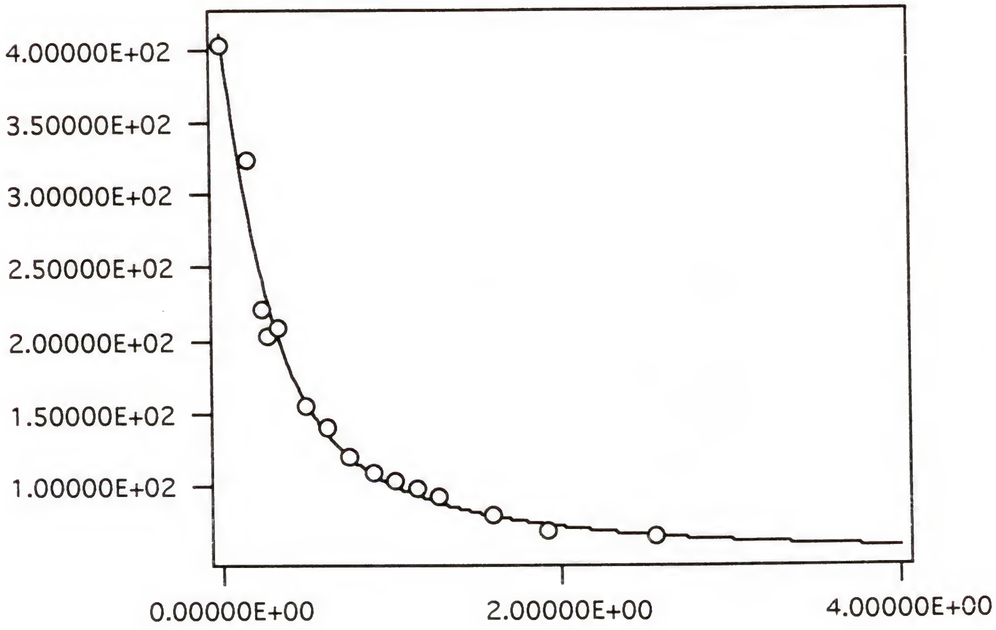

Ala-H22
Thr-H92

Antigen Quenching [scFv]=0.0042 μM

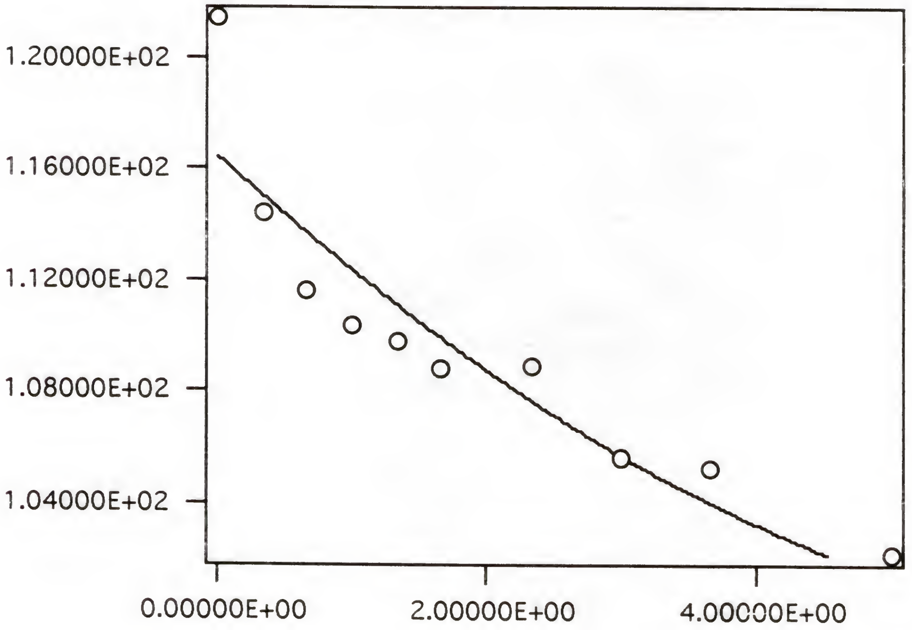

Ala-H22
Thr-H92

p-Nitrophenol Quenching

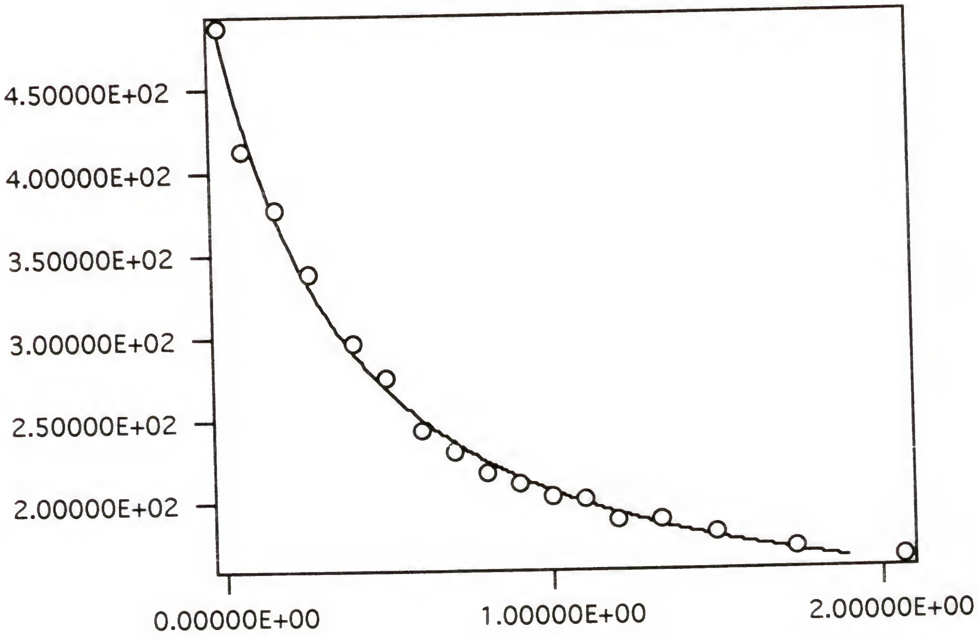

Val-H22 Antigen Quenching [scFv]=0.0874 μM
Leu-H92

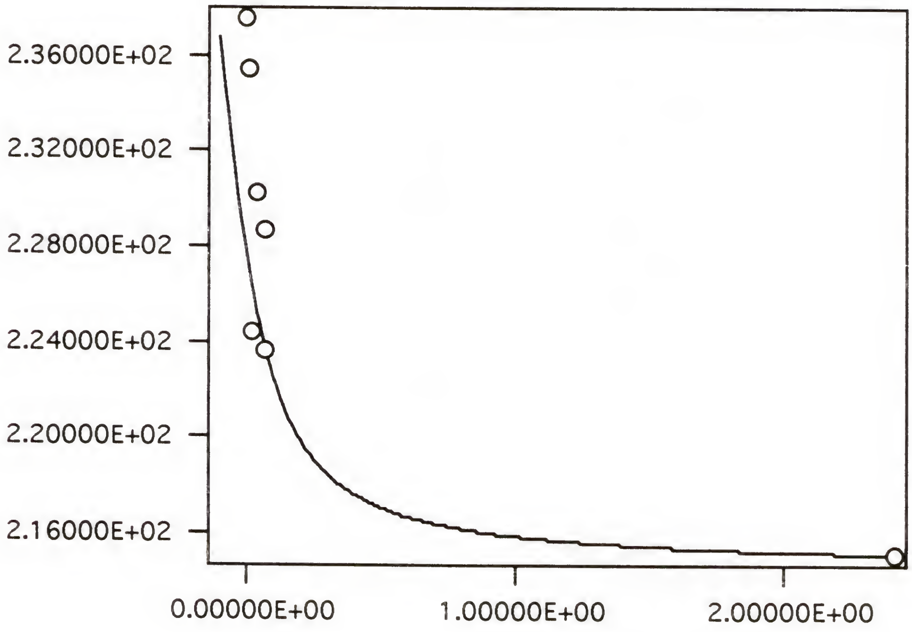

Val-H22 p-Nitrophenol Quenching
Leu-H92

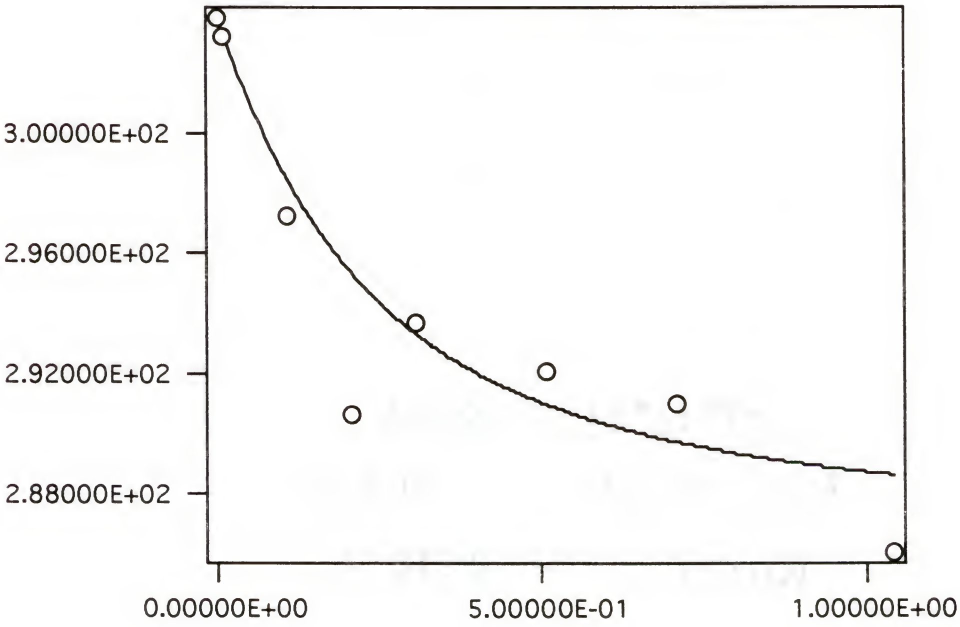

Val-H22 Acid Product Quenching
Leu-H92

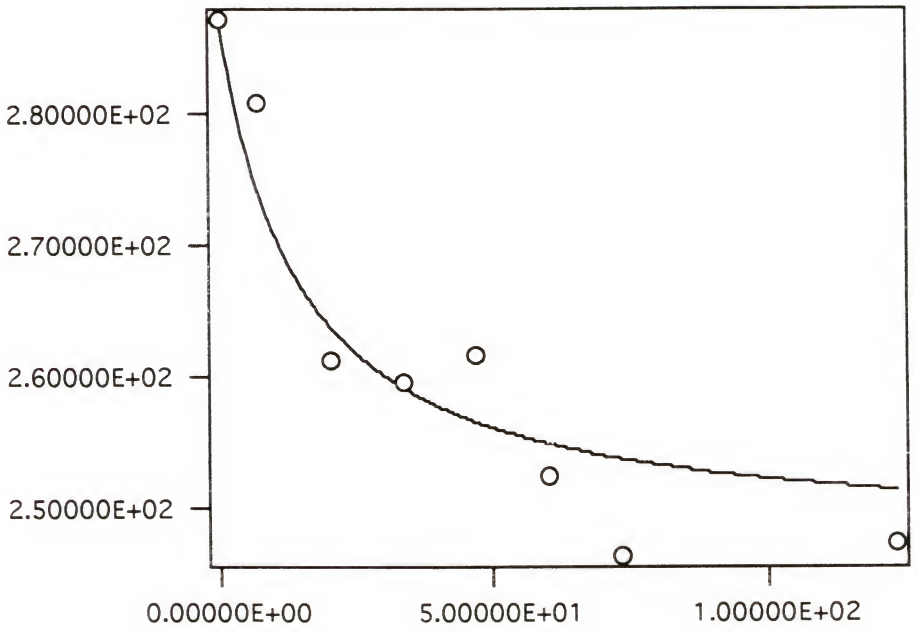

Arg-H22 Antigen Quenching [scFv]=0.00257 μM
Ser-H92

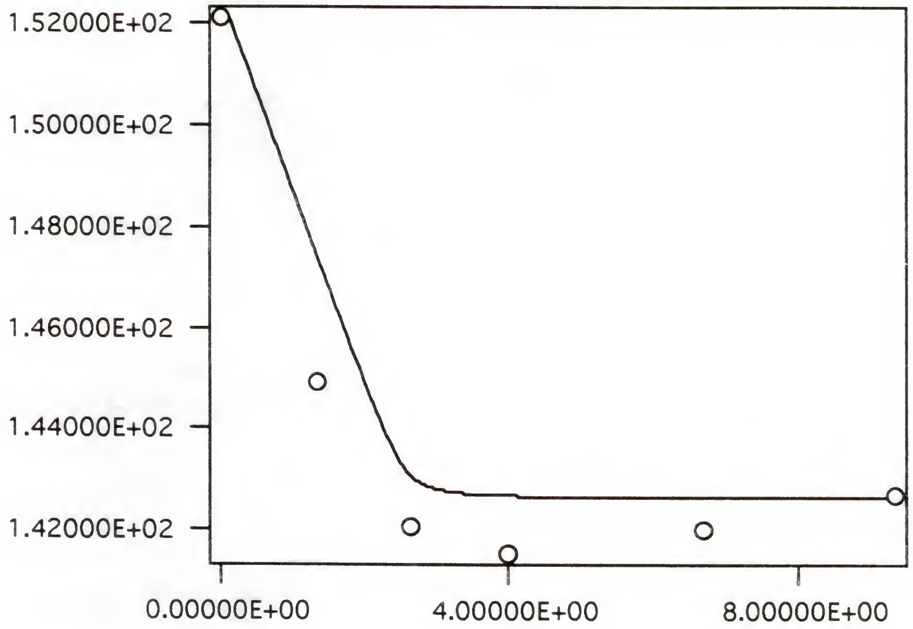

Arg-H22 p-Nitrophenol Quenching
Ser-H92

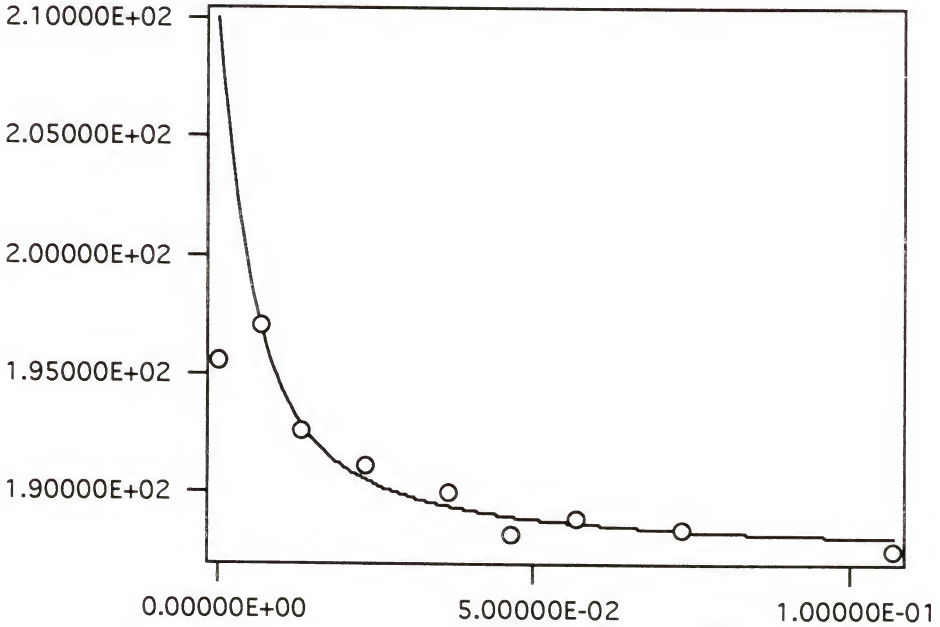

Arg-H22 Acid Product Quenching
Ser-H92

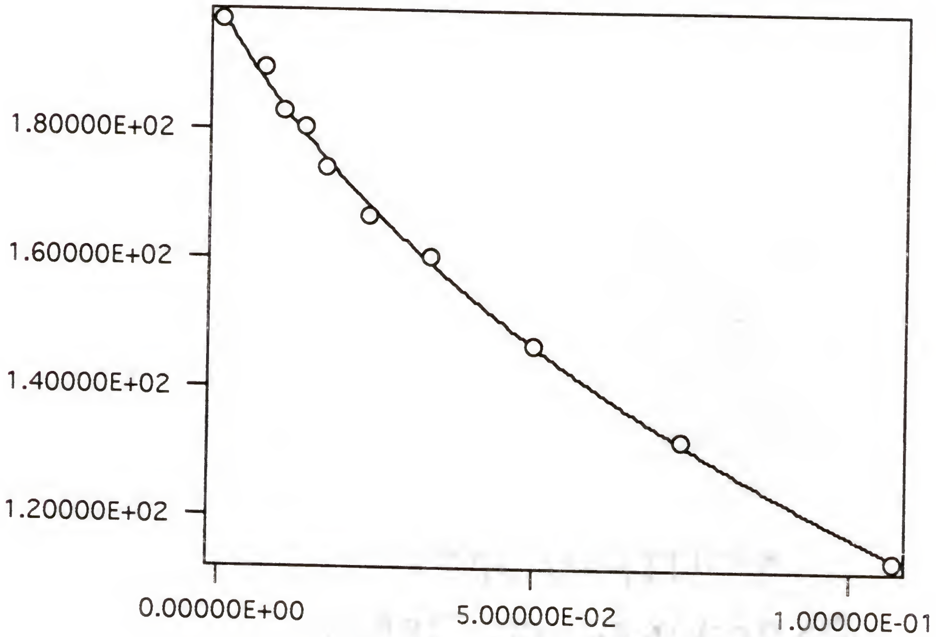

Phe-H22
Ser-H92

Antigen Quenching [scFv]=0.0064 μM

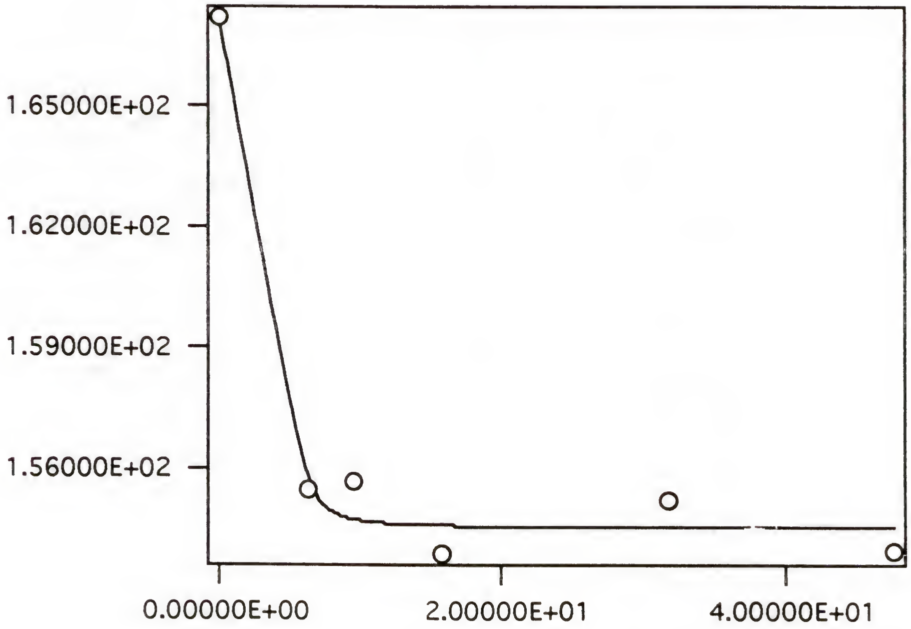

Phe-H22
Ser-H92

p-Nitrophenol Quenching

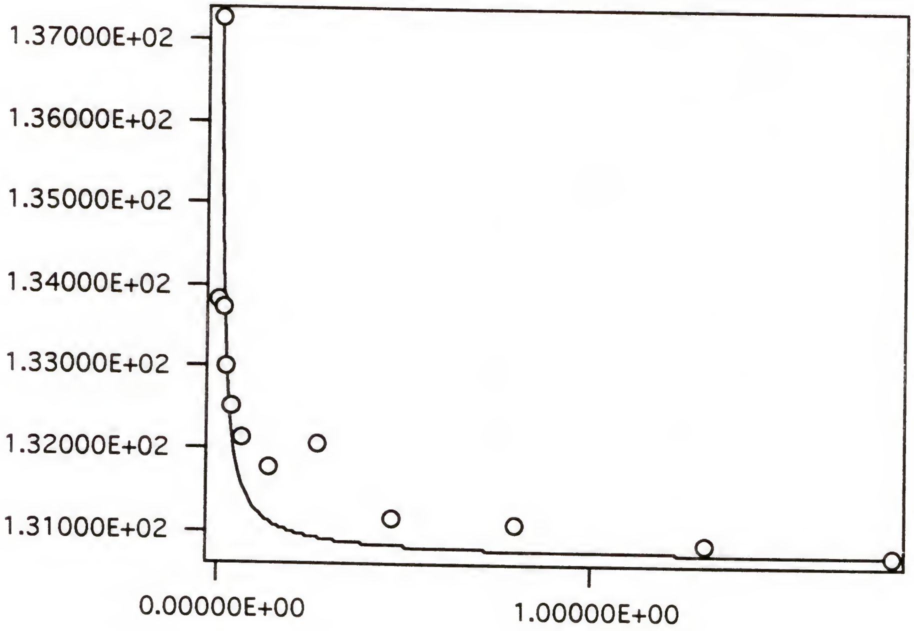

Phe-H22 Acid Product Quenching
Ser-H92

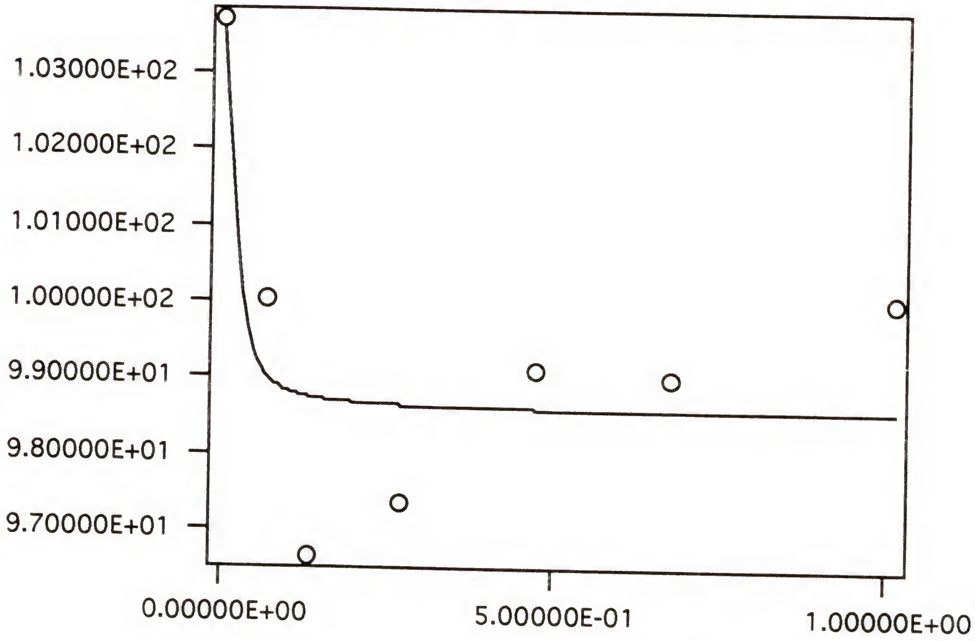

Leu-H22 Antigen Quenching [scFv]=0.0081 μM
Pro-H92

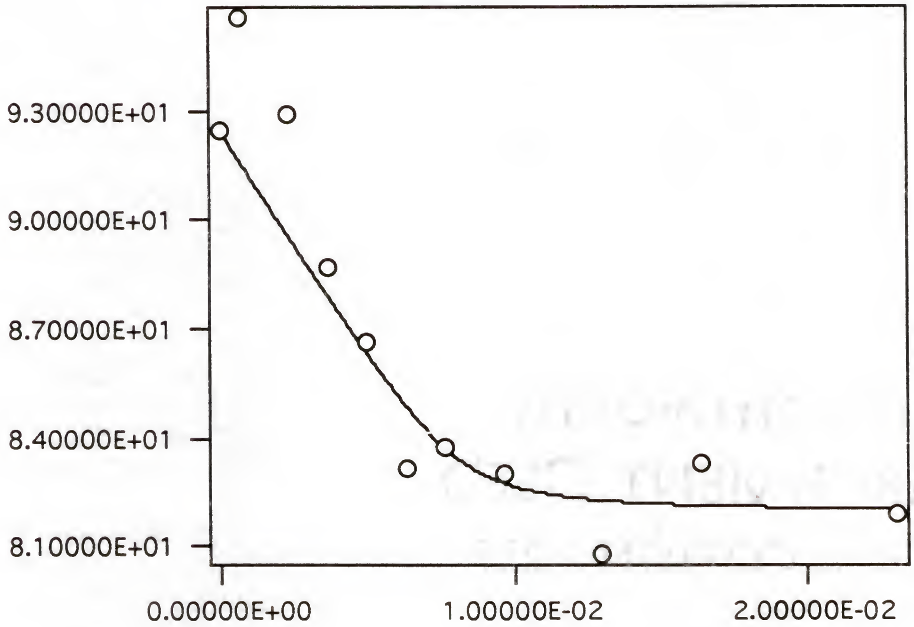

Leu-H22 p-Nitrophenol Quenching
Pro-H92

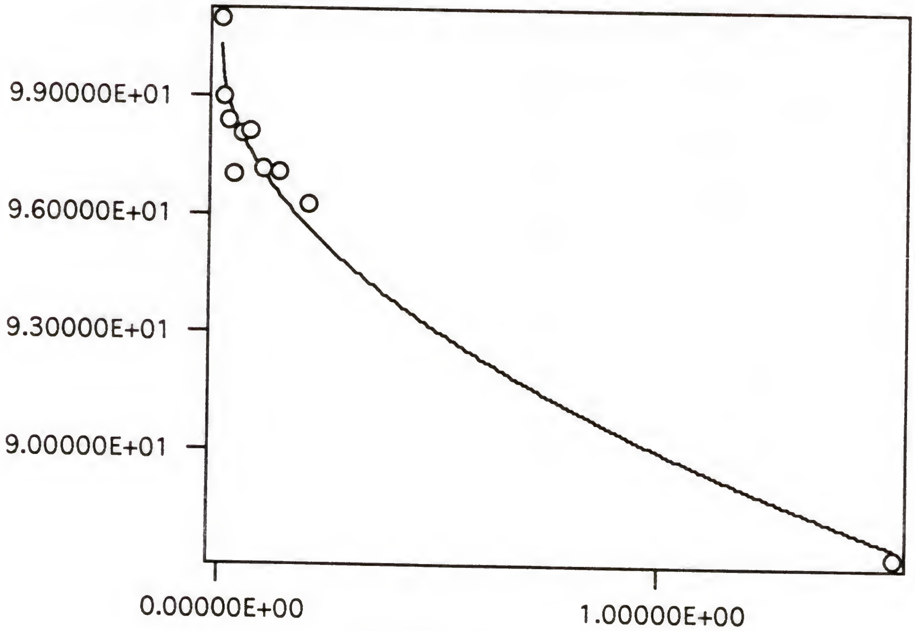

Met-H22 Antigen Quenching [scFv]=Not Determined
Pro-H92

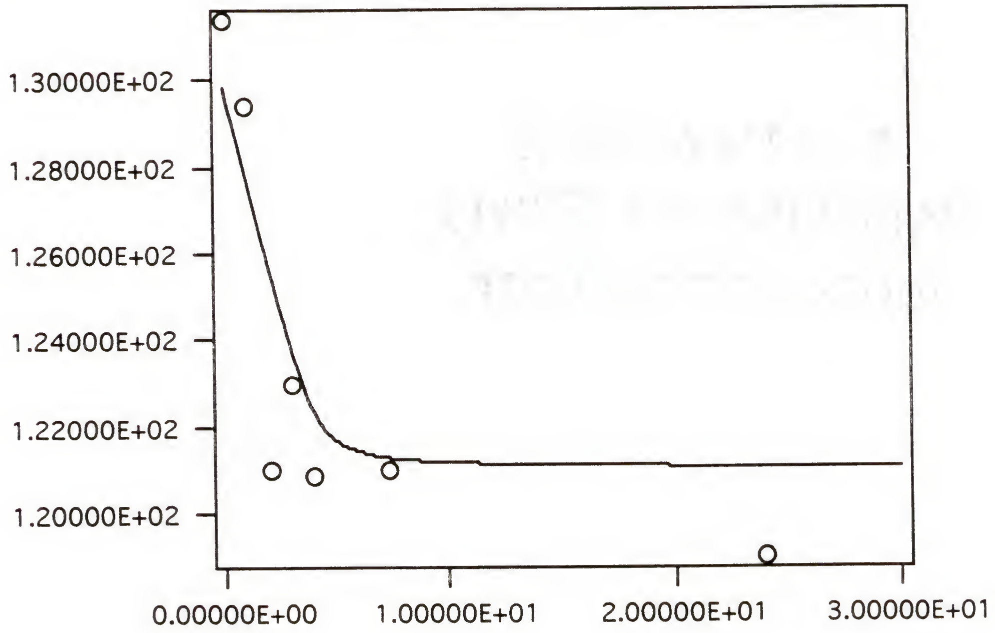

Met-H22 p-Nitrophenol Quenching
Pro-H92

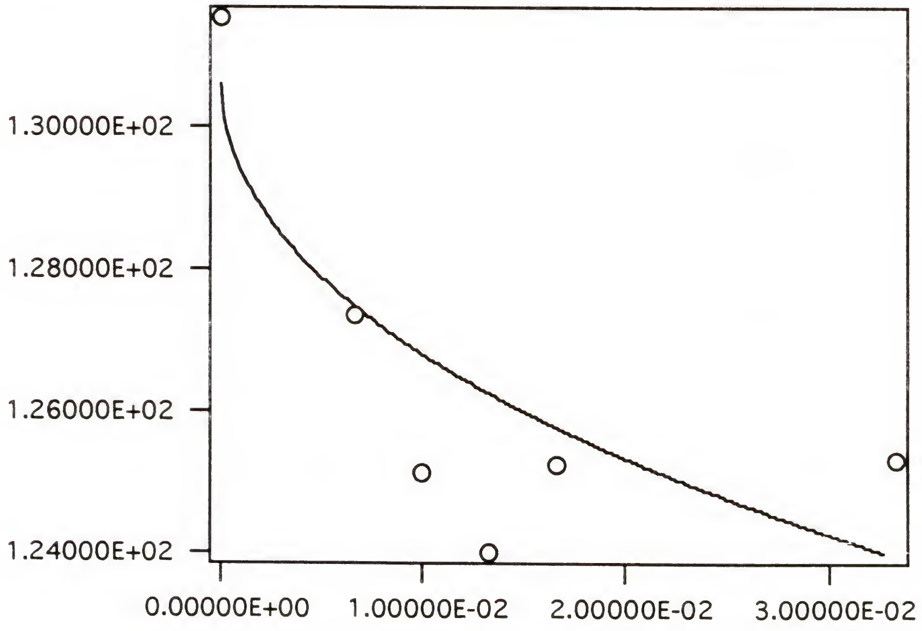

Thr-H22 Antigen Quenching [scFv]=Not Determined
Pro-H92

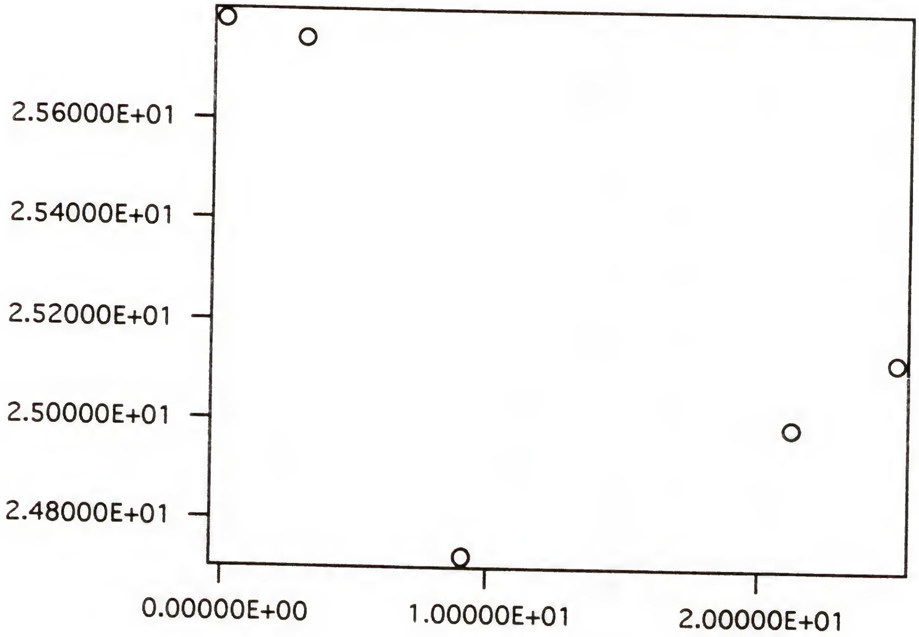

APPENDIX C
GENE SEQUENCES

General Sequences

Promoters

T3 Promoter:
`5′-A ATT TAA TTA CCC TCA CTA AAG-3′`

T7 Promoter:
`5′-A ATT TAA TAC GAC TCA CTA TAG-3′`

Leader Sequences

Native-*pelB* leader sequence:
`5′-ATG AAA TAC CTA TTG CCT ACG GCA GCC GCT GGA TTG TTA TTA CTC GCT GCC CAA CCA GCC ATG GCC-3′`

Codon optimized-*pelB* leader sequence:

`5′-ATG AAA TAC CTG CTG CCG ACC GCT GCT GCT GGT CTG CTG CTC CTC GCT GCC CAG CCG GCG ATG GCC ATG GCC-3′`

Codon optimized-*pelB* leader sequence that is completely cleaved by signal peptidase:
`5′-ATG AAA TAC CTG CTG CCG ACC GCT GCT GCT GGT CTG CTG CTC CTC GCT GCC CAG CCG GCG ATG GCC-3′`

Tags

c-myc tag:
`5′-AGA GAA CAG AAA CTG ATC TCT GAA GAA GAC CTG AAC AAC AGA TCT GGG CCC`

his6 tag:
`5′-CAC CAC CAC CAC CAC CAC-3′`

scFv 43C9 Gene Sequence

```
5′-GAG CTC GTG ATG ACC CAG ACT CCA TCC TCC CTG GCT ATG TCA
GTA GGA CAG AAG GTC ACT ATG AGC TGC AAG TCC AGT CAG AGC CTT
TTA AAT ATT AGC AAT CAA AAG AAC TAT TTG GCC TGG TAC CAG CAG
AAA CCA GGA CAG TCT CCT AAA CTT CTG GTA TAC TTT GCA TCC ACT
AGG GAA TCT GGG GTC CCT GAT CGC TTC ATA GGC AGT GGA TCT GGG
ACA GAT TTC ACT CTT ACC ATC AGC AGT GTG CAG GCT GAA GAC CAG
GCA GAT TAC TTC TGT CAG CAA CAT TAT AGG GCT CCT CGG ACG TTC
GGT GGA GGC ACC AAG CTT GAA ATA AAA GGC TCT ACT TCC GGT AGC
GGC AAA TCC TCT GAA GGC AAA GGT CAG GTT CAG CTG GTC GAG TCT
GGA CCT GGC CTG GTG GCA CCC TCA CAG AGC CTG TCC ATC ACA TGC
ACT GTC TCT GGG ATC TCA TTA TCC AGA TAT AAT GTA CAC TGG GTT
CGC CAG TCT CCA GGA AAG GGT CTG GAG TGG CTG GGA ATG ATA TGG
GGT GGT GGA AGT ATA GAG TAT AAT CCA GCG CTC AAA TCC AGA CTG
AGC ATC AGC AAG GAC AAC TCC AAG AGC CAA ATA TTC TTA AAA ATG
AAC AGT CTG CAA ACT GAT GAC TCA GCC ATG TAT TAC TGT GTC AGT
TAT GGT TAC GGC GGG GAC AGG TTT TCT TAC TGG GGC CAA GGG ACT
CTG GTC ACT GTC TCT-3′
```

scFv PN2A

Variable Fragments of mAb PN2A

Legend for the Alignments below:	Example:
Kabat numbering	1
DNA sequence of PN2A	GAG
amino acid sequence of PN2A	E
Aligned consensus sequence from Kabat Database	Q

PN2A gene sequence that contained variants to the consensus sequence are underlined. Variant residue positions are also bolded for the amino acid sequence.

Light Chain of mAb PN2A

Kabat Database Subgroup: Kappa light chains VI V region- Mouse

Kabat Number	Region
1-24	Framework 1
25-41	CDR 1
42-56	Framework 2
64-95	Framework 3
96-110	CDR3

Note: All invariant residues of the consensus sequence were conserved in the PN2A gene.

1	2	3	4	5	6	7	8	9	10	11	12	13	14	15
GAG	CTC	GTG	CTC	ACC	CAG	TCT	CCA	GCA	ATC	ATA	TCT	GCC	TCT	CCA
E	**L**	V	L	T	Q	S	P	A	I	**I**	S	A	S	S
Q	**I**	V	L	T	Q	S	P	A	I	**M**	S	A	S	S

16	17	18	19	20	21	22	23	24	25	26	27	29	30	31
GGG	GAG	AAG	GTC	ACC	ATA	ACC	TGC	AGT	GCC	AGC	TCA	AGT	GTT	ATT
G	E	K	V	T	**I**	T	C	S	A	S	S	S	V	**I**
G	E	K	V	T	**M**	T	C	S	A	S	S	S	V	**S**

32	33	34	35	36	37	38	39	40	41	42	43	44	45	46
TAC	ATG	TAC	TGG	TTC	CAG	CAG	AAG	CCA	GGC	ACT	TCT	CCC	AAA	CTC
Y	M	**Y**	W	**F**	Q	Q	K	**P**	G	T	S	P	K	**L**
Y	M	**H**	W	**Y**	Q	Q	K	**S**	G	T	S	P	K	**R**

47	48	49	50	51	52	53	54	55	56	57	58	59	60	61
TGG	ATT	TAT	AGT	ACA	TCC	AAT	TTG	GCT	TCT	GGA	GTC	CCT	GCT	CGC
W	I	Y	**S**	T	S	**N**	L	A	S	G	V	P	A	R

W	I	Y	**D**	T	S	**K**	L	A	S	G	V	P	A	R

62	63	64	65	66	67	68	69	70	71	72	73	74	75	76
TCC	AGT	GGC	AGT	GGA	TCT	GGG	ACC	TCT	TAC	TCT	CTC	ACA	ATC	AGC
R	S	G	S	G	S	G	T	S	Y	S	L	T	I	S
R	S	G	S	G	S	G	T	S	Y	S	L	T	I	S

77	78	79	80	81	82	83	84	85	86	87	88	89	90	91
CGA	ATG	GAG	GCT	GGA	GAT	GCT	GCC	ACT	TAT	TAC	TGC	CAG	CAA	AGG
R	M	E	A	E	D	A	A	T	Y	Y	C	Q	Q	**R**
S	M	E	A	E	D	A	A	T	Y	Y	C	Q	Q	**W**

92	93	94	95	96	97	98	99	100	101	102	103	104	105	106
ACT	AGT	TTC	CCG	CTC	ACG	TTC	GGT	GCT	GGG	ACC	AAG	CTG	GAG	CTG
T	S	**F**	P	L	T	F	G	A	G	T	K	L	E	L
S	S	**N**	P	L	T	F	G	A	G	T	K	L	E	L

107	108	109	110
ACA	CGG	GCT	GAT
T	R	A	D
K	R	A	

Heavy Chain of mAb PN2A

Kabat Database Subgroup: MH2A, Heavy chain subgroup II(A) V region- Mouse

Kabat Number	Region
1-30	Framework 1
31-35B	CDR 1
36-49	Framework 2
50-65	CDR 2
66-94	Framework 3
95-	CDR3

Note: Position 103 had a mismatch at an invariant residue in the consensus sequence of the Kabat Subgroup. The remaining mismatches were located at positions with variants in the subgroup.

1	2	3	4	5	6	7	8	9	10	11	12	13	14	15
						TCT	GGA	CCT	GAG	TTG	GTA	AAG	CCT	GGG
						S	G	P	E	L	V	K	A	G
				Q	Q	S	G	P	E	L	V	K	A	G

16	17	18	19	20	21	22	23	24	25	26	27	28	29	30
GCT	TCA	GTG	AAG	ATG	TCC	TGC	AAG	GCT	TCT	GGA	TAC	ACA	TTC	ACT
A	S	V	K	**M**	S	C	K	A	S	G	Y	T	F	T
A	S	V	K	**I**	S	C	K	A	S	G	Y	T	F	T

31	32	33	34	35	36	37	38	39	40	41	42	43	44	45
AGT	TAT	GTT	ATA	CAC	TGG	GTG	AGG	CAG	AAG	CCT	GGG	CAG	GGC	CTT
S	Y	**V**	**I**	**H**	W	V	**R**	Q	**K**	P	G	**Q**	**G**	L
D	Y	**Y**	**M**	**N**	W	V	**K**	Q	**S**	P	G	**K**	**S**	L

46	47	48	49	50	51	52	52A	53	54	55	56	57	58	59
GAG	TGG	ATT	GGA	TTC	ATT	AAC	CCT	TAC	AAT	GAT	GGT	ACT	AAT	TAC
E	W	I	G	**F**	I	N	**P**	**Y**	N	**D**	G	T	N	Y
E	W	I	G	**D**	I	N	**G**		N	**G**	G	T	**S**	Y

60	61	62	63	64	65	66	67	68	69	70	71	72	73	74
AAT	GAG	AAG	TTC	AAA	GGC	AAG	GCC	ACA	CTG	ACT	TCA	GAC	AAA	TCC
N	**E**	K	F	K	G	K	A	T	L	T	**S**	D	**L**	S
N	**Q**	K	F	K	G	K	A	T	L	T	**V**	D	**K**	S

76	77		78	79	80	81	82	82A	82B	82C	83	84	85	86
TCC	ACC	ACA	GCC	TAC	ATG	GAG	CTC	AGC	AGC	CTG	ACC	TCT	GCG	GAC
S	T	**T**	A	Y	M	**E**	L	S	S	L	T	S	E	D
S	T		A	Y	M	**Q**	L	S	S	L	T	S	E	D

87	88	89	90	91	92		93	94	95	96	97	98	99	100
TCT	GCG	GTC	TAT	TAC	TGT	GTT	AAG	AGG	GGG	GAC	TTT	GAA	ACT	CCC
S	A	V	Y	Y	C	**V**	**K**	R	G	**D**	**F**	**Q**	T	P
S	A	V	Y	Y	C		**A**	R	G	**Y/G**	**Y**	**Y**	**S**	**S**

100 A-K	101	102	103	104	105	106	107	108	109	110
TTT	GCT	CAC	TGG	GGC	CAA	GGG	ACT	CTG	GTC	ACT
Many	**A**	**H**	**T**	G	Q	G	T	**L**	V	T
Many	**D**	**Y**	**W**	G	Q	G	T	**T**	V	T

REFERENCES

(1)http://antibodyresource.com.

(2)Stryer, L. *Biochemistry*; Third ed.; W. H. Freeman and Company: New York, 1988.

(3)Glockshuber, R.; Schmidt, T.; Plückthun, A. *Biochemistry* **1992**, *31*, 1270-1279.

(4)Kabat, E. A.; Wu, T. T.; Perry, H. M.; Gottesman, K. S.; Foeller, C. *Sequences of Proteins of Immunological Interest*; Fifth ed.; US Department of Health and Human Services: Washington, DC, 1991.

(5)Bera, T. K.; Onda, M.; Brinkman, U.; Pastan, I. *J. Mol. Biol.* **1998**, *281*, 475-483.

(6)Chowdhury, P. S.; Vasmatzis, G.; Beers, R.; Lee, B.; Pastan, I. *J. Mol. Biol.* **1998**

(7)Stewart, J. D.; Lee, I.; Posner, B. A.; Benkovic, S. J. *Methods in Enzymology* **1995**, *249*, 507-519.

(8)Kuan, C. T.; Pastan, I. *Biochemistry* **1996**, *35*, 2872-2877.

(9)Pauling, L. *Am. Sci.* **1948**, *36*, 51.

(10)Tramontano, A.; Janda, K. D.; Lerner, R. A. *Science* **1986**, *234*, 1566-1569.

(11)Benkovic, S. J. *Nature* **1996**, *383*, 23-24.

(12)Benkovic, S. J. *Annu. Rev. Biochem.* **1992**, *61*, 29.

(13)Lerner, R. A.; Benkovic, S. J. *Science* **1991**, *252*, 659.

(14)Thayer, M. M.; Olender, E. H.; Arvai, A. S.; Koike, C. K.; Canestrelli, I. L.; Stewart, J. D.; Benkovic, S. J.; Getzoff, E. D.; Roberts, V. A. *J. Mol. Biol.* **1999**, *291*, 329-345.

(15)Stewart, J. D.; Krebs, J. F.; Siuzdak, G.; Berdis, A. J.; Smithrud, D. B.; Benkovic, S. J. *Proc. Natl. Acad. Sci. USA* **1994**, *91*, 7404-7409.

(16)Stewart, J. D.; Benkovic, S. J. *Chem. Soc. Rev.* **1993**, 213-219.

(17)Benkovic, S. J.; Adams, J. A.; Borders, C. L.; Janda, K. D.; Lerner, R. A. *Science* **1990**, *250*, 1135-1139.

(18)Pastan, I.; Lee, P.; Brinkmann, U.; FitzGerald, D. 1993.

(19)FitzGerald, D.; Pastan, I. *Journal of Controlled Release* **1996**, *39*, 261-265.

(20)Schmidt, M.; Maurer-Gebhard, M.; Groner, B.; Köhler, G.; Brochmann-Santos, G.; Wels, W. *Oncogene* **1999**, *18*, 1711-1721.

(21)Bera, T.; Viner, J.; Brinkmann, E.; Pastan, I. *Cancer Res.* **1999**, *59*, 4018-4022.

(22)Chen, S. Y.; Zani, C.; Khouri, Y.; Marasco, W. A. *Gene Therapy* **1995**, *2*, 116-123.

(23)Pai, L. H.; Bookman, M. A.; Ozol, R. F.; Young, R. C.; Smith, J. W.; Longo, D. L.; Gould, B; Frankel, A.; McClay, E. F.; Howells, E. F.; Reed, E.; Willingham, M. C.; Fitzgerald, D. J.; Pastan, I. *J. Clin. Oncol.* **1991**, *9*, 2095-2103.

(24)Selvaggi, K.; Saria, E. A.; Schwartz, R.; Vlock, D. R.; Ackerman, S.; Wedel, N.; Kirkwood, J. M.; Jones, H.; Ernstoff, M. S. *J. Immunotherapy* **1993**, *1993*, 201-207.

(25)Carlson, J. R. *Mol. Cell. Bio.* **1988**, *8*, 2638-2646.

(26)Richardson, J. H.; Marasco, W. A. *Tibtech* **1995**, *13*, 306-310.

(27)Chen, S. Y.; Bagley, J.; Marasco, W. A. *Human Gene Ther.* **1994**, *5*, 595-601.

(28)Marasco, W. A.; Haseltine, W. A.; Chen, S. Y. *Proc. Natl. Acad. Sci. USA* **1993**, *90*, 7889-7893.

(29)Beerli, R. R.; Wels, W.; Hynes, N. E. *J. Biol. Chem.* **1994**, *269*, 23932-23936.

(30)Deshane, J.; Siegal, G. P.; Alvarez, R. D.; Wang, M. H.; Feng, M.; Cabrera, G.; Liu, T.; Kay, M.; Curiel, D. T. *J. Clin. Invest.* **1995**, *96*, 2980-2989.

(31)Graus-Porta, D.; Berrli, R. R.; Hynes, N. E. *Mol. and Cell. Biol.* **1995**, *15*, 1182-1191.

(32)Ohage, E. C.; Wirtz, P.; Barnikow, J.; Steipe, B. *J. Mol. Biol.* **1999**, *291*, 1129-1134.

(33)Biocca, S.; Neuberger, M.; Cattaneo, A. *EMBO J.* **1990**, *9*, 101-108.

(34)Biocca, S.; Cattaneo, A. *Trends Cell Biol.* **1995**, *5*, 248-254.

(35)Biocca, S.; Pierandrei-Amaldi, P.; Cattaneo, A. *Biochem. Biophys. Res. Comm.* **1993**, *197*, 422-427.

(36)Richardson, J. H.; Sodroski, J. G.; Waldmann, T. A.; Marasco, W. A. *Proc. Natl. Acad. Sci. USA* **1995**, 3137-3141.

(37)Biocca, S.; Tafani, M.; Cattaneo, A. *Biochem. Biophys. Res. Comm.* **1998**, *246*, 518-523.

(38)Duan, L.; Bagasra, O.; Laughlin, M. A.; Oakes, J. W.; Pomerantz, R. J. *Proc. Natl. Acad. Sci. USA* **1994**, *91*, 5075-5079.

(39)Duan, L.; Zhang, H.; Oakes, J. W.; Bagasra, O.; Pomerantz, R. J. *Human Gene Ther.* **1994**, *5*, 1315-1324.

(40)Biocca, S.; Pierandrei-Amaldi, P.; Campioni, N.; Cattaneo, A. *Bio/Technology* **1994**, *12*, 396-399.

(41)Cochet, O.; Keningsberg, M.; Delumeau, I.; Virone-Oddos, A.; Multon, M. C.; Fridman, W. H.; Schweighoffer, F.; Teillaud, J. L.; Tocqué, B. *Cancer Res.* **1998**, *58*, 1170-1176.

(42)Ohage, E. C.; Steipe, B. *J. Mol. Biol.* **1999**, *291*, 1119-1128.

(43)Wirtz, P.; Steipe, B. *Prot. Science* **1999**, *8*, 2245-2250.

(44)Taviadorakl, P.; Benvenuto, E.; Trinca, S.; De Martinis, D.; Cattaneo, A.; Galeffi, P. *Nature* **1993**, *366*, 469-472.

(45)Tavladoraki, P.; Girotti, A.; Donini, M.; Arias, F. J.; Mancini, C.; Morea, V.; Chiaraluce, R.; Consalvi, V.; Benvenuto, E. *Eur. J. Biochem.* **1999**, *262*, 617-624.

(46)Bowdish, K.; Tang, Y.; Hicks, J. B.; Hilvert, D. *J. Biol. Chem.* **1991**, *266*, 11901-11908.

(47)Wörn, A.; Plückthun, A. *Biochemistry* **1999**, *38*, 8739-8750.

(48)Wörn, A.; Plückthun, A. *FEBS Letters* **1998**, *427*, 357-361.

(49)Proba, K.; Ge, L.; Plückthun, A. *GENE* **1995**, *159*, 203-207.

(50)Steipe, B.; Schiller, B.; Plückthun, A.; Steinbacher, S. *J. Mol. Biol.* **1994**, 188-192.

(51)Proba, K.; Worn, A.; Honegger, A.; Plückthun, A. *J. Mol. Biol.* **1998**, *275*, 245-253.

(52)Martineau, P.; Jones, P.; Winter, G. *J. Mol. Biol.* **1998**, *280*, 117-127.

(53)Langedijk, A.; Honegger, A.; Maat, J.; Planta, R.; van Schaik, R.; Plückthun, A. *J. Mol. Biol.* **1998**, *283*, 95-110.

(54)Frisch, C.; Kolmar, H.; Fritz, H. J. *Biol. Chem. Hoppe-Seyler* **1994**, *375*, 353-356.

(55)Passafiume, M.; Vulliez-le Normand, B.; Riottot, M. M.; Bentley, G. A. *FEBS Letters* **1998**, *441*, 407-412.

(56)Rudikoff, S.; Pumphrey, J. G. *Proc. Natl. Acad. Sci. USA* **1986**, *83*, 7875-7878.

(57)Proba, K.; Honegger, A.; Plückthun, A. *J. Mol. Biol.* **1997**, *265*, 161-172.

(58)Wörn, A.; Plückthun, A. *Biochemistry* **1998**, *37*, 13120-13127.

(59)Jäger, M.; Plückthun, A. *J. Mol. Biol.* **1999**, *285*, 2005-2019.

(60)Ramm, K.; Gehrig, P.; Plückthun, A. *J. Mol. Biol.* **1999**, *290*, 535-546.

(61)Gibbs, R. A.; Posner, B. A.; Filula, D. R.; Dodd, S. W.; Finkelman, M. A.; Lee, T. K.; Wroble, M.; Whitlow, M.; Benkovic, S. J. *Proc. Natl. Acad. Sci. USA* **1991**, *88*, 4001-4004.

(62)Gibbs, R. A.; Benkovic, P. A.; Janda, K. D.; Lerner, R. A.; Benkovic, S. J. *J. Am. Chem. Soc,* **1992**, *114*, 3528-3534.

(63)Gibbs, R. A.; Taylor, S.; Benkovic, S. J. *Science* **1992**, *258*, 803-805.

(64)Benkovic, S. J.; Adams, J. A.; Borders, C. L.; Janda, K. D.; Lerner, R. A. *Science* **1990**, *250*, 1135-1139.

(65)Krebs, J. F.; Suizdak, G.; Dyson, H. *Biochemistry* **1995**, *34*, 720-723.

(66)Janda, K. D.; Ashley, J. A.; Jones, T. M.; MeLeod, D. A.; Schloeder, D. M.; Weinhouse, M. I.; Lerner, R. A.; Gibbs, R. A.; Benkovic, P. A.; Hilhorst, R.; Benkovic, S. J. *J. Am. Chem. Soc.* **1991**, *113*, 291-297.

(67)Stewart, J. D.; Roberts, V. A.; Thomas, N. R.; Getzoff, E. D.; Benkovic, S. J. *Biochemistry* **1994**, *33*, 1994-2003.

(68)Roberts, V. A.; Stewart, J. D.; Benkovic, S. J.; Getzoff, E. D. *J. Mol. Biol.* **1994**, *235*, 1098-1116.

(69)Lee, I.; Stewart, J. D.; Zhong, W.; Benkovic, S. J. *Anal. Biochem.* **1995**, *230*, 62-67.

(70)Wood, C. R.; Dorner, A. J.; Morris, G. E.; Alderman, E. M.; Wilson, D.; O'Hara, R. M.; Kaufman, R. J. *J. Immunol.* **1990**, *145*, 3011-3016.

(71)Brüggemann, M.; Neuberger, M. S. *Methods: A Companion to Methods in Enzymology* **1991**, *2*, 159-165.

(72)Bebbington, C. R. *Methods: A Companion to Methods in Enzymology* **1991**, *2*, 136-145.

(73)Wu, X. C.; Ng, S. C.; Near, R. I.; Wong, S.L. *Bio/Technology* **1993**, *11*, 71-76.

(74)Hasemann, C. A.; Capra, J. D. *Methods: A Companion to Methods in Enzymology* **1991**, *2*, 146-158.

(75)Wright, A.; Shin, S.U. *Methods: A Companion to Methods in Enzymology* **1991**, *2*, 125-135.

(76)Wülfing, C.; Plückthun, A. *Mol. Microbiol.* **1994**, *12*, 685-692.

(77)Ostermeier, M.; De Sutter, K.; Georgiou, G. *J. Biol. Chem.* **1996**, *271*, 10616-10622.

(78)Rietsch, A.; Belin, D.; Martin, N.; Beckwith, J. *Proc. Natl. Acad. Sci. USA* **1996**, *93*, 13048-13053.

(79)Sone, M.; Akiyama, Y.; Ito, K. *J. Biol. Chem.* **1997**, *272*, 10349-10352.

(80)Derman, A. I.; Prinz, W. A.; Belin, D.; Beckwith, J. *Science* **1993**, *262*, 1744-1747.

(81)Buchner, J.; Pastan, I.; Brinkmann, U. *Anal. Biochem.* **1992**, *205*, 263-270.

(82)Buchner, J.; Rudolph, R. *Bio/Technology* **1991**, *9*, 157-162.

(83)Kobayashi, H.; Morioka, H.; Tobisawa, K.; Torizawa, T.; Kato, K.; Shimada, I.; Nikaido, O.; Stewart, J. D.; Ohtsuka, E. *Biochemistry*, **1999**, *38*, 532-539.

(84)DiGiovanna, M. P.; Stern, D. F. *Cancer Res.* 1995, *55*, 1946-1955.

(85)DiGiovanna, M. P.; Carter, D.; Flynn, S. D.; Stern, D. F. *Brit. J. Cancer* **1996**, *74*, 802-806.

(86)Ruddon, R. W. *Cancer Biology*; Oxford University Press: New York, 1995.

(87)Weinberg, R. A. *Oncogenes and the Molecular Origins of Cancer*; Cold Spring Harbor Laboratory Press: New York, 1989.

(88)Ullrich, A.; Schlessinger, J. *Cell* **1990**, *61*, 203-212.

(89)Testsu, A.; Namba, Y.; Saito, T.; Toyoshima, K.; Yamamoto, T. *Cell. Biol.* **1991**, 833-842.

(90)Stern, D. F.; Kamps, M. P. *EMBO J.* **1988**, *7*, 995-1001.

(91)Schmidt, M.; Reiser, P.; Hills, D.; Gullick, W. J.; Wels, W. *Int. J. Cancer* **1998**, *75*, 878-884.

(92)Hynes, N. E.; Stern, D. F. *Biochim. Biophy. Acta* **1994**, *1198*, 165-184.

(93)Bangalore, L.; Tanner, A. J.; Laudano, A. P.; Stern, D. F. *Proc. Natl. Acad. Sci. USA* **1992**, *89*, 11637-11641.

(94)Stern, D.; Kamps, M.; Cao, H. *Mol. Cell. Biol.* **1988**, 3969-3973.

(95)Neu, H. C.; Heppel, L. A. *J. Biol. Chem.* **1965**, *240*, 3685-3692.

(96)Gibbs, R. A.; Benkovic, P. A.; Janda, K. D.; Lerner, R. A.; Benkovic, S. J. *J. Am. Chem. Soc.* **1992**, *114*, 3534-3534.

(97)Suizdak, G.; Krebs, J. F.; Benkovic, S. J.; Dyson, J. *J. Am. Chem. Soc.* **1994**, *116*, 7937-7938.

(98)Veleick, S. F.; Parker, C. W.; Eisen, H. N. *Biochemistry* **1960**, *46*, 1470-1482.

(99)Taira, K.; Benkovic, S. J. *J. Med. Chem.* **1988**, *31*, 129-137.

(100)Pace, N. C.; Shirley, B. A.; Thomson, J. A. *Protein Structure and Function: A Practical Approach*; Creighton, T. E., IRL Press: Oxford, 1989; p. 311-330.

(101)Pace, C. N. *Trends in Biotechnology* **1990**, *8*, 93-98.

(102)Callahan S. M.; Cornell, N. W.; Dunlap, P. V. *J. Biol. Chem.* **1995**, *270*,17627-17632.

(103)Orlandi, R.; Gussow, D. H.; Jones, P. T.; Winter, G. *Proc. Natl. Acad. Sci. USA* **1989**, *86*, 3833-3837.

(104)Huse, W. D.; Sastry, L.; Iverson, S. A.; Kang, A. S.; Alting-Mees, M.; Burton, D. R.; Benkovic, S. J.; Lerner, R. A. *Science* **1989**, *246*, 1275-1281.

(105)Sastry, L.; Alting-Mees, M.; Huse, W. D.; Short, J. M.; Sorge, J. A.; Hay, B. N.; Janda, K. D.; Benkovic, S. J.; Learner, R. A. *Proc. Natl. Acad. Sci. USA* **1989**, *86*, 5728-5732.

(106)Whitlow, M.; Filpula, D. *Methods* **1991**, *2*, 97.

(107)Sambrook, J.; Fritsch, E. F.; Maniatis, T. *Molecular Cloning. A Laboratory Manual;* Cold Spring Harbor: Cold Spring Harbor, 1989.

(108)Bradford, M. M. *Anal. Biochem.* **1976**, *72*, 248-254.

(109)Suttnar, J.; Dyr, J.; Hamsikova, J.; Novak, J.; Vonka, V. *J. Chrom. B.* **1994**, *656*, 123-126.

(110)Kobayashi, H.; Morioka, H.; Nikaido, O.; Stewart, J. D.; Ohtsuka, E. *Protein Engineering* **1998**, *11*, 1089-1092.

BIOGRAPHICAL SKETCH

Jennifer Tonzello was born in Bethesda, Maryland on August 30, 1972. After her family relocated to Florida, she was raised in Rockledge, which is located on the East Coast of Central Florida. She attended high school at Rockledge High and graduated in 1990. Her education was continued at the Florida State University where she earned a Bachelors of Science in Chemistry. Her undergraduate project in Chemistry was under the direction of Dr. R. Rill. She then accepted a position at EG&G Florida, Inc. as an Environmental Health Specialist at Kennedy Space Center Florida. While at Kennedy Space Center she was fortunate to work in Hazardous Operations and on the Launch Team that surveyed the pad after lift-off. In August of 1995 she elected to attend graduate school at the University of Florida and began working towards a doctoral degree in chemistry under the supervision of Dr. Jon Stewart. Upon completion of her studies in biochemistry she will accept a position at Research Corporation Technologies as an Analyst in the Gene Expression Technology Group.

I certify that I have read this study and that in my opinion it conforms to acceptable standards of scholarly presentation and is fully adequate, in scope and quality, as a dissertation for the degree of Doctor of Philosophy.

Jon D. Stewart, Chair
Assistant Professor of Chemistry

I certify that I have read this study and that in my opinion it conforms to acceptable standards of scholarly presentation and is fully adequate, in scope and quality, as a dissertation for the degree of Doctor of Philosophy.

Steven A. Benner
Professor of Chemistry

I certify that I have read this study and that in my opinion it conforms to acceptable standards of scholarly presentation and is fully adequate, in scope and quality, as a dissertation for the degree of Doctor of Philosophy.

Benjamin A. Horenstein
Associate Professor of Chemistry

I certify that I have read this study and that in my opinion it conforms to acceptable standards of scholarly presentation and is fully adequate, in scope and quality, as a dissertation for the degree of Doctor of Philosophy.

David E Richardson

David Richardson
Professor of Chemistry

I certify that I have read this study and that in my opinion it conforms to acceptable standards of scholarly presentation and is fully adequate, in scope and quality, as a dissertation for the degree of Doctor of Philosophy.

Harry S. Nick

Harry S. Nick
Professor of Neuroscience